NUREG/CR-4438
EGG-2424
November 1985

Results of Semiscale Mod-2C Small-Break (5%) Loss-of-Coolant Accident Experiments S-LH-1 and S-LH-2

Guy G. Loomis
John E. Streit

F O R M A L R E P O R T

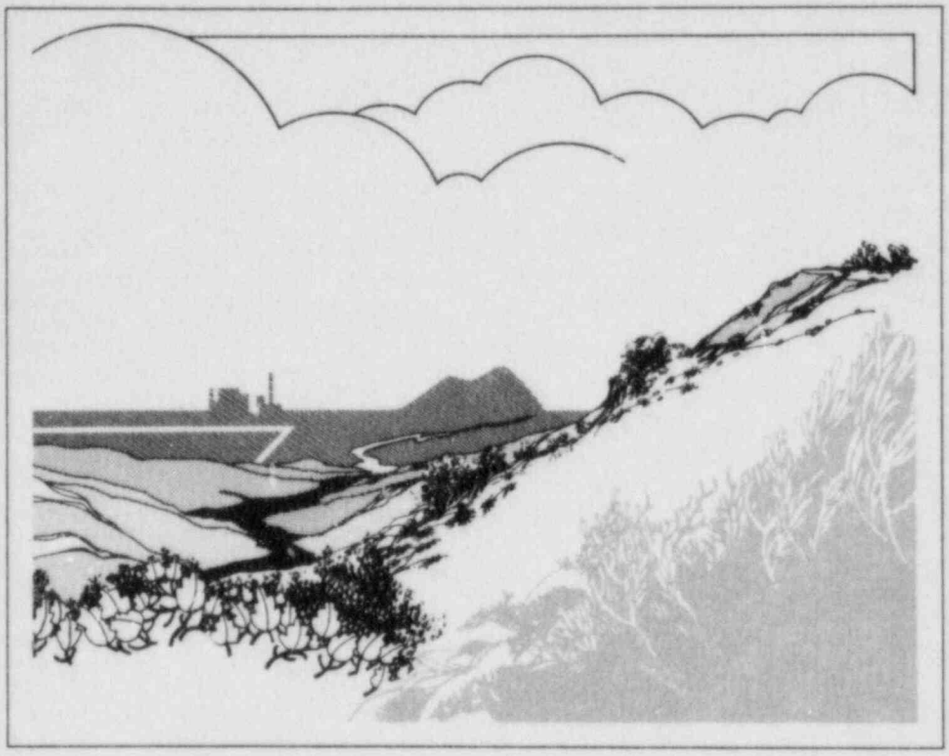

EG&G Idaho

Work performed under
DOE Contract No. DE-AC07-76ID01570

for the ***U.S. Nuclear Regulatory Commission***

Idaho National Engineering Laboratory

Managed by the U.S. Department of Energy

Available from

Superintendent of Documents
U.S. Government Printing Office
Post Office Box 37082
Washington, D.C. 20013-7982

and

National Technical Information Service
Springfield, VA 22161

NUREG/CR-4438
EGG-2424
Distribution Category: R2

RESULTS OF SEMISCALE MOD-2C SMALL-BREAK (5%) LOSS-OF-COOLANT ACCIDENT EXPERIMENTS S-LH-1 AND S-LH-2

Guy G. Loomis
John E. Streit

Published November 1985

EG&G Idaho, Inc.
Idaho Falls, Idaho 83415

Prepared for the
Division of Accident Evaluation
Office of Nuclear Regulatory Research
U.S. Nuclear Regulatory Commission
Washington, D.C. 20555
Under DOE Contract No. DE-AC07-76IDO1570
FIN No. A6038

ABSTRACT

Two experiments simulating small break (5%) loss-of-coolant accidents (5% SBLOCAs) were performed in the Semiscale Mod-2C facility. These experiments were identical except for downcomer-to-upper-head bypass flow (0.9% in Experiment S-LH-1 and 3.0% in Experiment S-LH-2) and were performed at high pressure and temperature [15.6 MPa (2262 psia) system pressure; 37 K (67°F) core differential temperature; 595 K (610°F) hot leg fluid temperature]. From the experimental results, the signature response and transient mass distribution are determined for a 5% SBLOCA. The core thermal-hydraulic response is characterized, including core void distribution maps, and the effect of core bypass flow on transient severity is assessed. Comparisons are made between postexperiment RELAP5 calculations and the experimental results, and the capability of RELAP5 to calculate the phenomena is assessed.

FIN No. A6038—Semiscale Program

SUMMARY

The Semiscale experimental program, conducted by EG&G Idaho, Inc., is part of the overall research and development program sponsored by the U.S. Nuclear Regulatory Commission (NRC) through the Department of Energy (DOE) to evaluate the behavior of pressurized-water-reactor (PWR) systems during hypothesized accident sequences. Its primary objective is to obtain representative integral and separate-effects thermal-hydraulic response data to provide an experimental basis for analytical model development and assessment. This report presents the results obtained from Semiscale experiments S-LH-1 and S-LH-2, performed in the Semiscale Mod-2C system, and a comparison of RELAP5 postexperiment calculations with the experimental data. The Mod-2C system is a small-scale, nonnuclear, experimental system in which nuclear heating is simulated by an electrically heated core. The system includes a vessel and two operating loops, both of which contain an active steam generator and active pumps. Experiments S-LH-1 and S-LH-2 were performed at typical PWR system pressure and temperature [15.6 MPa (2262 psia) pressure; 37 K (67°F) core differential temperature].

Experiments S-LH-1 and S-LH-2 simulated centerline cold leg small break loss-of-coolant accidents (5% SBLOCAs). The two experiments differed only in the initial amount of allowed downcomer-inlet-annulus-to-upper-head bypass flow (core bypass flow). Experiment S-LH-1 had a 0.9% core bypass flow, and Experiment S-LH-2 had a 3.0% core bypass flow. Comparison of results from these two experiments allowed an assessment of the effect of the amount of bypass flow on accident severity in the Semiscale system. Since both S-LH-1 and S-LH-2 had similar basic hydraulic response during the 5% SBLOCA, details relative to S-LH-1 data are discussed. Differences in phenomena between S-LH-1 and S-LH-2 are discussed separately. The capability of RELAP5 to correctly calculate the phenomena observed during S-LH-1 and S-LH-2 is assessed.

Both S-LH-1 and S-LH-2 had similar signature pressure responses for a 5% SBLOCA. This signature response is characterized as a primary system depressurization with significant loss of primary system mass inventory. Before accumulator recovery, the system fluid mass inventory was reduced to 10% of initial inventory and was accompanied by core rod heat-ups. Once accumulator injection started, the core rod heat-ups were mitigated. Starting from subcooled conditions, opening the break caused a primary system depressurization with various inflection points as primary system fluid mass inventory escaped through the break. Major inflection points included a large increase in depressurization rate, when core power was ramped down on the ANS decay curve following a low primary pressure trip, and a large decrease in depressurization rate caused by flashing when fluid throughout the loop reached saturation conditions. The vessel fluid was the first to reach saturation conditions at about 5 s, followed by the hot legs at 9 s. By 40-45 s, fluid in the cold leg and thus the entire loop reached saturation conditions and was accompanied by flashing and a significant reduction in the depressurization rate. Other inflection points were caused by pump suction clearing of liquid (increasing the depressurization rate) and accumulator injection (decreasing the depressurization rate).

The system fluid mass distribution during a 5% SBLOCA can be characterized by five distinct time periods. These periods are distinguishable according to the amount of mass in the system, fluid thermodynamic conditions, pump operation, and mode of natural circulation. The first period (0 to 40 s) covers the rapid drain of the pressurizer and the beginning of upper head drain. The second period (40 to 90 s) starts when loop saturation conditions are achieved in the loop and ends when the pumps have coasted down. The third period (90 to 140 s) starts when the pumps achieve zero speed and ends with the initiation of natural circulation. The fourth period (140 to 300 s) is distinguished by development of a complicated transient manometric balance of loop fluid heads and a rapid (25 s duration) core liquid level depression, with or without core rod heat-ups depending on core bypass flow. The fifth period (300 to 1000 s) is characterized by a long-term boil-off of vessel fluid accompanied by core rod heat-ups in both experiments and ends with accumulator coolant injection.

Upon initiation of blowdown, the first components in the loop to begin draining were the pressurizer and upper head. Eighty percent of the fluid that left the system via the break during the first period (0 - 40 s) was accounted for by the pressurizer drain. The remainder of the fluid came from the vessel upper head. The upper head and pressurizer drained in a differential manner because of differences in fluid conditions for the two

components. For the pressurizer, the initial condition of the fluid was saturated; and the expanding steam bubble pushed liquid out of the pressurizer. The vessel upper head fluid remained subcooled with no flashing, and the drain of this component was minimal during the first period.

The second distinct time period included pump coastdown (40-90 s). During pump coastdown, there was relatively slow depressurization with a much reduced break flow due to saturation conditions (two-phase flow) at the break. During this period, the upper head continued to drain; however, most of the mass lost from the system came from lower regions of the vessel. During pump coastdown, the general loop fluid condition was two-phase, with the pressurizer steam-filled. The broken loop hot leg was stratified, and the intact loop hot leg was a homogeneous, two-phase mixture. The cold leg fluid in both loops remained nearly liquid throughout this period. Due to the flow splits throughout the loop, the vessel drained more than other components during this period. The flow direction in the broken loop went from the vessel to the steam generator and then to the break, where some of the flow was diverted to the break and a reduced amount reentered the vessel at the downcomer. Since the hot leg flow split (broken to intact loop) remained about one to three, the vessel fluid had to be diminished by simple mass balance. The pump operation during this period was found to have a 130 cm (52 in.) effect on calculated collapsed liquid levels throughout the loops. When the pumps coasted down from about 20% initial speed to zero speed (between 80 and 90 s), the levels in the primary U-tubes and vessel exhibited about a 130 cm (52 in.) change, indicating the effect of pumped flow on calculated liquid level.

The third period (90 to 140 s) was dominated by the drain of the steam generator primary U-tubes, which was controlled by the transition from pumped flow to natural circulation. The fluid in the U-tubes drained in a top-down manner, and there were differences in the draining rate between intact and broken loop tubes. Collapsed liquid levels in the vessel remained stable at about 60 cm (24 in.) below the top of the core throughout this period. The drain of fluid in the primary steam generator tubes occurred because of the loss of head across the pumps when zero speed was achieved. Immediately after the pumps achieved zero speed, natural circulation heads alone could not support the broken loop U-tube level and the fluid drained concurrently (upflow and downflow sides at the same rate). However, during drain of the broken loop tubes, intact loop two-phase natural circulation flow supported the ongoing primary tube fluid level until the broken loop primary tubes had drained, thus establishing a reflux mode of natural circulation. When the reflux mode was established in the broken loop, the intact loop steam generator primary tubes drained concurrently (upflow and downflow sides) accompanied by a marked increase in hot leg volumetric flow (toward the intact loop steam generator) which replaced the fluid as it drained out of the tubes. After both intact and broken loop tubes had drained, the reflux mode of core heat rejection occurred in both loops, which appears as a differential head between the upflow and downflow sides. This differential head has been referred to previously as "liquid hold-up induced," but in reality it is simply the ongoing reflux process.

The fluid distribution during the forth period (140 to 300 s) was dominated by a manometric balance of heads throughout the loop. Following draining of the steam generator U-tubes, liquid seals were left in the pump suction of both loops and in the vessel downcomer and vessel. These liquid seals caused a blockage to steam flow (steam created in the core region) around the loop to the break. The vessel upper plenum and hot legs were pressurized, causing a manometric depression in both the liquid level in the downflow side of the pump suction seals and the liquid level in the vessel. The loop seals in both the intact and broken loops were eventually cleared of liquid, allowing a steam relief path to the break and a relaxation of manometric balance of heads throughout the loop. The clearing of the pump suction seal can be envisioned as a steam/water interface simply moving down the downflow side and around the U-bend of the pump suction and up the upflow side. For S-LH-1, the intact loop seal was cleared first at 180 s, followed by the broken loop at 280 s. This preferred clearing for the intact loop is due to the 9-to-1 hydraulic resistance split between the broken loop and intact loop. With a 9-to-1 resistance split with pumps off, break flow was preferentially supplied from the less hydraulically resistant intact loop suction rather than from the more resistant broken loop suction.

The fifth period (300 to 1000 s) was characterized as a core boil-off period. Following clearing of the loop seals, the remaining mass in the system was centered in the vessel and downcomer; and

fluid in the core simply boiled off with a differential fluid head between the downcomer and core. This differential head was supported by pressurization in the core, as needed to support steam flow to the break, even though both loop pump suction seals and the bypass between the vessel upper head and downcomer were cleared of fluid and could pass steam. The vessel and downcomer liquid levels depleted concurrently as the core boiled off. Eventually, primary system pressure decreased to the accumulator set point [4.2 MPa (600 psia)], initiating accumulator water flow into the system. Accumulator flow reflooded hot core structures and rods, causing a reduction in ongoing depressurization rate due to steam production. The experiment was terminated at about 1000 s with a quenched core and an increasing core liquid level.

The core thermal-hydraulic response during S-LH-1 was dominated by two liquid level depressions. The first liquid level depression, to 110 cm (43 in.) above the bottom of the core, was of relatively short duration (~25 s) and was caused by the manometric head balance associated with pump suction clearing. The second liquid level depression, to 116 cm (46 in.) above the bottom of the core, was ~250 s in duration and was caused by core boil-off. Both of these depressions resulted in core rod temperature excursions. The maximum cladding temperature achieved for any rod position was 624 K (663°F) during the seal-clearing period and 764 K (915°F) during the boil-off period. The temperature excursions during the manometric balance period were terminated naturally following clearing of the pump suction seals in both loops. Accumulator injection terminated the core rod temperature excursions during the boil-off period. Even though core rod heat-ups occurred during both liquid level depressions, the characteristics of the heat-ups were dependent on the mechanism of depression. During the first rapid depression, drops or films of water on portions of the rods caused multidimensional heat-up effects. During the relatively slow second depression, core rod heat-up followed a uniform top-down pattern. During both liquid level depressions, the core axial void fraction distribution was stratified. This stratification was supported by boiling in the core due to core decay heat. Heat-up occurred only if the local void fraction was 1 (+0; -0.02).

The amount of core bypass flow had a strong effect on SBLOCA severity. Experiments S-LH-1, with 0.9% of initial core flow bypassed, and S-LH-2, with 3.0% of initial core flow bypassed, showed that the core liquid level depression during the manometric depression period was greater for lower bypass flow. (The 0.9% bypass flow case had a minimum core level of 110 cm (43 in.) above the bottom of the core, whereas the 3.0% bypass flow case had a minimum core level of 220 cm (86 in.) above the bottom of the core.) Core rod heat-ups occurred during the vessel manometric level depression for the low bypass flow case (S-LH-1) but not for the higher bypass flow case (S-LH-2). Previous studies on the effect of core bypass flow attributed the difference in core liquid level depression to a difference in net head of steam generator primary tubes for high and low bypass flows. However, for S-LH-1 and S-LH-2, the net head of liquid in both steam generators was identical during the depression period; therefore, the additional bypass flow alone (upper head cleared for steam flow) relieved enough steam to minimize the core level depression. On an overall basis, the same phenomena occurred for S-LH-1 as S-LH-2. Both experiments exhibited vessel level depression and seal clearing and core boil-off, with only the timing and severity of events altered. The major difference between S-LH-1 and S-LH-2 other than the severity of core level depression was that the broken loop pump suction seal never did clear for the higher bypass flow case (S-LH-2). The flow through the intact loops plus the additional bypass flow was sufficient to relieve steam generated in the core.

RELAP5/MOD2 calculated the major phenomena that occurred during these transients. The RELAP5 calculation shows that the buildup of liquid due to reflux on the up side of the U-tubes contributed to the core level depression in S-LH-1. Although major phenomena were calculated, the duration and the magnitude of their effect on the transient were not always well calculated. During the manometric period, the core liquid level was calculated to be depressed much more severely than was measured for S-LH-1; however, no heater rod temperature excursion was calculated. In addition, when the break was uncovered, the RELAP5-calculated depressurization rate was higher than was observed, resulting in an earlier activation of the accumulators; therefore, the heater rod temperature excursions due to core boil-off were not calculated. RELAP5, however, did calculate the trend that lower bypass flow causes a more severe core liquid level depression.

CONTENTS

FIGURES

TABLES

RESULTS OF SEMISCALE MOD-2C SMALL-BREAK (5%) LOSS-OF-COOLANT ACCIDENT EXPERIMENTS S-LH-1 AND S-LH-2

INTRODUCTION

The Semiscale experimental program conducted by EG&G Idaho, Inc., is part of the overall research and development program sponsored by the U.S. Nuclear Regulatory Commission (USNRC) through the Department of Energy (DOE) to evaluate the behavior of pressurized-water-reactor (PWR) systems during hypothesized accident sequences. Its primary objective is to obtain representative integral- and separate-effects thermal-hydraulic response data to provide an experimental basis for analytical model development and assessment. The subject Semiscale Mod-2C experiments, S-LH-1 and S-LH-2, were authorized and performed under this program. Experiments S-LH-1 and S-LH-2 simulated small break (5%) loss-of-coolant accidents (5% SBLOCAs)[a] and were identical except for downcomer-to-upper-head bypass flow (0.9% for S-LH-1 and 3.0% for S-LH-2).

SBLOCAs are considered relatively probable during the normal operating lifetime of a commercial PWR. In fact, small breaks in the form of steam generator tube ruptures, pump seal leaks, and stuck open pressurizer power operated relief valves (PORVs) have already occurred. Additional anticipated small breaks include instrumentation lines and small pipe cracks associated with normal or abnormal operation. The real safety issue associated with small breaks is the possibility of severe voiding of vessel liquid before primary pressure decreases to accumulator and low pressure injection pressure set points. If the core liquid level is depressed to a low enough level, core rod heat-up and possible fuel damage may result before safety injection initiates a reflood of the core. In large break LOCA's (>10%), the vessel liquid inventory quickly flashes; and core heat-up can start early in the transient. However, because of the accompanying rapid depressurization, both accumulator and low pressure injection systems (LPIS) refill and reflood the vessel before significant core rod heat-up occurs. Previous Semiscale studies[1,2] have indicated that 5% SBLOCAs produce the most severe core liquid level depressions and that core bypass flow affects the severity of the accident. However, data from these previous studies were incomplete; and hardware differences other than allowed core bypass flow were made, disallowing a clear comparison.[3] Therefore, the characteristic signature response could not be accurately described and the effect of bypass flow alone could not be determined. Experiments S-LH-1 and S-LH-2 were performed in Semiscale Mod-2C, a state-of-the-art SBLOCA facility, to gain insight into the phenomena and provide data for code assessment and development purposes.

This report presents the results of Experiments S-LH-1 and S-LH-2. First, the historical background of these 5% SBLOCA experiments is discussed. In the "results" section, specific topics include the characteristic signature response of a 5% SBLOCA, the transient fluid mass distribution, the core thermal and hydraulic response, and an assessment of the affect of bypass flow on transient severity. Finally, a comparison of experiment data with RELAP5 posttest calculations is given. Conclusions based on these results are then offered.

a. A 200% break equals a double-ended offset shear of the main coolant piping in one loop of a four-loop PWR. Small pipe breaks are assumed to be centerline tears or cracks in the main coolant piping.

HISTORICAL BACKGROUND

On December 9, 1981, a 5% SBLOCA experiment, S-UT-8, was performed in the Semiscale Mod-2A system.[4] The purpose of this experiment was to provide a thermal-hydraulic test bed for the Westinghouse Reactor Vessel Level Indicating System (WRVLIS). Westinghouse requested that certain modifications be made to the Mod-2A system to better simulate actual PWR behavior.[5] These modifications involved adjusting the initial vessel downcomer-to-upper-head flow rate (core bypass flow) to 2.3% of the total core flow rate. In addition, it was requested that the ratio for the pressure drop between the upper head and upper plenum to the pressure drop between the downcomer and upper head (R_{DP}) be 9.3%. In actual practice, the core bypass flow rate was adjusted to 1.1% of total core flow and R_{DP} was only 5.6%. Even though the desired vessel/downcomer hydraulic paths were not achieved, the experiment was a success in providing hydraulic conditions similar to those expected during small-break transients.

Current interest in additional SBLOCA experiments centers on certain phenomena that occurred during S-UT-8. Phenomena of interest include condensation-induced filling of intact loop primary steam generator tubes and pump suction liquid seal formation and resulting manometric hydrostatic balance that caused an extreme core liquid level depression. Both of these phenomena had been witnessed in a previous 5% SBLOCA experiment (S-UT-6);[6] however, the core liquid level depression was considerably greater during S-UT-8 than during S-UT-6.

The decision to run additional 5%[a] SBLOCA experiments similar to S-UT-8 and S-UT-6 (named S-LH-1 and S-LH-2, respectively) centered around differences in hydraulic response between S-UT-6 and S-UT-8. Both experiments were 5% SBLOCAs with essentially identical initial and boundary conditions; however, many system hardware changes were made between the two experiments that could have caused the observed differences in response. S-UT-6 had a vessel collapsed liquid core level depression to about 220 cm (87 in.) above the bottom of the heated length, whereas the S-UT-8 vessel collapsed liquid core level depressed to the bottom of the heated length.[5] This difference in phenomena could have been due to one or more of the hardware differences shown in Table 1.

The upper head drain characteristics and downcomer/upper-head bypass flow are considered most influential in explaining the differences between S-UT-6 and S-UT-8. A larger bypass flow path provides better pressure relief from core steam generation and thus less core liquid level depression. A faster upper-head drain for S-UT-8 tends to reduce available vessel inventory early in the transient.

With this historical background, two 5% SBLOCAs, S-LH-1 and S-LH-2, were performed in the Semiscale Mod-2C system in an attempt to duplicate certain thermal-hydraulic phenomena observed in previous Semiscale Mod-2A S-UT series experiments. The Mod-2C system is a better scaled and instrumented system than Mod-2A, and special emphasis was placed on measuring and controlling boundary conditions.

a. In general, 5% SBLOCA's were found to produce the maximum core liquid level depressions for a break spectrum from 2.5% to 10%.[7]

Table 1. Comparison of hardware for S-UT-6 and S-UT-8

Parameters	S-UT-6	S-UT-8
Downcomer/upper-head bypass	4.0%	1.1%
R_{DP}	Unknown	5.6%
Intact loop steam generator inlet piping	10.16 cm (4.0 in.) pipe (pant legs)	6.35 cm (2.5 in.)
Intact loop pump suction piping	7.62 cm (3.0 in.)	6.35 cm (2.5 in.)
Guide tube drain characteristics	No holes below support plate	Eight -0.79 cm (5/16 in.) holes drilled in guide tube below support plate.
Upper head ECC injection tube	Installed	Removed
Bypass standpipe	88.9 cm (35 in.) above core support plate	74.5 cm (29.33 in.) above core support plate
Support columns	Scaled flow allowed between upper head and upper plenum; existing turbine meter functional	Plugged; turbine meter removed; however, instrumentation hole not plugged, causing a more rapid upper-head drain on S-UT-8 than S-UT-6
Downcomer initial differential pressure	50 kPa (7.25 psia)	102 kPa (14.8 psia); new downcomer instrumentation spool piece installed; turbine meter frozen
Accumulator set point pressure	2.86 MPa (414 psia)	4.2 MPa (600 psia)

SYSTEM DESCRIPTION AND EXPERIMENTAL PROCEDURE

System Description

Semiscale Mod-2C is a scaled model representation of a PWR plant, with a fluid volume of about 1/1705 of a PWR (Figure 1). The modified-volume scaling philosophy followed in the design of the Mod-2C system preserves most of the first-order effects thought important for SBLOCA transients. Most notably, the 1:1 elevation scaling of the Semiscale system is an important criterion for preserving the factors influencing signature response to a SBLOCA. The Mod-2C system consists of a pressure vessel with external downcomer and simulated reactor internals; an "intact loop," with a shell and inverted U-tube active steam generator, pressurizer, and pump; and a "broken loop," including an active pump, active steam generator, and associated piping to allow break simulations. The intact loop simulates three "unaffected loops" of a four-loop PWR, and the broken loop simulates an "affected loop" in which the small break is assumed to occur. The break simulates a 5% cold-leg, centerline, communicative break in the loop piping between the pump and vessel. The break is simulated by an orifice that has a scaled area equivalent to a 15.5-cm (6.1 in.) break diameter in a PWR. The unique feature of the Mod-2C system is the installation in the affected loop of a Type III steam generator that includes an external downcomer, allowing use of gamma densitometers to measure riser density. The unaffected loop steam generator consists of six inverted U-tubes, and the affected loop steam generator consists of two inverted U-tubes, both with 2.2-cm (0.86 in.) outer diameter. Vessel internals include a simulated core, consisting of a 5 x 5 array of internally heated electric rods, of which 23 were powered as shown on Figure 2. The rods are geometrically similar to nuclear rods, with a heated length of 3.66 m (12 ft) and an outside diameter of 1.072 cm (0.42 in.).

The vessel upper head simulates a Westinghouse inverted top hat upper head internal package design (see Figure 3) and accounts for about the top 25% of the pressure vessel volume. The Semiscale upper head contains a simulated control rod guide tube and two simulated support columns, with an upper core support plate providing the boundary between the upper head and upper plenum. The guide tube and the two support columns penetrate through the upper core support plate extending into the upper plenum region. The support columns are plugged, allowing draining only through the guide tube and downcomer/upper head bypass line. The downcomer/upper head bypass line simulates leakage between these two components in a commercial PWR, which varies between 0.5% and 4% of total core flow. For S-LH-1, a 0.317-cm (0.125-in.) thick flat plate orifice with a 0.295-cm (0.116-in.) diameter hole was installed in the 1.27-cm (0.5-in.) tubing bypass line. The flat plate orifice allowed a bypass line hydraulic resistance $(R')^a$ of 1.1×10^{10} m^{-4} (20537 $lbf\text{-}s^2/in^2\text{-}ft^3\text{-}lbm$) in either direction, creating an initial condition core bypass flow of 0.9%. For S-LH-2, the orifice was removed, resulting in an initial condition core bypass flow of 3.0%. The hydraulic resistance for this case was 9.9×10^8 m^{-4} (1842 $lbf\text{-}s^2/in^2\text{-}ft^3\text{-}lbm$). Both of these flow rates are thought to be within the range of PWR bypass flow. External heaters were installed in a relatively uniform manner on the vessel and loop piping to offset environmental heat loss. Reference 8 contains a more detailed description of the Mod-2C system.

Conditions in the system were monitored by an extensive network of metal and fluid thermocouples and differential pressure transducers. In the affected steam generator, both tubes were extensively instrumented with both primary and secondary-side fluid thermocouples and several primary-side differential pressure transducers. Average fluid density was measured in the loops and vessel (see Figure 2) with gamma densitometers, while volumetric flow was measured with turbine meters. Condensing systems and catch tanks were included to measure effluent from the steam generator atmospheric dump valves and the break assembly (break flow). The core rod thermocouple distribution is shown in Figure 2.

---

a. Hydraulic resistance (R') is defined as $R' = \Delta P \rho / m^2$, where ΔP is the differential pressure, ρ is the fluid density, and m is the fluid mass flow rate.

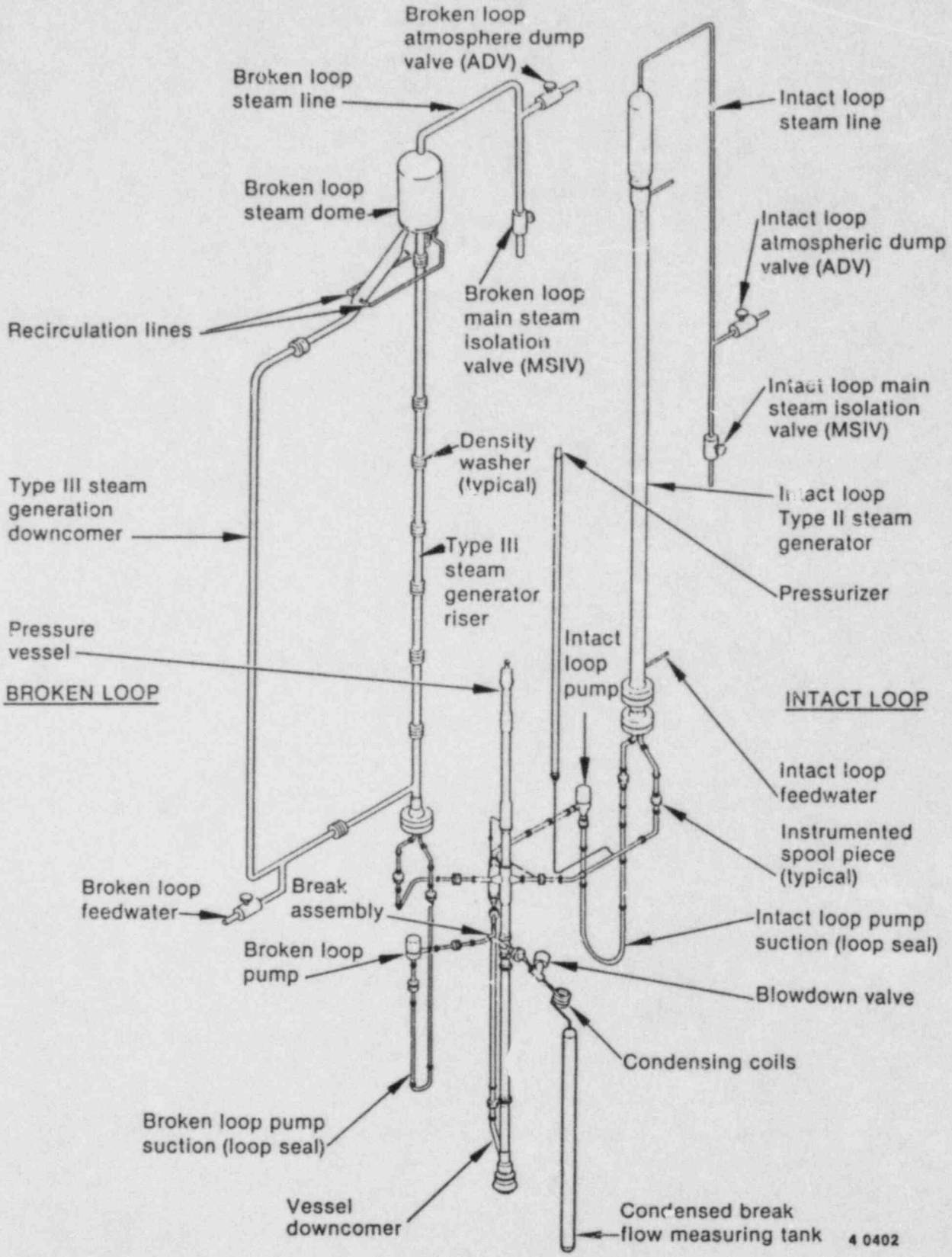

Figure 1. Semiscale Mod-2C system as configured for Experiments S-LH-1 and S-LH-2.

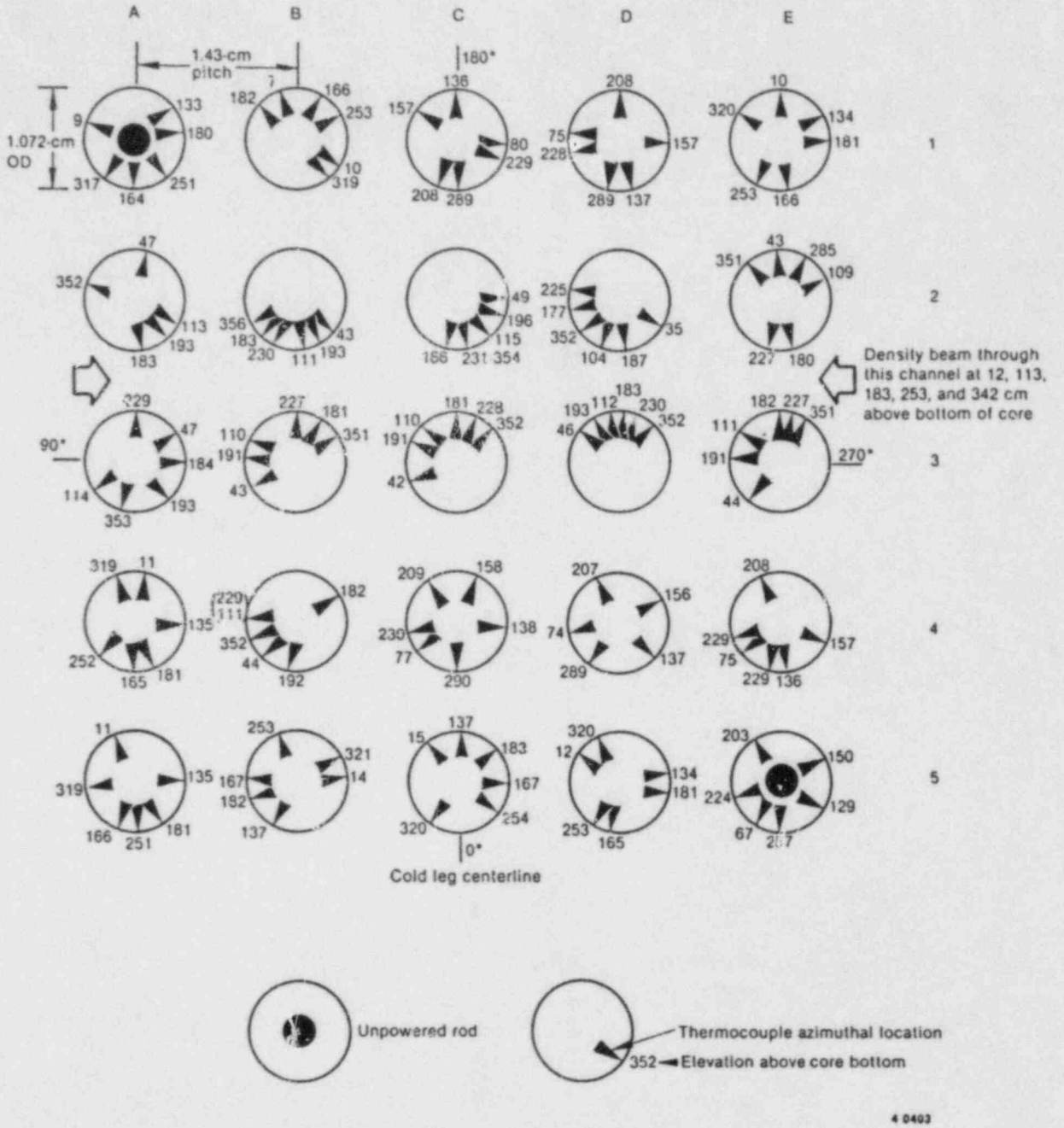

Figure 2. Semiscale Mod-2C core heater rod thermocouple orientation.

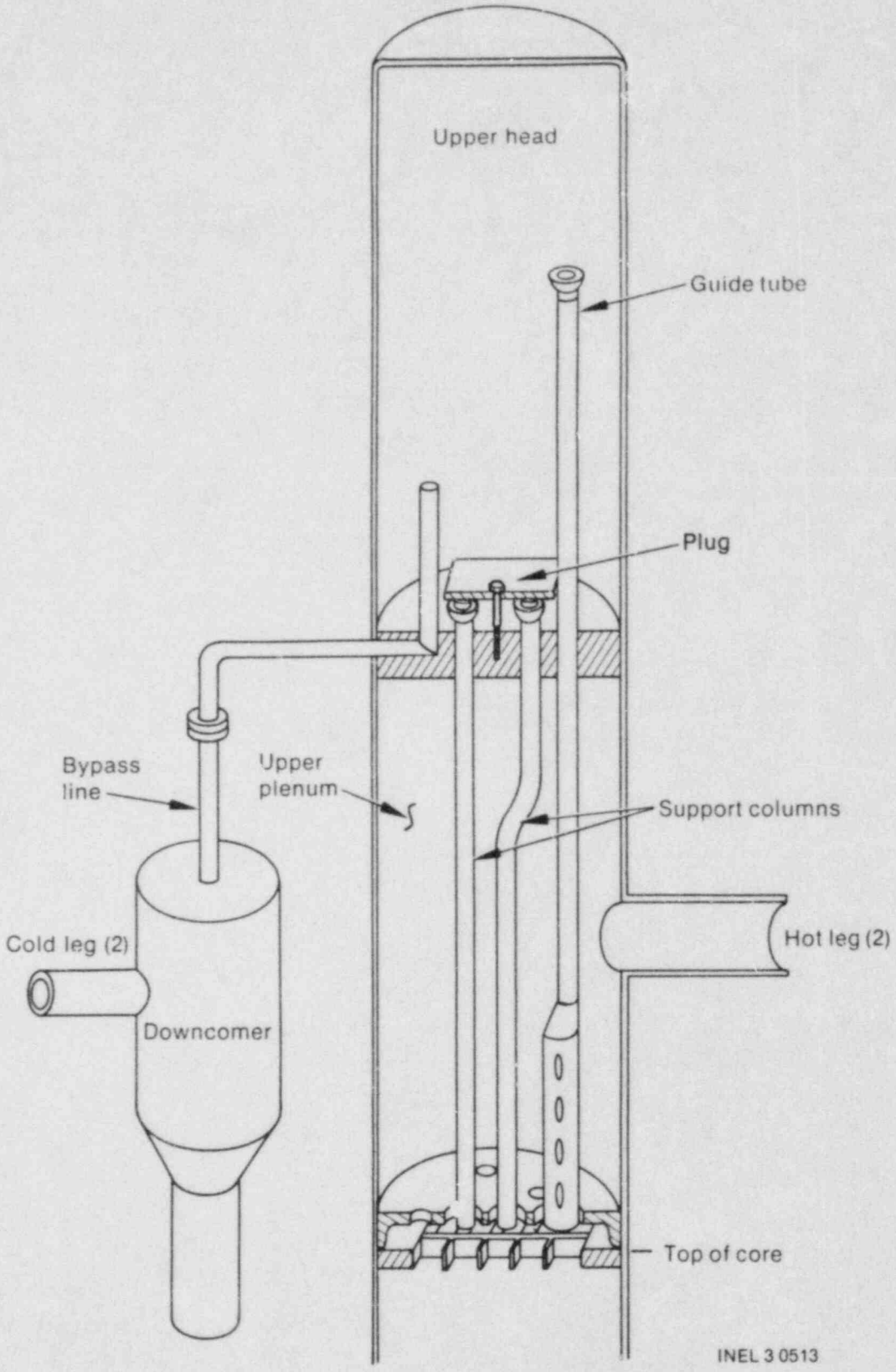

Figure 3. Semiscale Mod-2C vessel upper head configuration for Experiments S-LH-1 and S-LH-2.

Experimental Procedure

As a general procedure before initiation of the transient, the system was filled with demineralized water and vented to ensure a liquid-filled system. The system was heated to initial conditions, using core power and pumped flow, and pressurized, using pressurizer internal heaters to draw a steam bubble. The steam generator secondaries dissipated the core heat to atmosphere by steaming. The Semiscale initial conditions were typical of PWR full-power operation hydraulic conditions in the primary and secondary systems [15.6 MPa (2262 psia) primary pressure and 35 K (67°F) core differential temperature].

The transient was started at 0 s by opening a block valve, allowing primary fluid to flow through the break orifice to the break condensing system. A complete loss of off-site power was assumed; therefore, there were delays on certain automatically occurring events, such as high-pressure injection system (HPIS) flow [a 25-s delay[a] after a low pressurizer pressure trip at 12.6 MPa (1827 psia)]. Other automatically occurring events included core scram to the ANS decay curve (3.4 s after low pressurizer pressure trip to simulate control rod drop time), pump trip (2.0 s after low pressurizer trip), feedwater termination (0.0 s after low pressurizer pressure trip), main steam isolation valve (MSIV) closure (3.4 s after the low pressurizer pressure trip), and, finally, accumulator injection at 4.24 MPa (600 psia) primary pressure. No auxiliary feedwater was assumed available.

---

a. A 25-s delay is the time assumed to start the diesel generators that power the HPIS pumps.

EXPERIMENTAL RESULTS

This section presents an interpretive description of important thermal-hydraulic phenomena associated with Semiscale 5% SBLOCA Experiments S-LH-1 and S-LH-2. The discussion is aimed toward aiding code development and assessment efforts and concentrates on phenomena of particular challenge to code application. Most of this section refers to S-LH-1 data (the 0.9% core bypass flow case); therefore, unless otherwise specified, S-LH-1 results are presented. Following an overview of the gross system response to a 5% SBLOCA, the pressure signature response is discussed, along with major causal events that perturbed pressure response. Next, the fluid mass distribution throughout the transient is characterized. (Correct code calculation of the fluid mass distribution is mandatory to correctly calculating the major events.) Included in the discussion on fluid mass distribution is the drain behavior of the pressurizer, steam generator U-tubes, vessel upper head, and pump suctions, as well as a description of two prominent vessel fluid mass depletions associated with the blowdown. The core thermal response associated with the overall transient and the two prominent vessel liquid level depressions are then discussed. Finally, by comparing S-LH-1 and S-LH-2 results, the effect of core bypass flow on transient severity and overall transient response is examined.

Overview of a 5% SBLOCA (S-LH-1)

Preliminary to the detailed discussion of S-LH-1 and S-LH-2 results, this section presents a qualitative overview of the gross system response to a 5% SBLOCA, with special emphasis on major events that affect fluid mass inventory and thus transient severity. System response during a SBLOCA is characterized as a primary depressurization with significant loss of primary fluid mass inventory, as shown on Figure 4. The primary fluid mass inventory is controlled by the fluid mass balance formed by flow out the break and flow into the system from emergency core cooling systems (HPIS and accumulator flow). Figure 4 shows a continuous loss of primary fluid mass until after accumulator injection is initiated at about 504 s, shortly after which injection rate exceeds break flow. The relatively rapid loss of fluid mass inventory until

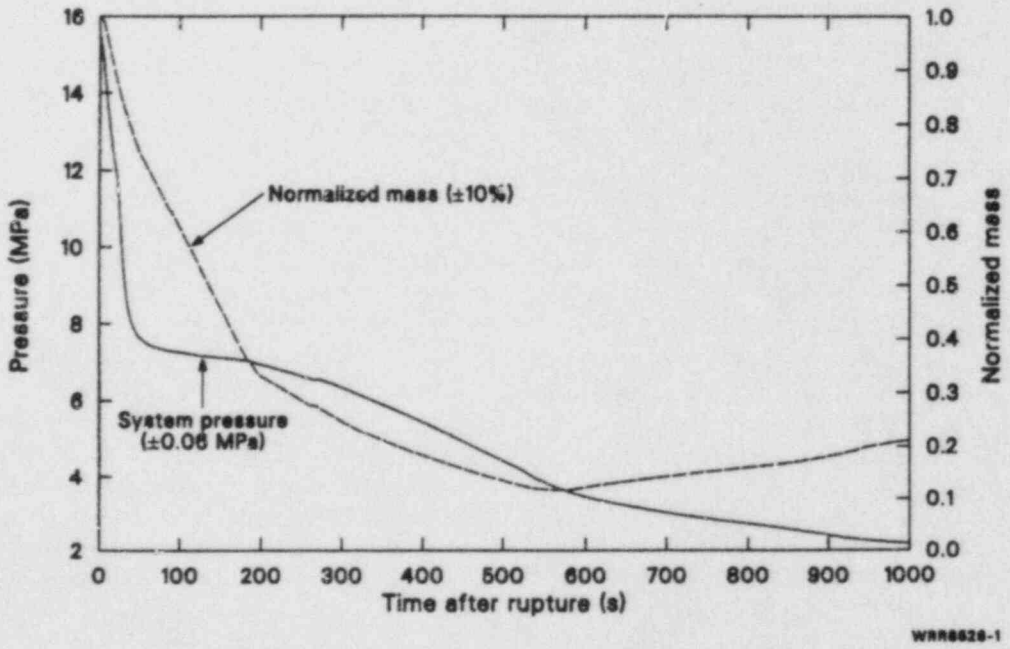

Figure 4. Primary system pressure and normalized primary fluid mass inventory during 5% SBLOCA Experiment S-LH-1.

accumulator injection is due to HPIS flow being smaller than break flow [an average of 0.004 kg/s (0.0088 lbm/s) for HPIS flow vs. a 0.6-kg/s (1.32 lbm/s) break flow]. Thus, at the time of accumulator injection, system fluid mass inventory was only about 10% of the initial inventory and was located primarily in the vessel downcomer and lower vessel. (A detailed description of the fluid mass inventory distribution will be presented later.)

The primary fluid mass inventory reduction (Figure 4) was relatively rapid until about 175 s, at which time a dramatic change in break flow caused an even more dramatic change in the rate of primary fluid mass inventory decrease. The break flow was affected by clearing of the intact loop pump suctions and a resulting stratification of fluid near the break. With a centerline break and the pipe full of liquid, the mass flow rate is maximized; however, when the intact loop suction cleared, the ongoing supply of liquid to the break diminished, resulting in a stratification of fluid near the break and a change from mostly liquid flow (high mass flow rate) to mostly steam flow (low mass flow rate). Once initiated, the accumulator fluid mass flow was greater than break mass flow, thus increasing the mass inventory in the system. Although low pressure injection (LPIS) was not used during S-LH-1, the experiment was terminated at 1000 s with an increasing primary fluid mass inventory and the primary pressure near the LPIS pressure set point [normally about 1.38 MPa (200 psia)].

Examining fluid mass inventory alone is misleading in judging transient severity. For instance, core rod heat-ups occurred for a wide range of overall mass inventories starting at about 35%; however, once accumulator injection was initiated, the core remained cool with mass inventory as low as 15%. The fluid mass distribution in the system (particularly the vessel), rather than overall mass inventory, determines the core thermal response to the accident. The transient mass distribution in the system is a major topic in this report. The next section discusses in detail the major inflection points in the primary pressure shown on Figure 4 and relates these inflection points to thermal-hydraulic events in the system.

Pressure Response

Understanding the primary pressure response during a SBLOCA is important, because emergency core cooling systems are controlled by the primary pressure. Basically, the pressure response is controlled by an overall energy balance involving break flow, heat loss, core power, safety injection into the system, primary-to-secondary heat transfer, and the thermodynamic state of the loop fluid (flashing). There are several characteristic inflection points in the system pressure response to a 5% SBLOCA. Since both of the subject experiments had similar signature pressure response, this discussion refers to S-LH-1 data only.

The transient was initiated at 0 s [system pressure 15.5 MPa (2248 psia)] by opening a block valve downstream of the break assembly, causing a flow of subcooled primary flow out the break. This initiated a rapid depressurization (see Figure 5) due to the steam bubble in the pressurizer expanding as fluid mass exited the system. When the primary pressure reached 12.6 MPa (1837 psia), several automatically occurring events transpired that greatly increased the primary depressurization rate, most importantly core scram and MSIV closure. Core scram reduced heat input to the fluid, while the secondary remained a heat sink relative to the primary even though the MSIVs in both loops were closed. The increased depressurization rate was due to a general shrinkage of primary fluid as the fluid density increased. Closing the MSIVs caused a pressurization of both loop secondaries (see Figure 6); however, the relief valve set point [7.22 MPa (1047 psia)] was not achieved in either loop secondary.

The next major inflection point in primary pressure was caused by achieving saturation conditions throughout the loop at about 40 s accompanied by flashing, which greatly retarded the depressurization rate. Figure 7 shows the vessel, hot leg, and cold leg fluid temperatures compared to saturation temperature. The vessel fluid (Figure 7a) was the first to reach saturation conditions, at about 5 s, followed by the hot leg (Figure 7b) at 9 s. By 40 to 45 s, the cold leg fluid (Figure 7c) was also saturated. At this time, break flow (Figure 8) decreased as the break flow out the cold leg changed from single-phase subcooled flow to two-phase saturated flow. Following attainment of saturation conditions, a relatively slow depressurization occurred as the effect of flashing throughout the system countered the energy lost in break flow. As noted previously, HPIS flow was insignificant when compared to break flow and is a trivial component of the overall energy balance controlling depressurization.

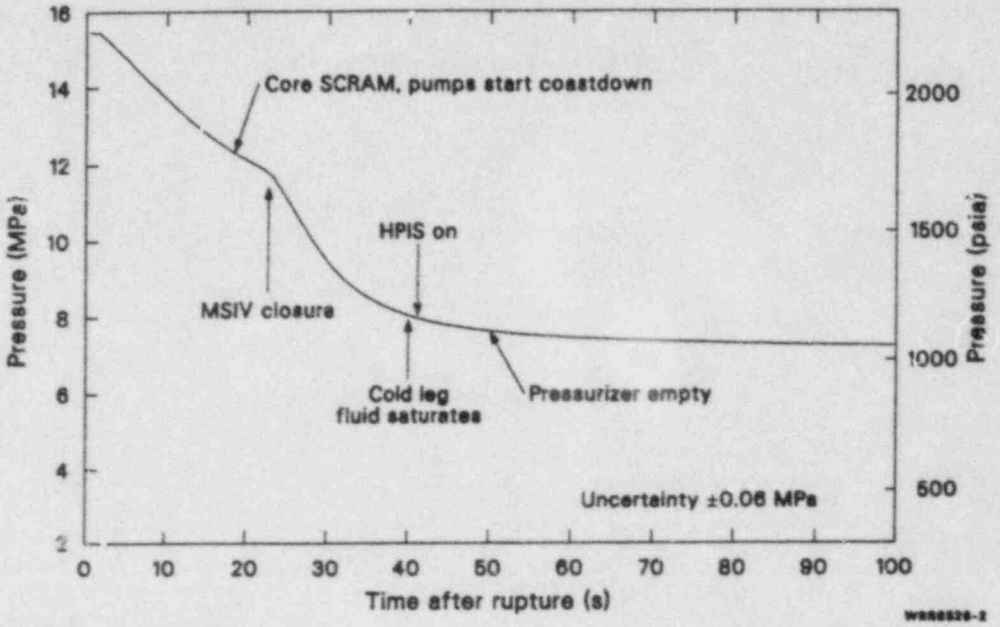

Figure 5. Primary system pressure response during 5% SBLOCA Experiment S-LH-1.

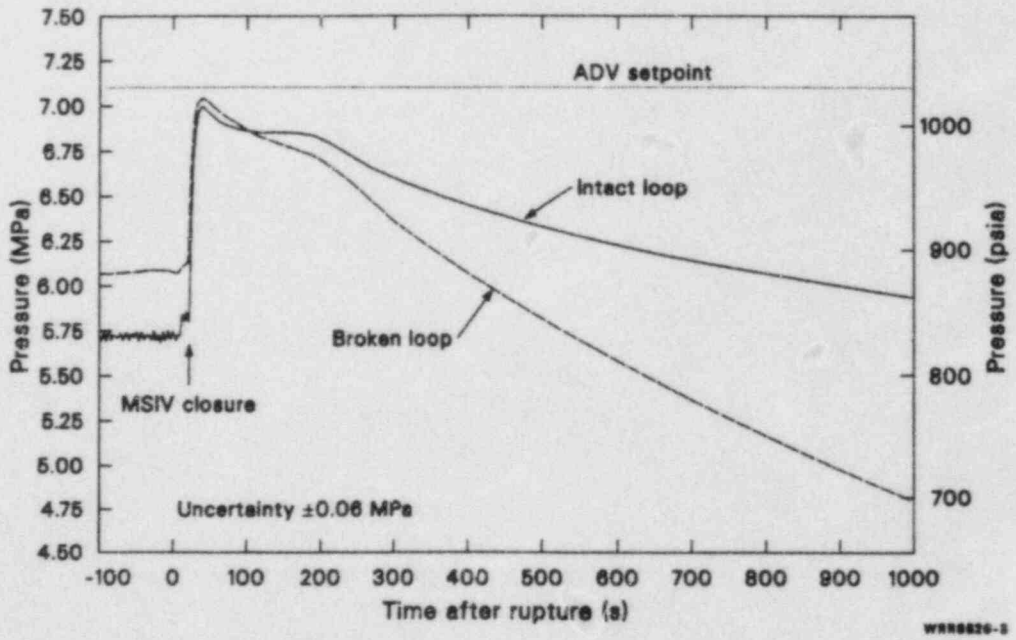

Figure 6. Secondary system pressure response during 5% SBLOCA Experiment S-LH-1.

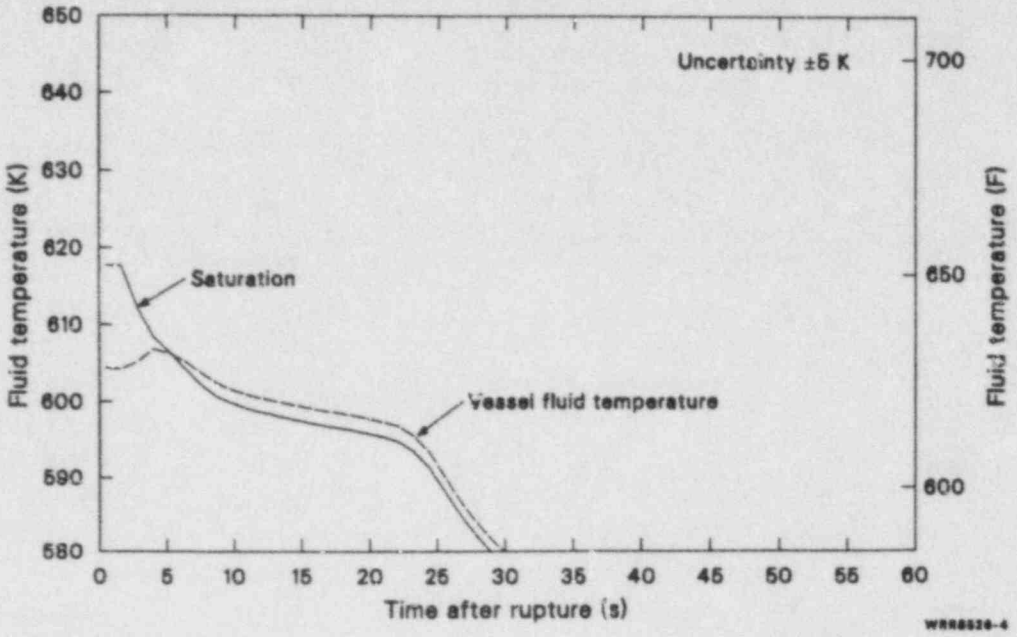

Figure 7a. Saturation temperature and fluid temperature in the vessel upper plenum during a 5% SBLOCA.

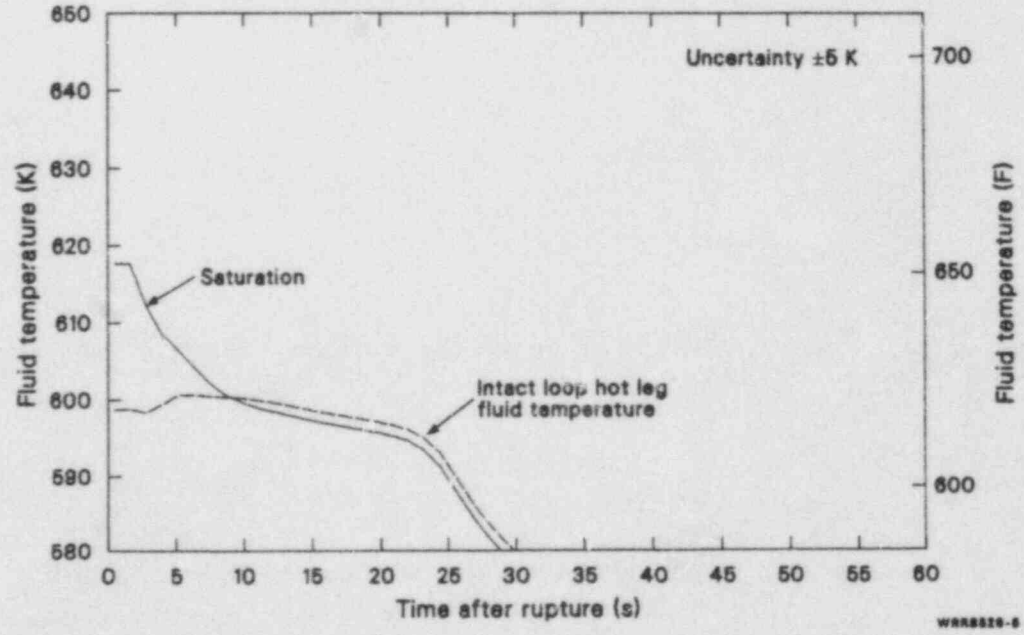

Figure 7b. Saturation temperature and fluid temperature in the intact loop hot leg during a 5% SBLOCA.

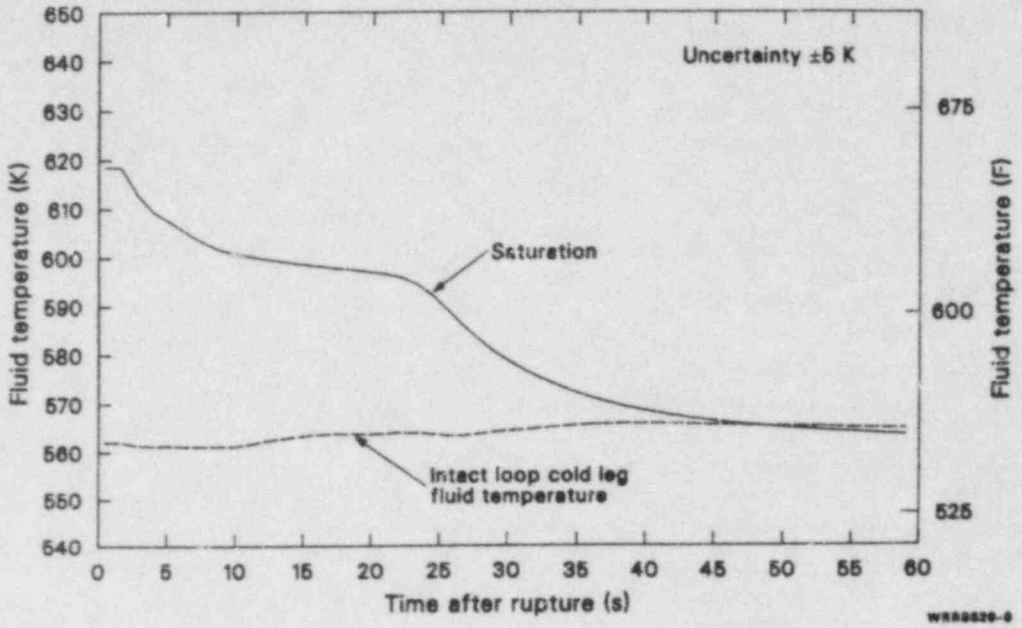

Figure 7c. Saturation temperature and fluid temperature in the intact loop cold leg during a 5% SBLOCA.

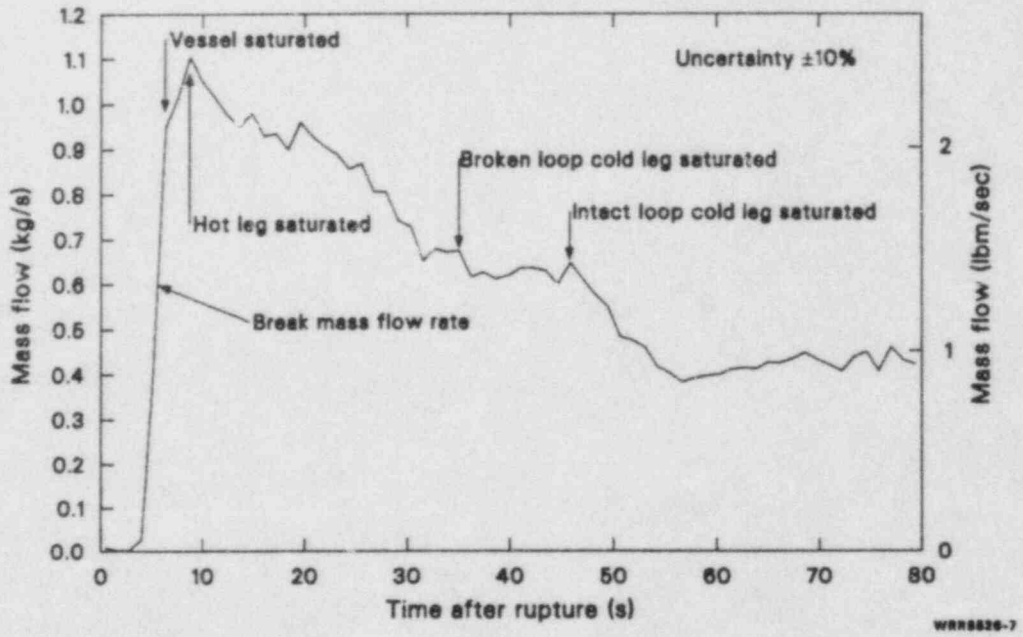

Figure 8. Break mass flow rate during a 5% SBLOCA.

On an extended time basis, other automatically occurring events and phenomena also had a large impact on depressurization rate, as shown on Figure 9. Clearing of both the intact and broken loop pump suction seals tended to increase the depressurization rate. (Seal clearing is related to break uncovery of liquid, which will be discussed in detail in a following section.) Briefly, as long as a pump suction fluid seal exists, a fluid plug extends throughout the cold leg to the break, thus supplying a two-phase fluid mixture to the break and precluding steam venting through the loop. As a seal clears, steam is allowed to reach the break, causing an increase in volumetric flow and a decrease in fluid mass flow. With increased volumetric flow out the break, the depressurization rate is increased. Once accumulator injection starts, there is a net increase in liquid mass in the system, causing reflood of the hot core accompanied by steam generation. This steam generation tends to offset the flow of steam out the break, causing a reduction in the depressurization rate. By the time the experiment was terminated at 1000 s, the primary pressure was decreasing, the core liquid inventory was gradually increasing, and the core was cooled.

System Fluid Mass Distribution

The system fluid mass distribution during blowdown can be characterized by five distinct time periods. These periods are distinguishable according to the amount of fluid mass in the system, fluid thermodynamic conditions, pump operation, and mode of natural circulation. The first period covers the rapid drain of the pressurizer as the break mass flow is maximized by the presence of subcooled fluid upstream of the break. The drain of the vessel upper head starts during this period, and the pressurizer drain characteristics are compared and contrasted to the upper head drain. The second period covers the time when fluid throughout the loop becomes saturated until the pumps are coasted down to zero speed. Much of the fluid mass distribution information throughout the loop is highly uncertain during this period, because of the forced flow effects on differential pressure cells which are the principal liquid level measurement devices. A third unique period begins when the pumps have coasted down to zero speed and ends when the core decay heat rejection mode is two-phase natural circulation. This is a period characterized by differential draining of fluid in the steam generator primary U-tubes and establishment of a reflux mode of core decay heat rejection. A fourth period is distinguished by establishment of a complicated transient manometric balance of loop fluids. During this period, steam created in the core is bound by the liquid plugs in the pump suctions and in the downcomer and lower vessel. As more steam is created, the manometric balance is perturbed, accompanied by a core liquid level depression and pump

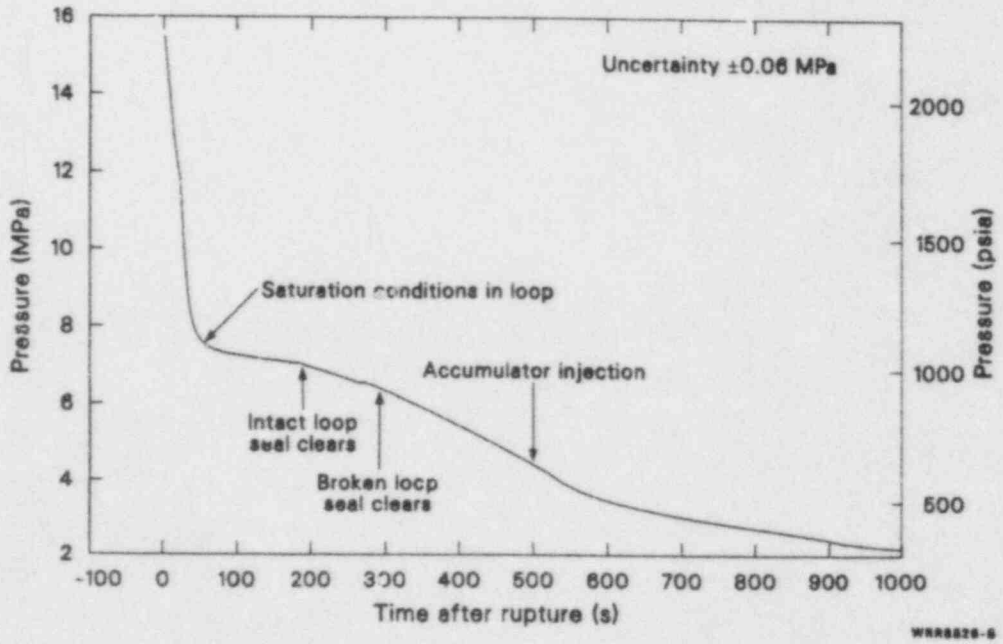

Figure 9. Overall primary system pressure response during 5% SBLOCA Experiment S-LH-1.

suction clearing of the liquid plugs. Once the liquid plugs have cleared from the pump suctions, steam vents directly to the break; and the fifth period is characterized as a long term boil-off of vessel fluid. During this period, the critical issue is the rate of core boil-off versus the depressurization rate until the accumulator pressure set points are reached. Once the accumulators inject, the core heat-ups are mitigated.

The discussion of system fluid mass distribution is presented chronologically according to the five periods. Since break flow is affected by system fluid mass distribution, the influence of upstream thermal-hydraulic events on break flow during these periods is also discussed.

Period 1—Upper Head/Pressurizer Drain (0 to 40 s). Upon blowdown initiation, the first components in the loop to begin draining were the pressurizer and vessel upper head. However, the draining occurred in a differential manner (Figure 10); i.e., the pressurizer drained completely before the upper head fluid began to drain. During the first 20 s, the break flow averaged about 0.75 kg/s (1.65 lbm/s) (Figure 8); and the pressurizer drain rate was about 0.594 kg/s (1.31 lbm/s). Therefore, about 80% of the break flow was accounted for by the pressurizer drain, even though the hydraulic resistance between the vessel upper head and the rest of the system is less than the pressurizer surge line. In fact, the pressurizer surge line resistance is an order of magnitude higher than the combined parallel resistance of the two upper head drainage outlets, the guide tube [about 330 cm (130 in.) above the cold leg (Figure 3)] and bypass line [about 230 cm (91 in.) above the cold leg].[a]

A probable explanation for the sequential drainage between pressurizer and upper head is the immediate flashing of fluid everywhere in the pressurizer after blowdown initiation, causing liquid to be pushed out of the pressurizer by the expanding steam bubble. (Figure 11 shows saturation or superheated conditions in the pressurizer from 0 s until empty.) The vessel upper head fluid remained subcooled during the pressurizer drain period (Figure 12), and no flashing occurred in the upper head prior to the pressurizer emptying.

a. Hydraulic resistance of the guide tube is 1.76×10^8 m^{-4} (327 lbf-s^2/in^2-ft^3lbm); the hydraulic resistance of the bypass line is 1.1×10^{10} m^{-4} (20537 lbf-s^2/in^2-ft^3-lbm); and the hydraulic resistance of the surge line is 1.63×10^9 m^{-4} (3032 lbf-s^2/in^2-ft^3-lbm).

The sudden jump in temperature in the vessel upper head fluid shown in Figure 12 appears to be due to voiding of the vessel upper head to the level of the fluid thermocouple [402 cm (158 in.) above the cold leg]. Following attainment of saturation conditions in the upper head at about 65 s, flashing in the top of the upper head aided in pushing fluid out the bypass line. There was probably very little draining from the upper head through the guide tube, since vapor generated in the core would be passing up through that channel. At about 240 s, the upper head liquid drained to the level of the top of the bypass line, which is about 74 cm (29 in.) above the upper core support plate. This 74 cm (29 in.) of liquid remained trapped in the upper head for the remainder of the experiment.

The difference between upper head and pressurizer drain rate is due to flashing in the loop, which caused a lower break mass flow rate, as shown in Figure 13. The pressurizer drained more rapidly, since it was contributing fluid to the loops during a period of higher break mass flow rate. Primary depressurization was slower during the period of the upper head drain, and the fluid mass flow rate through the break was greatly reduced (Figure 13). With break mass flow rate reduced, the drain rate of the upper head fluid was also reduced compared to the drain rate of the pressurizer.

The following discussion on upper head drain spans several distinct time periods, including the manometric balance period. In a later section, it will be shown that the amount of fluid in the upper head figures into the overall head balance during the manometric balance period; however, in general, upper head drain did not greatly perturb other system response for S-LH-1.[a] Upper head drain did have an interesting effect on system response when the upper head fluid level dropped to the level of the bypass line. Clearing the bypass line of fluid had a temporary but dramatic impact on break flow, as shown in Figure 14. Clearing the top of the bypass line of fluid at about 240 s provided an additional path to the break for steam flow from the core. Allowing for bypass line clearing time and steam transient time to the break, the sudden interruption in break mass flow seen on Figure 14 at

a. A later section will contrast upper head drain characteristics for S-LH-1, with 0.9% core bypass flow, and S-LH-2, with 3.0% core bypass flow.

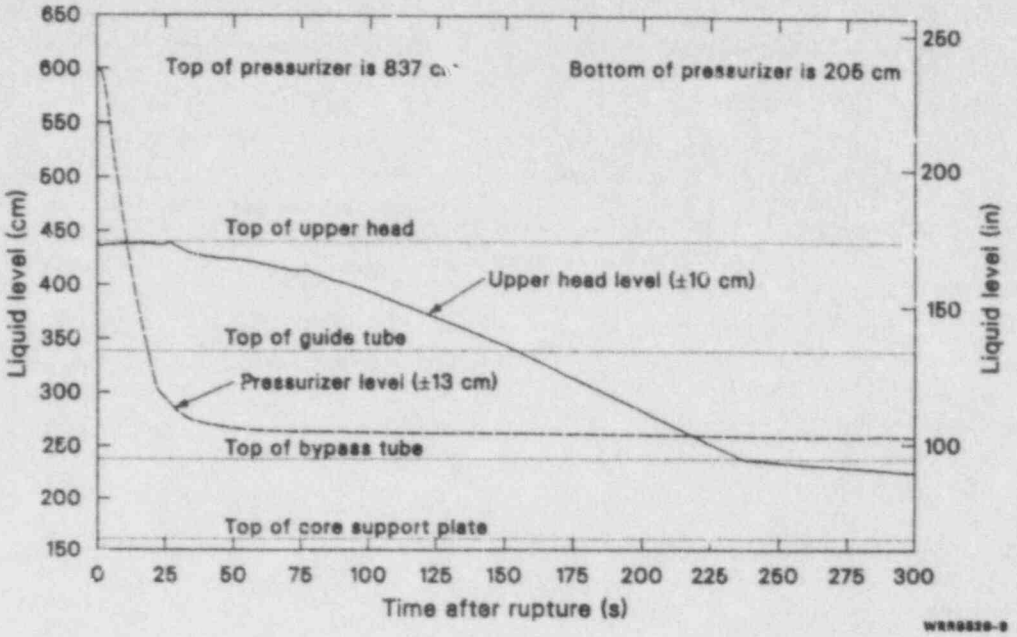

Figure 10. Comparison of upper head and pressurizer liquid level during 5% SBLOCA Experiment S-LH-1.

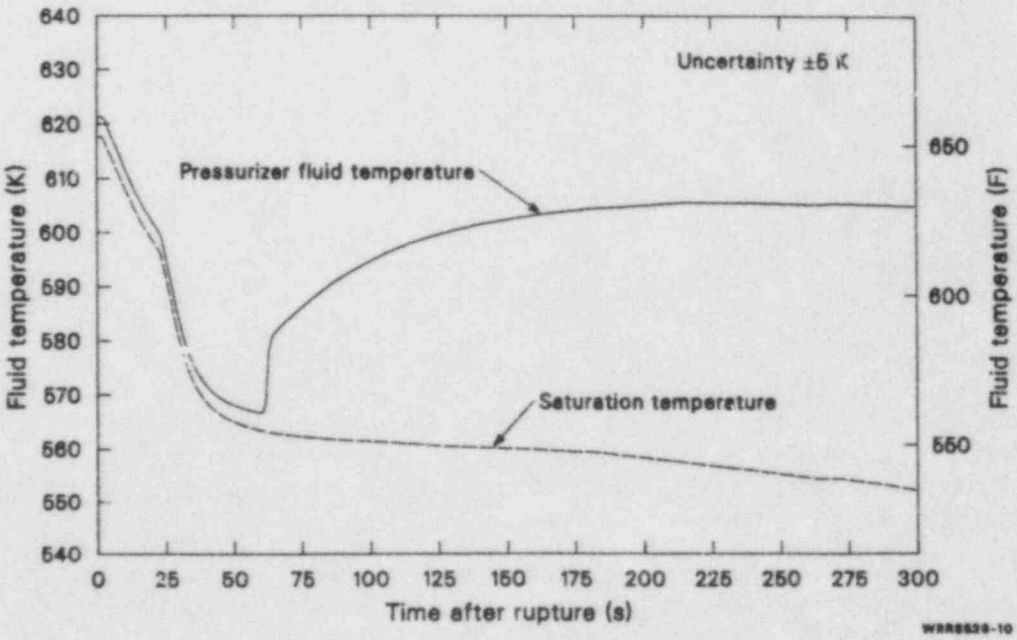

Figure 11. Comparison of saturation temperature and pressurizer fluid temperature during 5% SBLOCA Experiment S-LH-1.

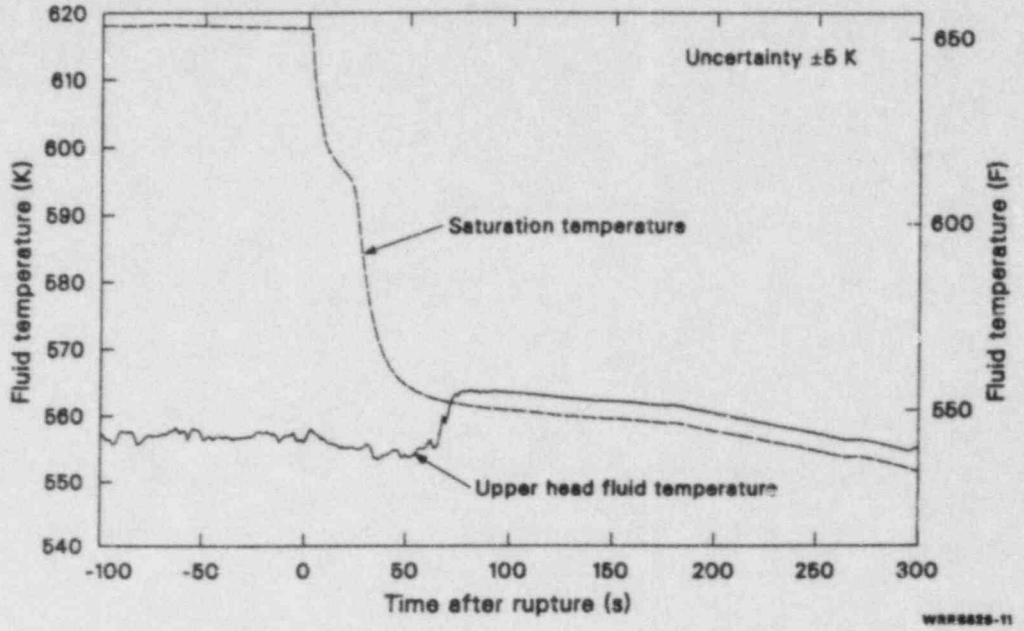

Figure 12. Comparison of upper head fluid temperature and saturation temperature during 5% SBLOCA Experiment S-LH-1.

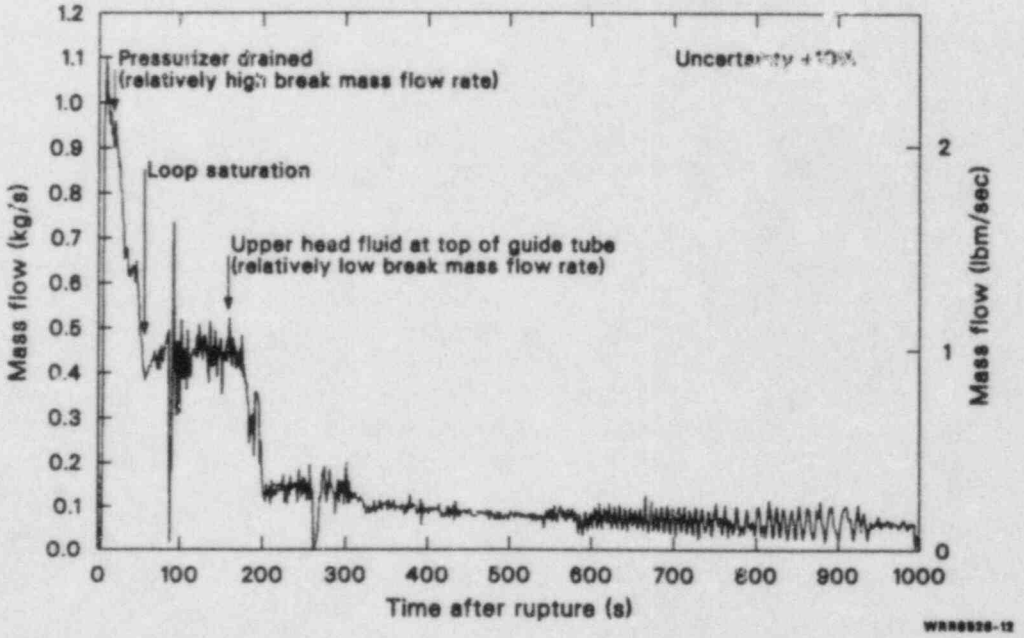

Figure 13. Break mass flow rate during upper head drain for 5% SBLOCA Experiment S-LH-1.

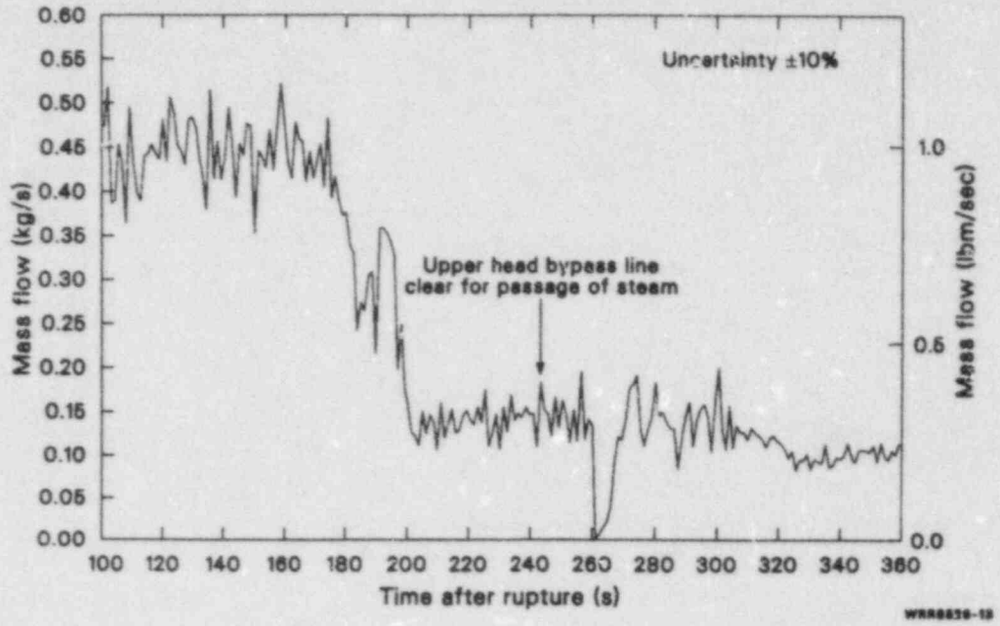

Figure 14. Break mass flow rate during the manometric depression period of 5% SBLOCA Experiment S-LH-1.

about 260 s corresponds to opening of the bypass line to steam flow at about 240 s. As shown in Figure 15, the sudden introduction of steam at the break caused an interruption in fluid mass flow, as the flow changed from a mostly two-phase mixture to single-phase steam upstream of the break toward the vessel.

Period 2—Pump Coastdown (40 to 90 s). Following the drain of the pressurizer at about 40 s and simultaneous attainment of saturation fluid conditions for most positions in the loop, a relatively slow depressurization period with a much reduced break flow was observed (Figure 13). During this period, the upper head continued to drain (Figure 10); however, most of the fluid mass lost from the system came from other loop components, most notably the vessel. Flashing occurred throughout the system during this period; therefore, the general fluid condition throughout the loop was a two-phase mixture, with the pressurizer steam-filled and the pumps coasting down, as shown in Figure 16, with coastdown complete at 90 s.

Figure 17 shows the fluid density of loop components throughout the hot and cold leg piping and the vessel upper head and lower vessel. The vessel upper head fluid density throughout this period is a fairly homogeneous liquid (not stratified), as shown in Figure 17a. The lower vessel develops a definite stratification of a two-phase mixture, with the collection of steam bubbles greater for upper regions (Figure 17b). Once the pump goes into final coastdown at 80 s (see Figure 16), the stratification of fluid in the lower vessel intensifies due to a decrease in flow.[a] Figure 17c shows the intact loop hot leg fluid to be a fairly homogeneous two-phase mixture with density similar to the top of the core; however, the broken loop density (Figure 17d) shows a definite hot leg fluid stratification. The difference in stratification between intact and broken loop hot legs is not related to the pipe size [area = 0.0035 m^2 (0.0376 ft^2) for the intact loop and area = 0.0009 m^2 (0.0097 ft^2) for the broken loop]. An approximate 3-to-1 flow split in the hot legs (see Figure 18) gives an average loop-to-loop fluid velocity ratio of about 0.77, which is too small a difference to cause the stratification seen on Figure 17c and 17d. The fluid in the intact and broken loop cold legs remains mostly single-phase liquid throughout the time period, mainly due to (a) subcooled conditions existing in the cold leg prior to 45 s, and (b) continued primary-to-secondary heat transfer with forced circulation from the pump operation. Following attainment of saturation

a. A change in forced circulation to natural circulation causes a collection of bubbles to form in upper regions of the core, because the bubble rise velocity is closer to the natural circulation flow rate than is the case for the forced flow rate.

fluid conditions in the cold leg at about 45 s (Figure 17c), the intact and broken loop cold legs show a developing stratification of fluid density, with lower densities at the top beam at 47 s for the broken loop cold leg (Figure 17d) and 68 s for the intact loop cold leg (Figure 17c).

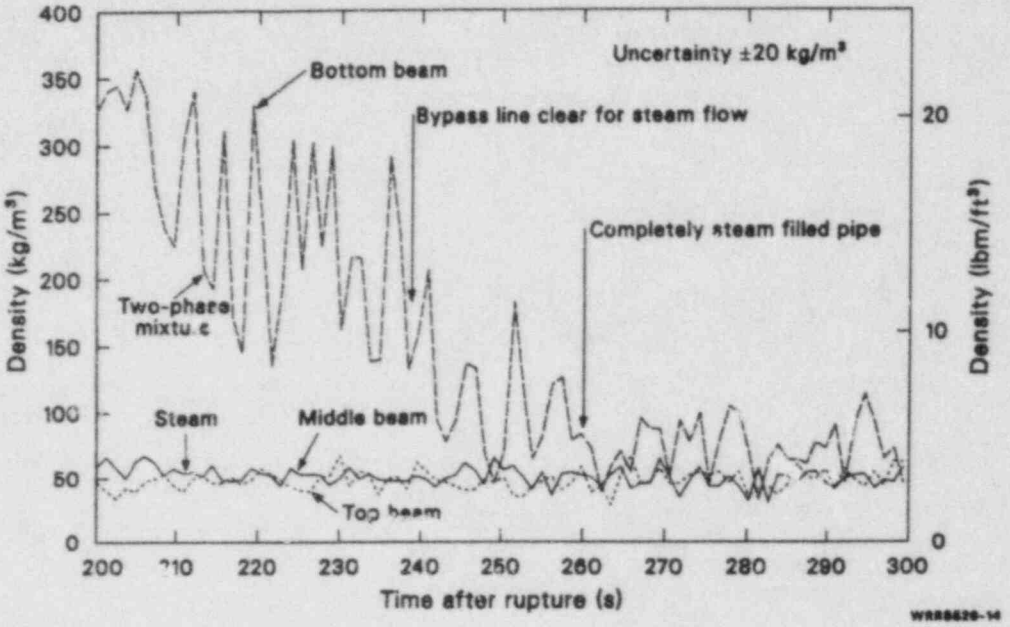

Figure 15. Broken loop cold leg fluid density during 5% SBLOCA Experiment S-LH-1.

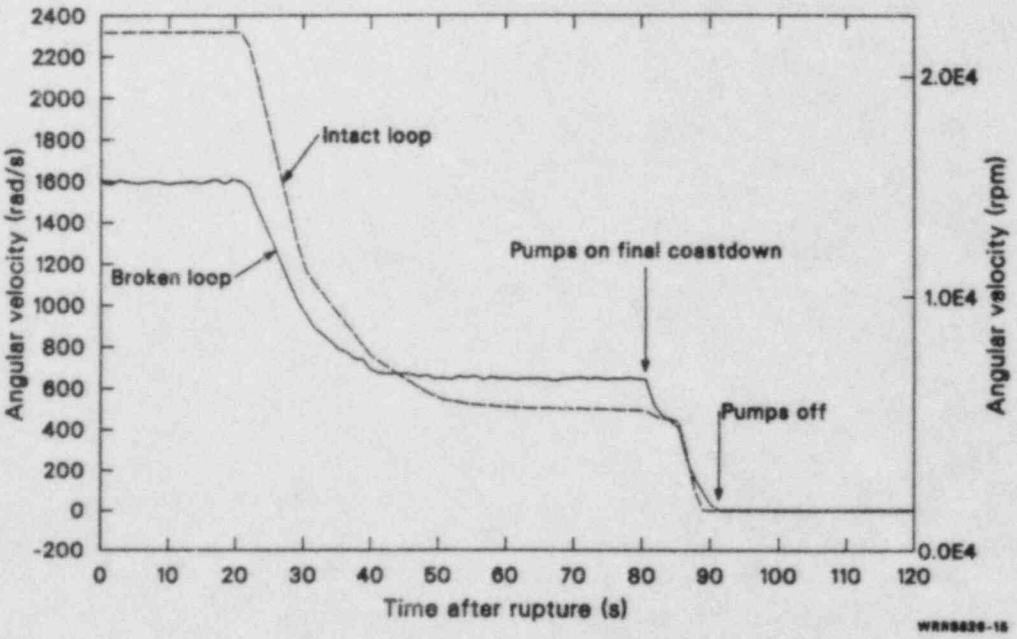

Figure 16. Pump speed in the intact and broken loops during 5% SBLOCA Experiment S-LH-1.

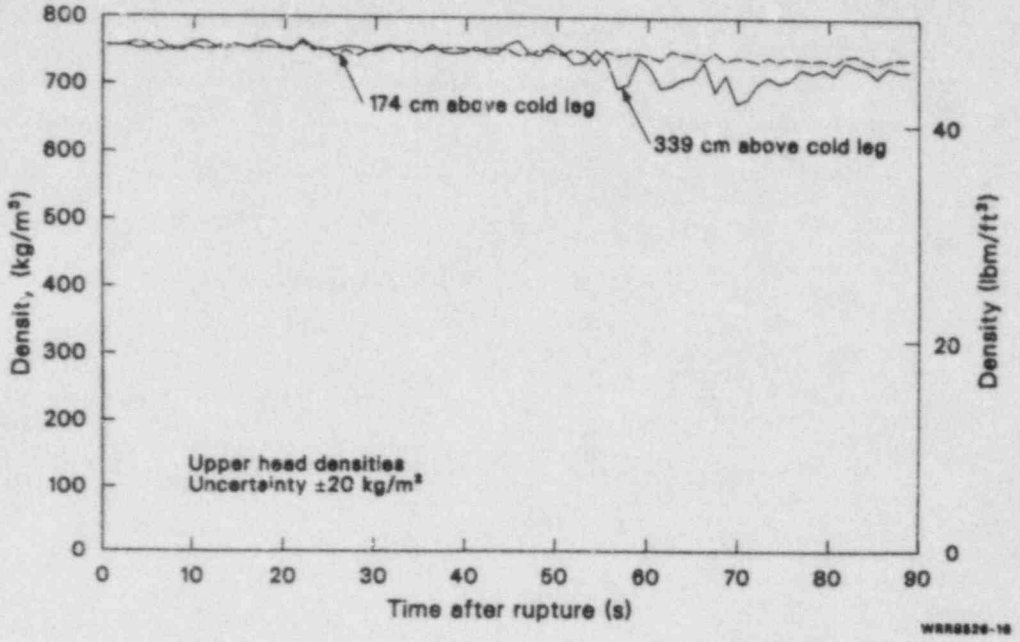

Figure 17a. System fluid density map for the vessel upper head during 5% SBLOCA Experiment S-LH-1.

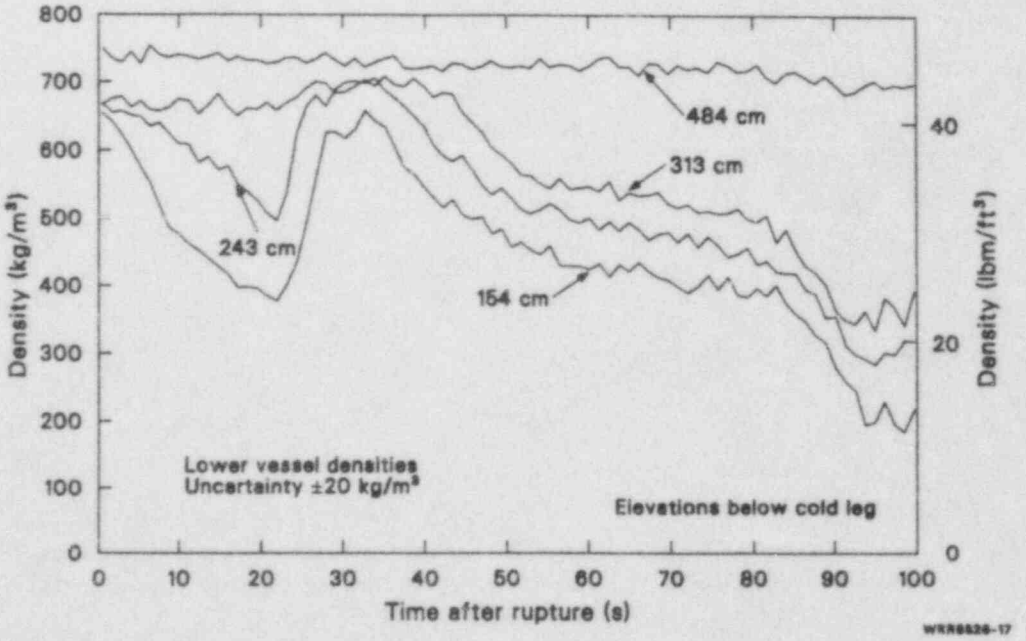

Figure 17b. System fluid density map for the lower vessel during 5% SBLOCA Experiment S-LH-1.

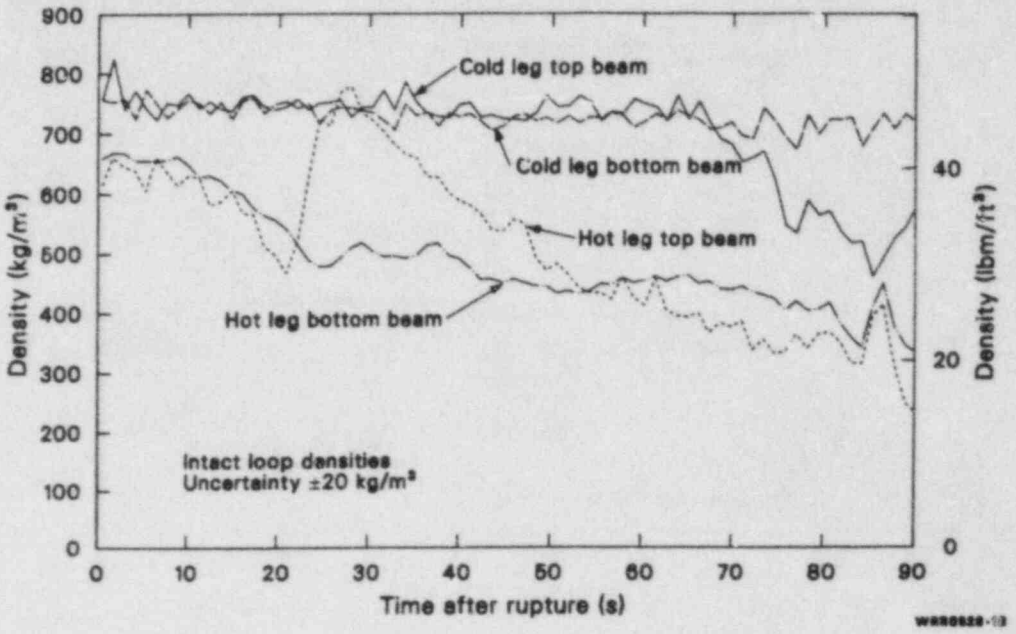

Figure 17c. System fluid density map for the intact loop during 5% SBLOCA Experiment S-LH-1.

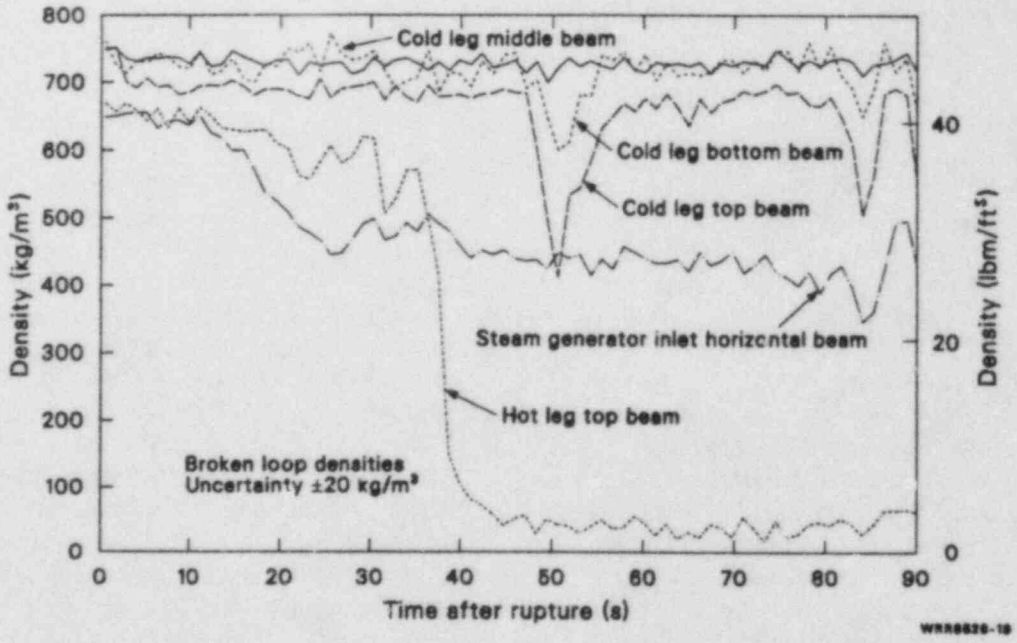

Figure 17d. System fluid density map for the broken loop during 5% SBLOCA Experiment S-LH-1.

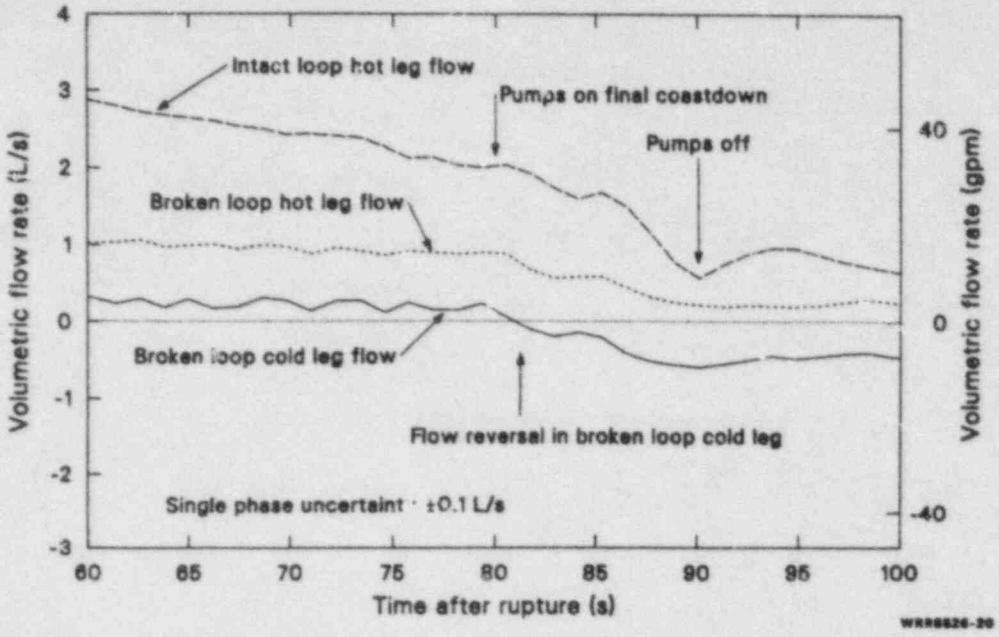

Figure 18. Loop volumetric flows during 5% SBLOCA Experiment S-LH-1.

Vessel fluid depletion was greater than for other components during this pump coastdown period. After the effects of the pump diminish, the vessel and intact and broken loop steam generator primary tube collapsed liquid level measurements show the vessel level to be about 60 cm (24 in.) below the top of the core, while the steam generator tubes are 500 to 600 cm (197 to 236 in.) above the tube sheet which is essentially full of a two-phase mixture (Figures 19 and 20, respectively). The vessel fluid was depleted to make up the break flow during this period in the following way. The flow split of fluid for the intact and broken loop hot leg remained approximately 1-to-3 for most of the period (see Figure 18), even though mass was diverted from the broken loop to the break. Therefore, the amount of flow entering the vessel from the broken loop cold leg was less than that leaving via the broken loop hot leg, resulting in a reduction in vessel fluid mass inventory. Prior to the end of pump coastdown at 90 s, the flow direction to the break was only via the broken loop hot leg/steam generator/pump suction; however, a flow reversal in the broken loop cold leg occurred after coastdown at about 82 s (see Figure 18). Therefore, after 82 s, break flow was fed from the inlet annulus as well as from the hot leg (Figure 18).

The effect of pump operation on the calculated collapsed liquid levels is quite prominent in both the vessel and steam generator primary U-tubes and is shown clearly on Figures 19 and 20. Between 80 and 90 s when the pumps are on final coastdown, the vessel level drops about 130 cm (51 in.); and the primary U-tube liquid levels change the same amount. Therefore, using the differential pressure cells from Semiscale data to estimate the collapsed liquid levels during pump operation appears to generate an error of 80 to 130 cm (32 to 51 in.) at about 20% of initial pump speed. Only after the pumped flow is zero can the differential pressure cells be used with confidence as a measurement of collapsed levels throughout the system.

A momentary interruption in break flow occurred at about 86 s (see Figure 21) that is attributed to the effects of the final pump coastdown to zero speed. Prior to coastdown, all the flow in the broken loop cold leg was either into the vessel or to the break (positive flow). Figure 18 shows that the broken loop cold leg flow stagnates, then reverses direction as the pumps are on final coastdown. This momentary flow stagnation partially voided the liquid density in the piping toward the vessel from the break and caused a filling of the piping toward the pump from the break. For the brief time period from 86 to 90 s, the break flow was therefore mostly steam, which had a trivial fluid mass flow compared to the two-phase mixture going out the break during pump operation.

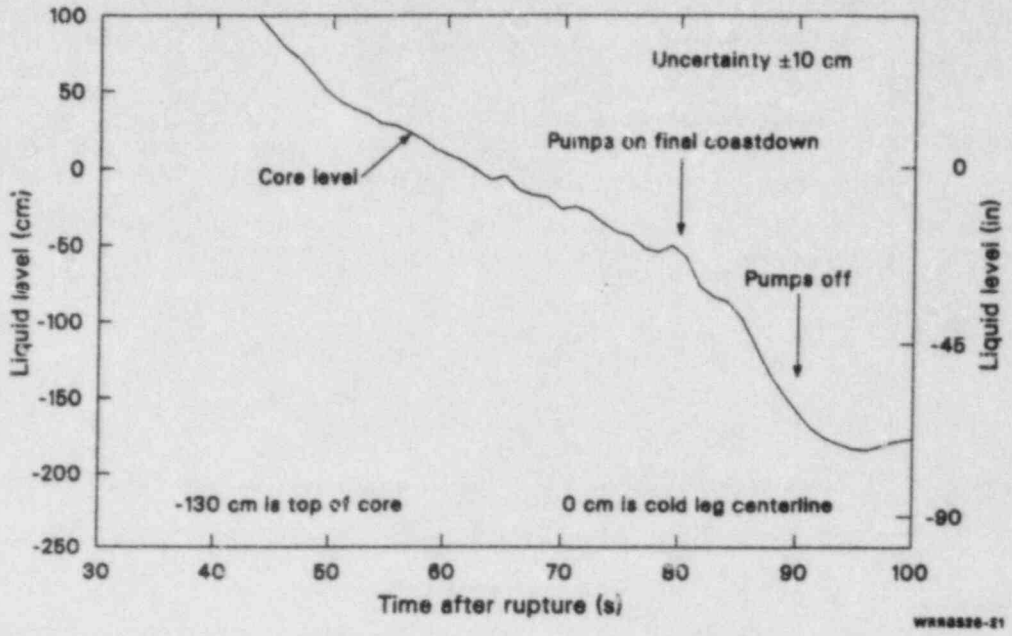

Figure 19. Vessel liquid level during 5% SBLOCA Experiment S-LH-1.

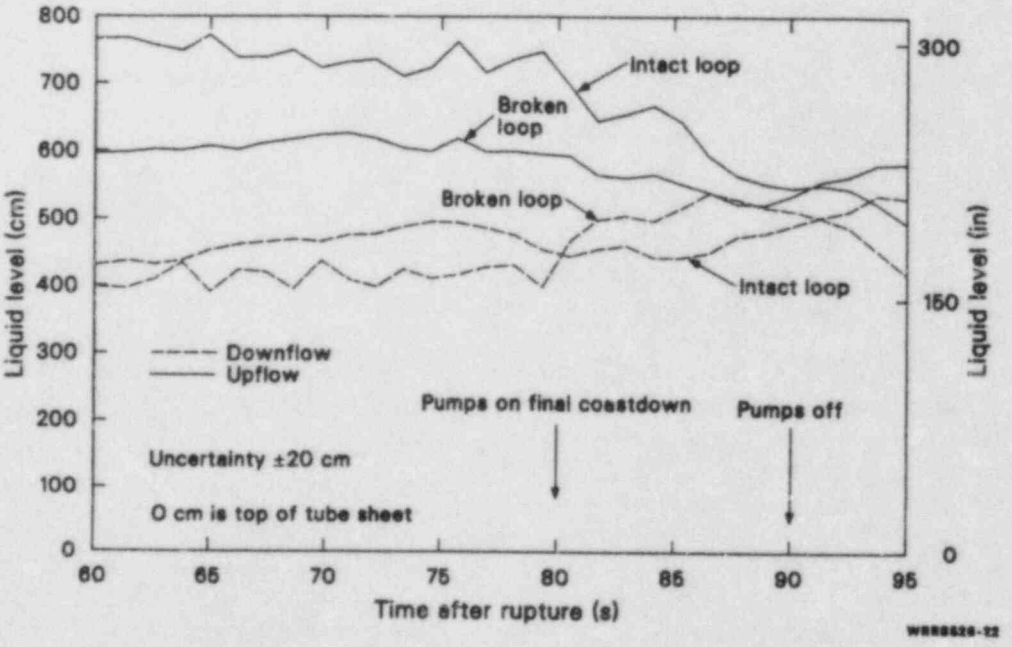

Figure 20. Intact and broken loop steam generator U-tube liquid levels during 5% SBLOCA Experiment S-LH-1.

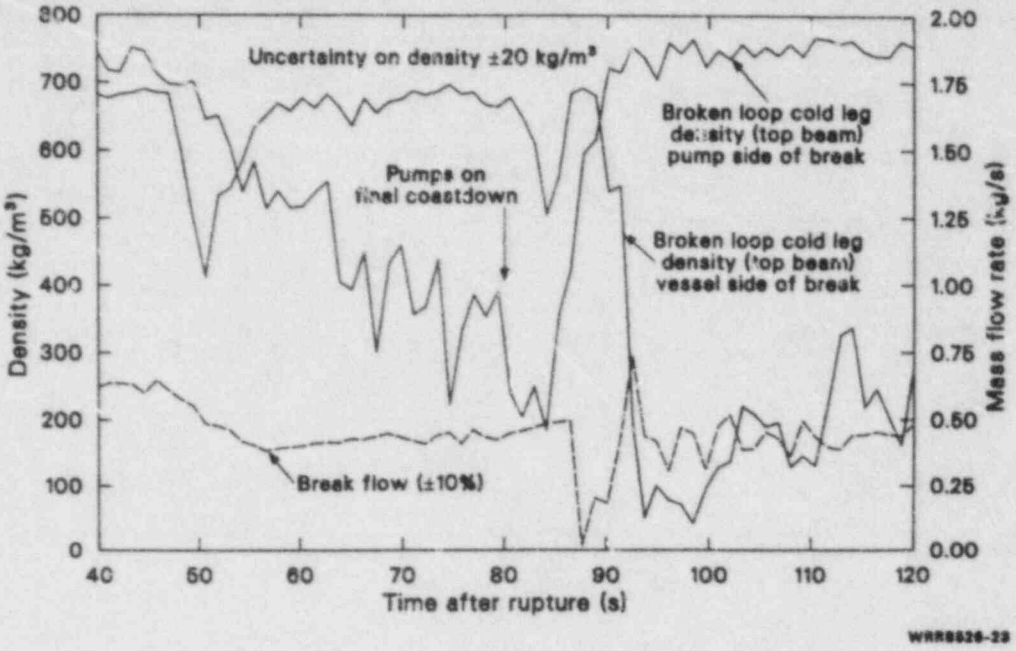

Figure 21. Break mass flow and broken loop cold leg density (top beam) either side of the break during 5% SBLOCA Experiment S-LH-1.

Period 3—Steam Generator U-tube Drain (90 to 140 s). After pump coastdown to zero speed, a distinct period of draining of the primary U-tubes in both the intact and broken loops followed. Fluid in the intact loop primary U-tubes drained at a different time than fluid in the broken loop U-tubes, which is related to the establishment of different natural circulation modes in the intact and broken loops. During this period, the fluid level in the vessel was fairly stable [~60 cm (24 in.) below the top of the core, which is at about the same level as when the pumps achieved zero speed]; therefore, the ongoing break mass flow throughout this period was mainly due to fluid draining from the tubes and was fairly constant, as shown on Figure 22.

Fluid in the intact and broken loop primary U-tubes drained from about the same level [500 to 600 cm (197 to 236 in.)] in a differential manner, as shown on Figure 23. In addition, draining of both the upflow and downflow sides of the tubes in each generator occurred symmetrically. The broken loop tubes drained immediately following pump coastdown at 90 s, and the intact loop tubes started draining at about 105 s. The start of draining in either case is related to the complete loss of pump head shown on Figure 24. By 86 s, the pump head for the broken loop was zero; by 95 s, the pump head in the intact loop was zero. Prior to pump coastdown, the 500 to 600 cm (197 to 236 in.)] of fluid in the primary U-tubes was supported by differential heads caused by condensation in the steam generator and steam generation in the core (tendency for two-phase natural circulation)[9] and the pump heads, which accounted for about 300 to 400 cm (118 to 157 in.) of the primary U-tube level. Following complete loss of the pump heads, fluid conditions in the hot leg piping caused draining to begin in the broken loop.

Figure 25 shows that following pump coastdown at 90 s the hot leg pipe fluid in the broken loop is highly stratified, with at least the top half of the pipe full of steam. (The bottom density measurement failed, and the middle density measurement can be taken as trend only.) The intact loop hot leg fluid was a more homogeneous two-phase mixture (Figure 25). Previous studies in Semiscale Mod-2A[9] have shown that even in steady-state cases one loop will remove all the energy via two-phase natural circulation while the other loop is stagnant; this appears to be the case for S-LH-1.

Figure 26 shows that following pump coastdown at 90 s there is actually an increase in intact loop hot leg flow, which is probably caused by that loop removing all the core decay heat via two-phase natural circulation while the broken loop tubes drain. Figure 27 also supports the concept of two-phase natural circulation with a slight plenum-to-plenum

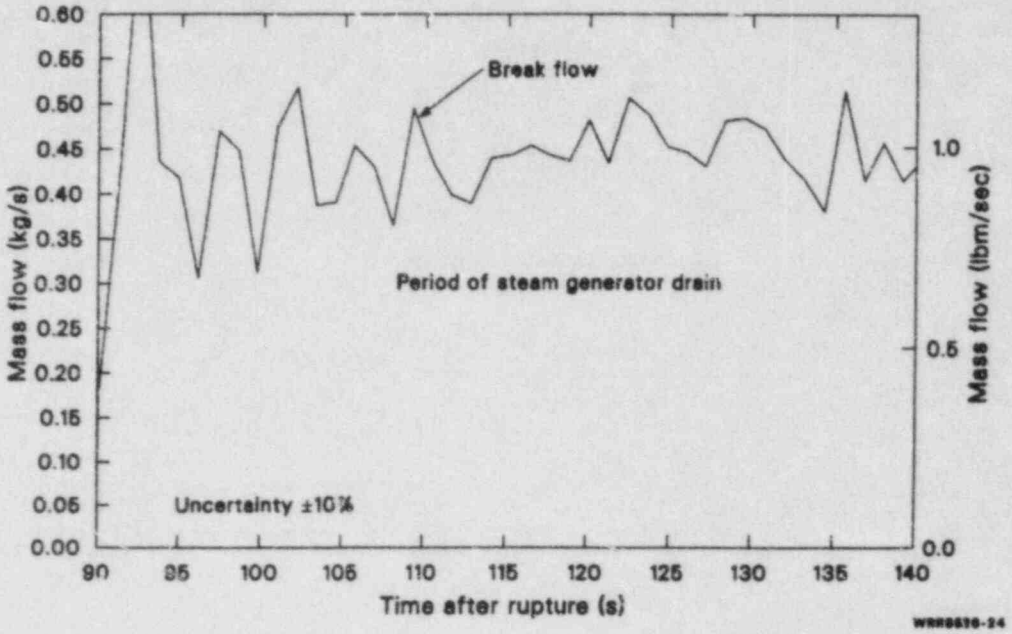

Figure 22. Break mass flow during steam generator U-tube drain for 5% SBLOCA Experiment S-LH-1.

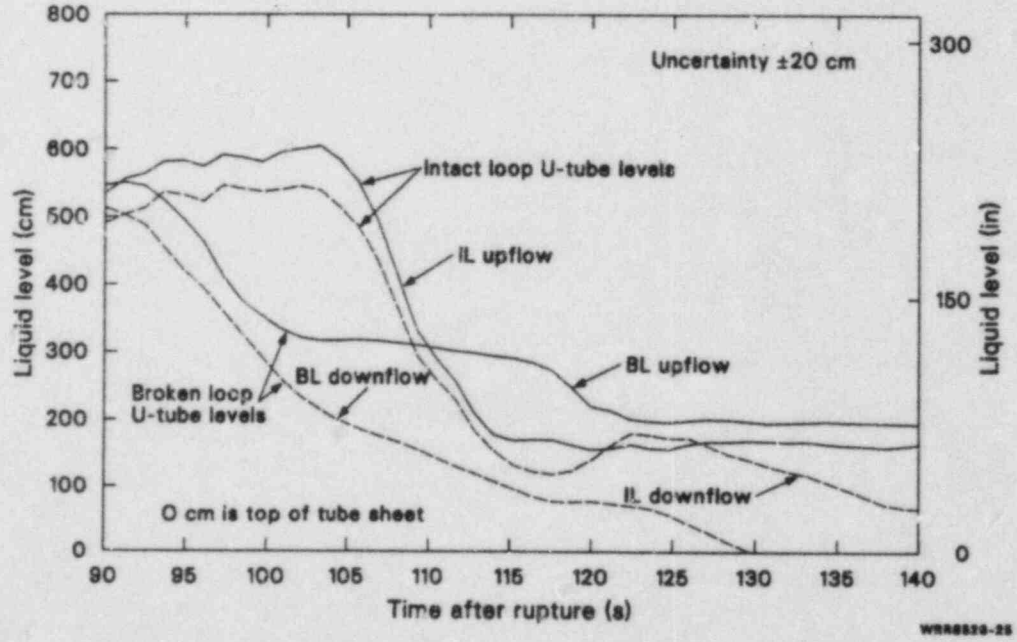

Figure 23. Comparison of steam generator primary U-tube liquid levels in the intact and broken loops during 5% SBLOCA Experiment S-LH-1.

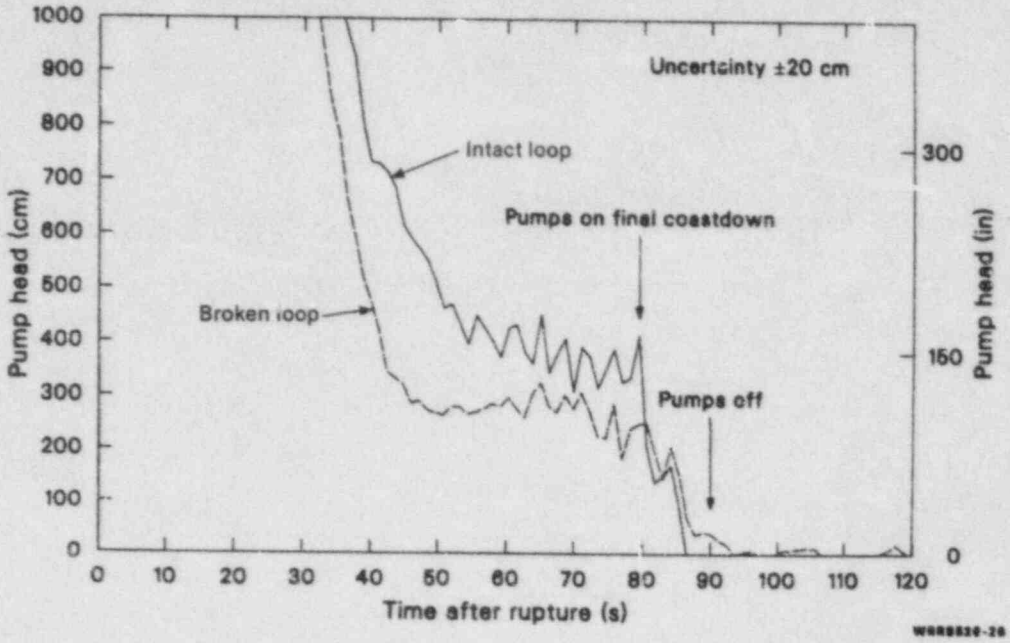

Figure 24. Pump head for the intact and broken loops during 5% SBLOCA Experiment S-LH-1.

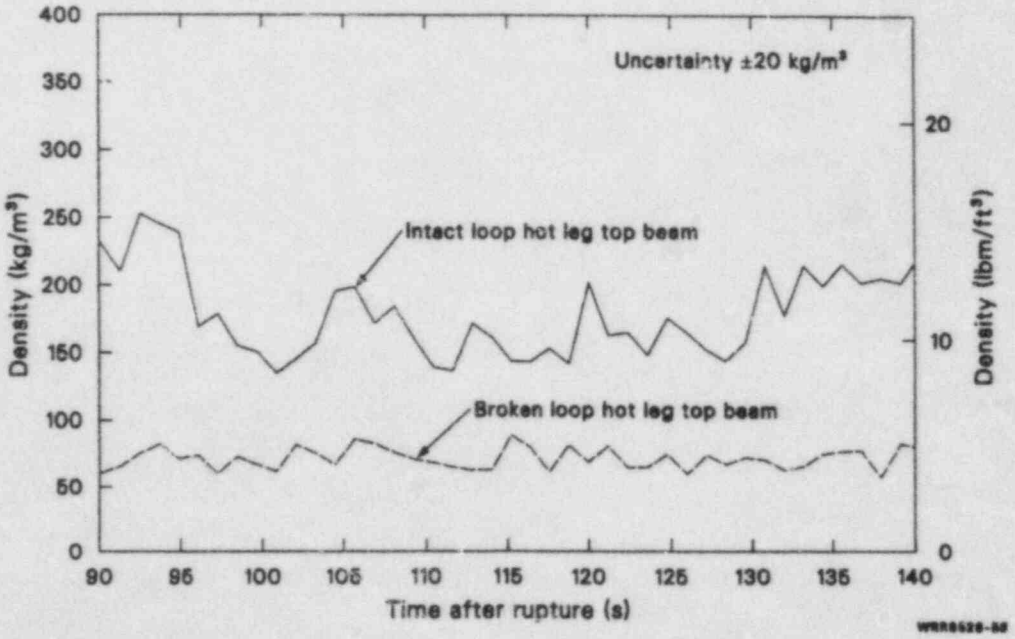

Figure 25. Comparison of intact and broken loop hot leg fluid densities (top beam) during 5% SBLOCA Experiment S-LH-1.

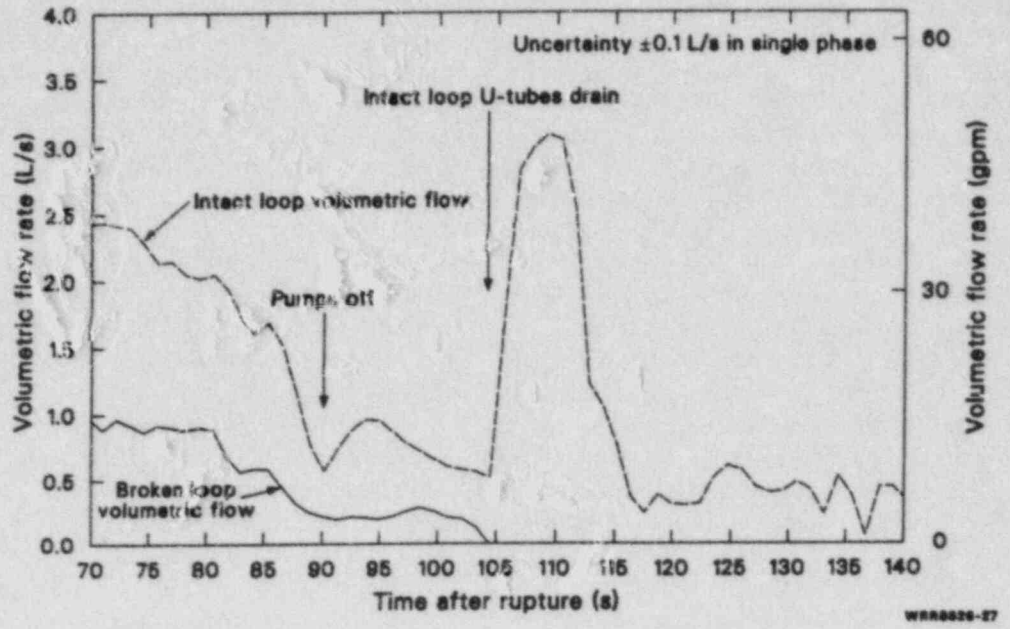

Figure 26. Volumetric flow in the intact and broken loop hot legs during 5% SBLOCA Experiment S-LH-1.

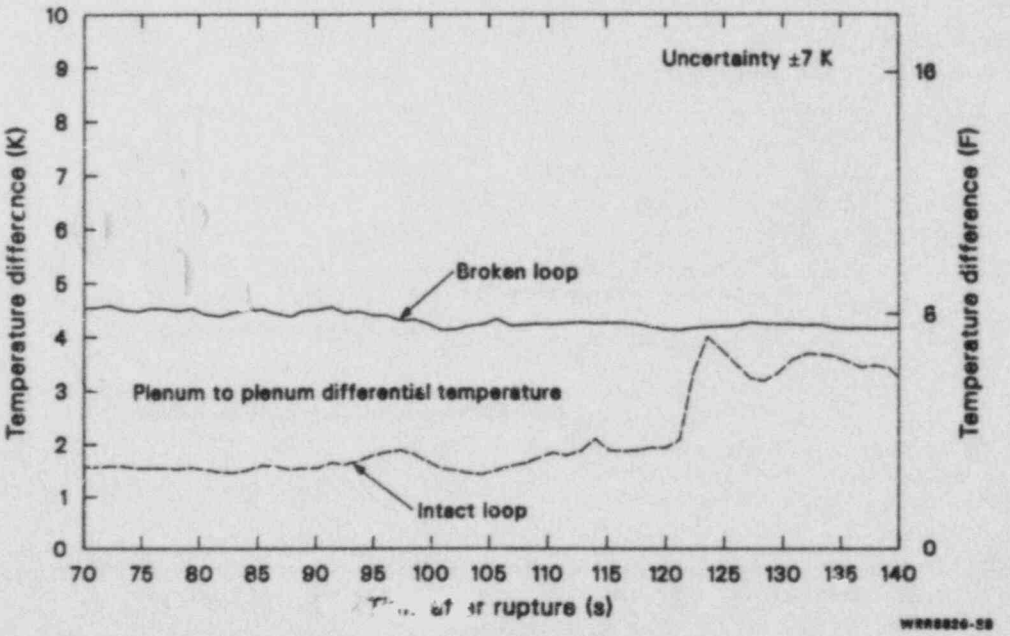

Figure 27. Steam generator primary-plenum to-plenum differential temperature for the intact and broken loops during 5% SBLOCA Experiment S-LH-1.

steam generator differential temperature [2 to 4 K (3.6 to 7.2°F)] in the intact loop. This increase in intact loop hot leg flow also caused a slight increase [0.5 m (19.7 in.)] in collapsed level in the intact loop primary tubes for both the upflow and downflow side (see Figure 23 between 90 to 105 s). This was possible because the intact and broken loop secondary fluid was still a heat sink relative to the primary. Without the support of both two-phase natural circulation and pumped flow in the broken loop primary tubes, fluid simply drained symmetrically into the vessel from the upflow side and into the suction from the downflow side. This symmetrical drain of the broken loop tubes persisted until the reflux[a] mode was established in the broken loop at about 102 s. The characteristic signature for reflux[9] is to have a voided pipe (Figure 25) and a 200- to 300-cm (79 to 118 in.) head of fluid on the primary upflow side depending on core decay heat (see Figure 23 at 102 s). This fluid head cannot be visualized as a liquid plug. Physically, fluid in the steam generator tubes is like a condensed film on the inside of the pipe, flowing down with steam flow up through the center. Depending on core steam generation rate, the film of liquid can increase or decrease, causing an increase or decrease in frictional pressure drop. Therefore, using the differential pressure drop to calculate fluid heads does not imply plugs of liquid in the tubes.

An additional requirement for reflux in the secondary has to be a heat sink relative to the primary (positive primary to secondary differential temperature),[b] which is the case for S-LH-1 for both intact and broken loops (Figure 28). As the reflux mode developed in the broken loop, core decay heat removal switched to the broken loop and allowed a symmetrical drain of the upflow and downflow side tubes in the intact loop beginning at 105 s. A dramatic spike in hot leg volumetric flow occurs at 105 s as steam travels to the intact loop tubes to replace the fluid that is draining out (see Figure 26). This draining of fluid from the upflow side of the tubes while steam is rushing toward the steam generator is a good example of countercurrent two-phase flow. At about 130 s, the characteristic signature response for reflux occurs in the intact loop tubes (a higher head on the upflow side of the tubes than the downflow side). These differential heads between upflow and downflow side have been referred to as "hold-up" and have an impact on the overall loop head balance during the next distinct time period—the manometric depression period.

Period 4—Manometric Depression (140 to 300 s). Following draining of the steam generator U-tubes, liquid seals were left in the pump suctions of both loops and in the vessel downcomer and vessel. These liquid seals caused a blockage of steam flow (steam created in the core region) around the loop to the break. As a result, the vessel upper plenum and hot legs were pressurized, causing manometric depressions in both the liquid level in the downflow side of pump suction seals and the vessel liquid level. Two things greatly affected the amount of core liquid level depression during these seal formations: (a) the amount of bypass steam flow from the vessel upper head to the downcomer (and then to the break)[a] and (b) the net head of liquid in the loops above the cold leg prior to the seal formation. In the Semiscale simulation, the loop seal (in both the intact and broken loop) was essentially cleared of liquid, allowing a steam relief path to the break and a relaxation of the manometric balance of pressure heads throughout the loop. The consequence and significance of this relaxation of heads is that the vessel liquid level increased, thus mitigating a core heat-up (discussed later under "Core Thermal Response"). The intact loop cleared first, pump seal followed by the broken loop pump seal. Both of these events were accompanied by changes in break flow characteristics and primary depressurization.

---

a. Reflux occurs when steam created in the core travels to the steam generator, where it is condensed, and the condensed liquid travels back to the vessel counter-current to the steam flow.

b. A previous 5% SBLOCA experiment (S-UT-8)[1,2] showed a 3-m (118-in.) increase in primary tube liquid levels that was attributed to a high condensation potential. Figure 20 shows only a 0.5-m (1.6-ft) increase in primary tube liquid level for S-LH-1. The condensation potential for S-UT-8 was considerably higher than for S-LH-1, with as much as 10 K (18°F) more differential temperature between primary and secondary for S-UT-8.[3]

---

a. The effect of bypass flow on the manometric balance is discussed in a later section. Basically, upper head drain was slow for Experiment S-LH-1; and the steam relief path through the bypass line was only used after the intact loop pump seal had cleared of fluid.

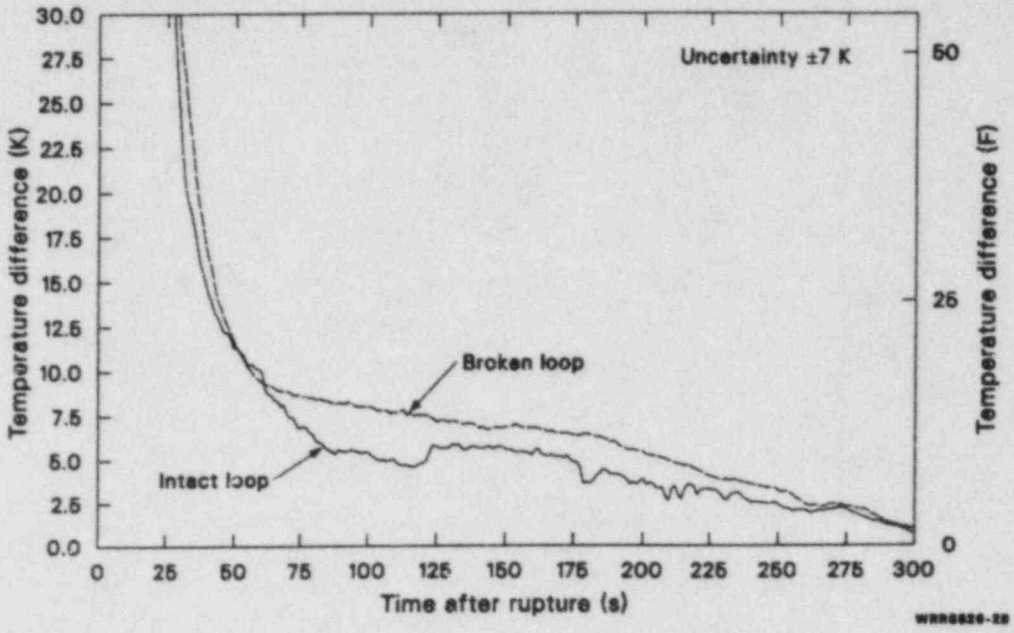

Figure 28. Primary-to-secondary differential temperature for the intact and broken loops during 5% SBLOCA Experiment S-LH-1.

The clearing of the pump suction seals in both loops occurred in a very steady manner rather than in the manner previously referred to as a blowout.[1,2] The downflow side emptied first, followed by a more rapid draining of the upflow side fluid. The intact loop seal cleared at about 180 s; and the broken loop seal cleared at about 280 s, as shown in Figures 29 and 30, respectively. This flushing action can be envisioned as a vapor/liquid interface simply moving down the downflow side, around the U-bend, and up the upflow side. The major effect of this seal clearing on vessel liquid level is shown in Figure 31. The vessel liquid level was depressed below the level associated with the bottom of the suctions during the manometric balance period prior to intact loop pump suction clearing. This extension of the vessel liquid level below the level associated with the suction can be understood by examining the overall head balance around the loop. Figure 32 demonstrates the collapsed liquid level head balance around the loop just prior to seal clearing (170 s), with arrows indicating the tendency to either push vessel fluid up or down. The fluid heads shown on Figure 32 represent a collapsed liquid level, although the head may be a frictional pressure drop. Heads are used for demonstration purposes only.

To estimate the cause of the vessel level depression below the level associated with the suction, the heads in the various components of any one of three parallel loops (intact, broken, or upper head bypass line) can be examined. The loops are not independent of each other and are interconnected through the upper plenum and downcomer inlet annulus. However, any one loop can be used to determine the overall head balance and the effect of this head balance on core liquid level. The net head in the steam generator primary tubes[a] is simply a natural part of the ongoing reflux mode, as discussed previously. Without the net head of fluid in the primary tubes, a core level depression below the bottom of the suction would not be possible; the downcomer head would simply partially reflood the core due to an imbalance of heads.

On Figure 32, at 170 s, the heads (either subtractive or additive) in the system balanced exactly to cause a core level depression about 100 cm (39 in.) below the elevation corresponding to the bottom of the pump suction. With the bottom of the suction the reference location, the net heads can be added or subtracted as shown in Table 2. For each of the

a. During previous 5% SBLOCA Experiment S-UT-8, it was thought that the net head across only the intact loop generator U-tubes caused the vessel level depression below the level of the suctions. This was incorrect; the overall heads throughout the loop, including the broken loop steam generator primary tube heads (for which data from S-UT-8 were not available), must be considered.

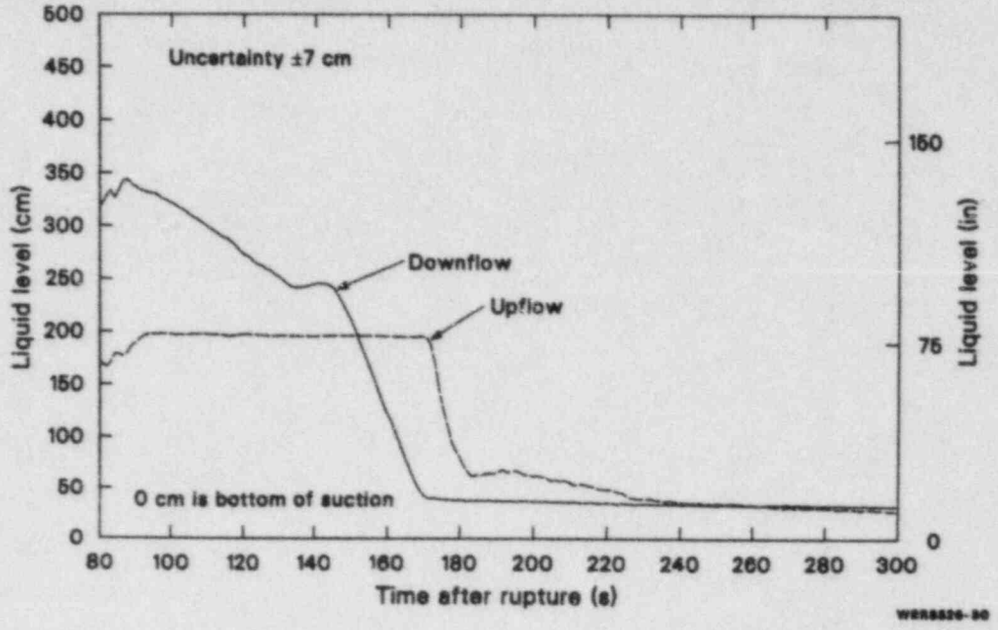

Figure 29. Liquid level in the intact loop pump suction during 5% SBLOCA Experiment S-LH-1.

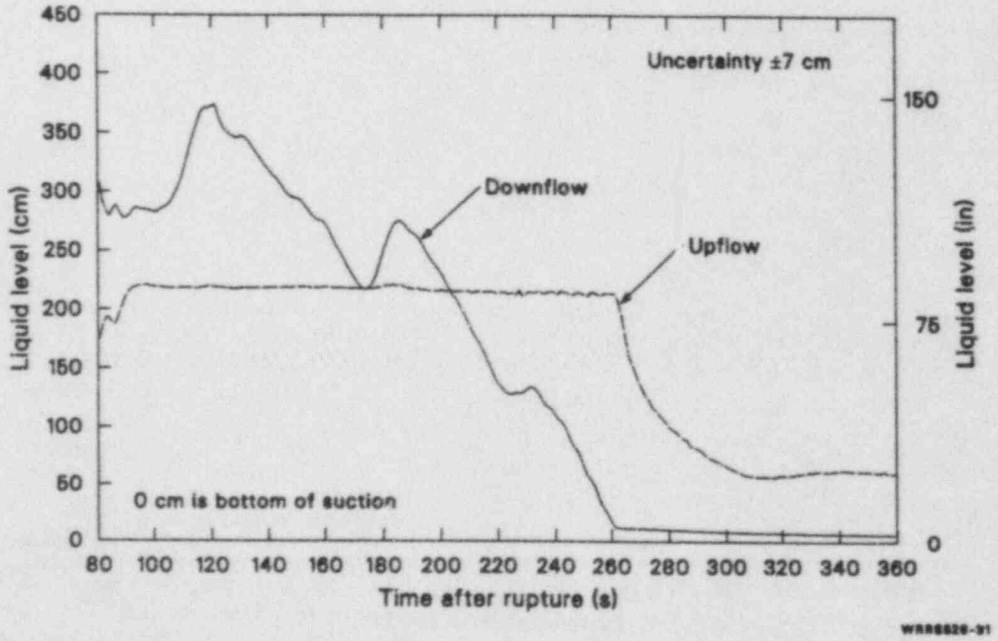

Figure 30. Liquid level in the broken loop pump suction during 5% SBLOCA Experiment S-LH-1.

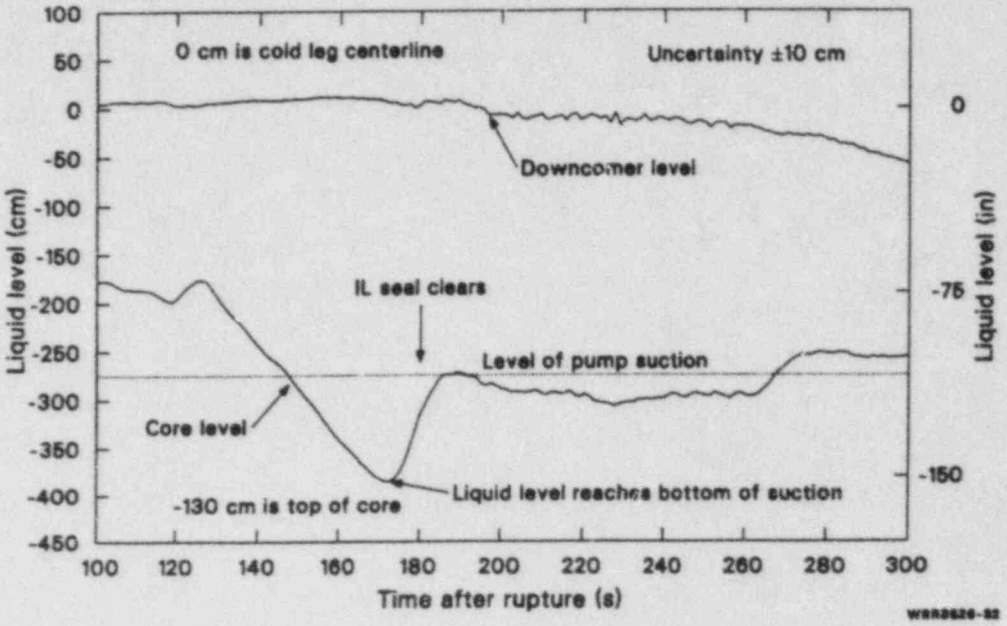

Figure 31. Vessel and downcomer liquid levels during 5% SBLOCA Experiment S-LH-1.

loops listed in Table 2, the calculated net amount of core liquid level depression below the level associated with the bottom of the pump suctions agrees with the measured core liquid level (Figure 31) within the uncertainties of the combined heads.

Following intact loop seal clearing at about 180 s, the core level increased to near the level of the suctions. The intact loop seal clearing was not able to cause the complete relaxation of the downcomer-to-core head difference, as depicted on Figure 31, since core steam generation was sufficient to maintain a depressed core level even with the intact loop clear. Following clearing of the intact loop seal, continued steam generation in the core, coupled with continued break flow, caused the broken loop seal to clear in the same manner (first the downflow side, then the upflow side, see Figure 30). After the broken loop seal cleared, the liquid level in the downcomer was still higher than in the core, as continued steam generation in the core depressed the vessel liquid level.

The preferential clearing of the intact loop before the broken loop is due to the 9-to-1 hydraulic resistance split between the broken and intact loops. With a 9-to-1 hydraulic resistance split, following pump coastdown, break flow will be supplied from the less resistive intact loop suction rather than the more resistive broken loop suction. It is not clear which loop would clear first in a symmetrical four-loop PWR; however, the proximity to the break favors the broken loop.

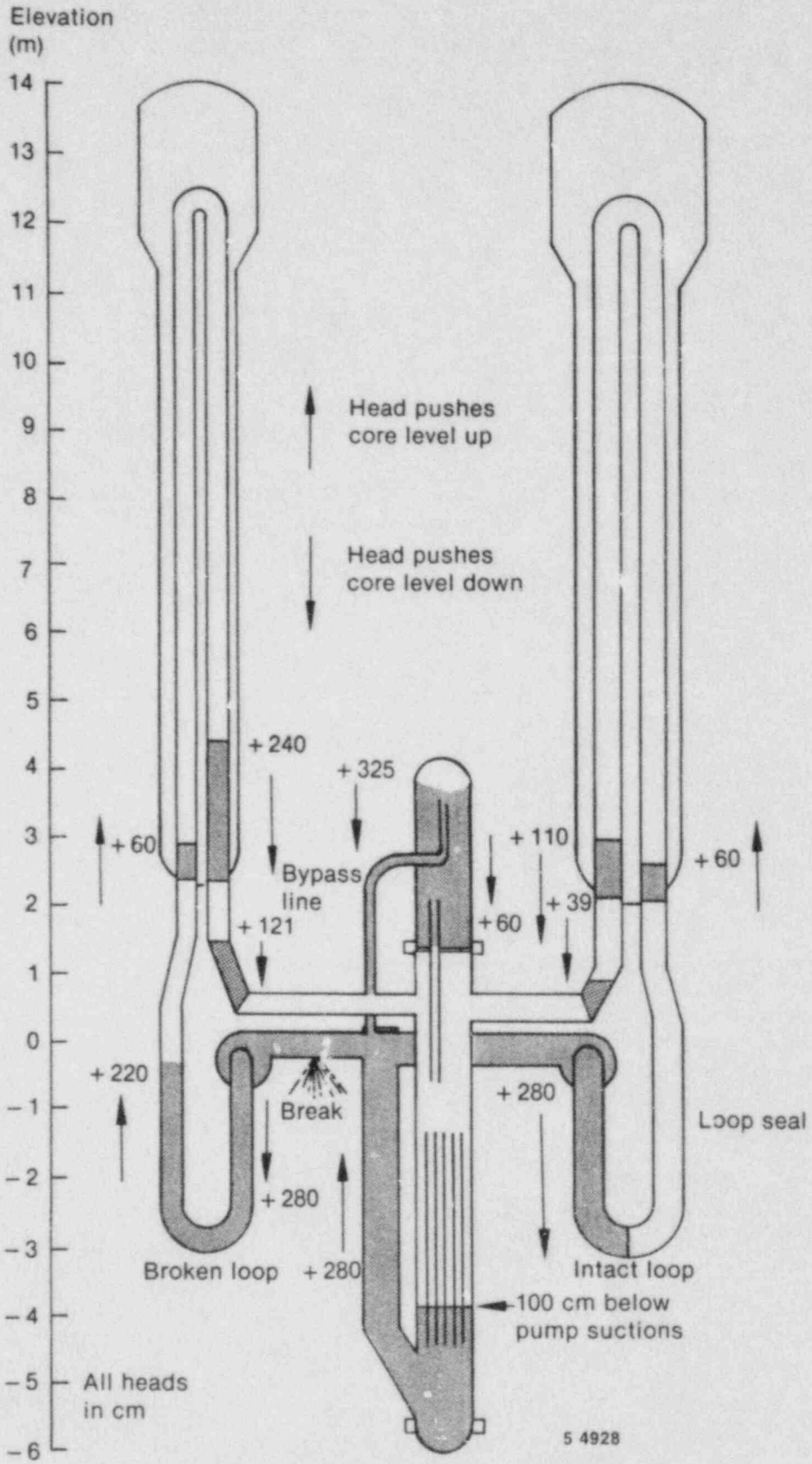

Figure 32. Manometric fluid head balance prior to intact loop pump suction seal clearing during 5% SBLOCA Experiment S-LH-1.

Table 2. System manometric head balance at 170 s

	Effect on Core Level			
	Pushes Up		Pushes Down	
	cm	in.	cm	in.
Intact loop				
Hot leg	—	—	39	15
Steam generator upflow	—	—	110	44
Steam generator downflow	60	24	—	—
Pump suction downflow	0	0	—	—
Pump suction upflow	—	—	280	110
Downcomer	280	110	—	—
	340	134	429	169
Net amount below suction level (cm) = 429 - 340 = 89 ± 16				
Net amount below suction level (in.) = 169 - 134 = 35 ± 6				
Broken loop				
Hot leg	—	—	121	48
Steam generator upflow	—	—	240	94
Steam generator downflow	60	24	—	—
Pump suction downflow	220	86	—	—
Pump suction upflow	—	—	280	110
Downcomer	280	110	—	—
	560	220	641	252
Net amount below suction level (cm) = 641 - 560 = 81 ± 16				
Net amount below suction level (in.) = 252 - 220 = 32 ± 6				
Upper head loop				
Upper core support plate	—	—	60	23
Bypass line[a]	—	—	325	128
Downcomer	280	110	—	—
	280	110	385	151
Net amount below suction level (cm) = 385 - 280 = 105 ± 15				
Net amount below suction level (in.) = 151 - 110 = 41 ± 6				

a. There is a large frictional pressure drop in the bypass line that overshadows the gravity head associated with fluid in the bypass line (steam binding) which in effect causes the core level to be depressed 325 cm (128 in.).

Break flow, and thus the primary depressurization rate, was greatly affected by the development of manometric heads in the loop. Figure 33 shows the break flow rate during the manometric seal-clearing period. The break remained covered with fluid as long as there was a liquid level in the intact loop suction. This suction fluid, even while decreasing in level, maintained the cold leg pipe full of liquid. As the supply of liquid was reduced due to the suction clearing, the break intermittently uncovered, causing a large decrease in fluid mass flow out the break. Therefore, as long as the pump suction had fluid, there was a large mass flux out of the system (Figure 33). When the break uncovered, the mass flux decreased; however, the volumetric flow increased, resulting in the increase in depressurization rate (Figure 9). Figure 34 compares the middle beam density measurement in the broken loop cold leg (on the same horizontal plane as the break) and the primary pressure during the period of intact loop seal clearing. Break uncovery, as evidenced by a decreasing density for the middle beam, occurred a few seconds before the intact loop suction was cleared of fluid. The density of the middle beam (which nearly bisects the middle of the pipe) began changing from solid liquid [700 kg/m^3 (44 lbm/ft^3)] to steam about 4 s before the suction cleared. As a result, the primary pressure started decreasing before the seal was clear. The implications of the break uncovery and pressure reduction are that the resulting increased flashing of fluid throughout the loop can imbalance the quasi-steady-state manometric balance that was established, resulting in a clearing of the intact loop of fluid.

Period 5—Core Boil-off (300 to 1000 s). Following clearing of the loop seals, the remaining fluid mass in the system was centered in the vessel and downcomer. With continued core power (core decay heat) and break flow, the core fluid simply boiled off with a differential fluid head between downcomer and core. This differential head was supported by pressurization in the core due to steam generated in the core as it flows to the break, even though the loop seals were clear and the upper head bypass line could pass steam. A heat-up of some rod positions occurred during this boil-off period.

Both the downcomer and vessel collapsed liquid levels followed a concurrent decrease in level as the core boiled off (Figure 35). A detailed description of core hydraulics and thermal response during this period is included in the next section. Meanwhile, the primary pressure (Figure 9) had decreased to the accumulator set point pressure (4.2 MPa, 600 psia), allowing flow of accumulator water

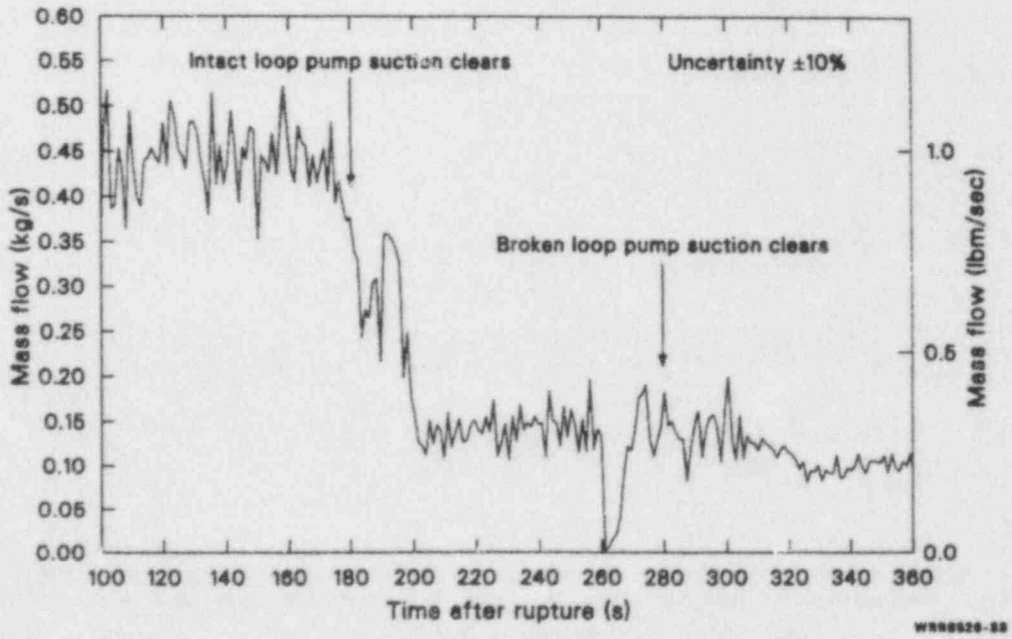

Figure 33. Break mass flow during pump suction seal clearing for 5% SBLOCA Experiment S-LH-1.

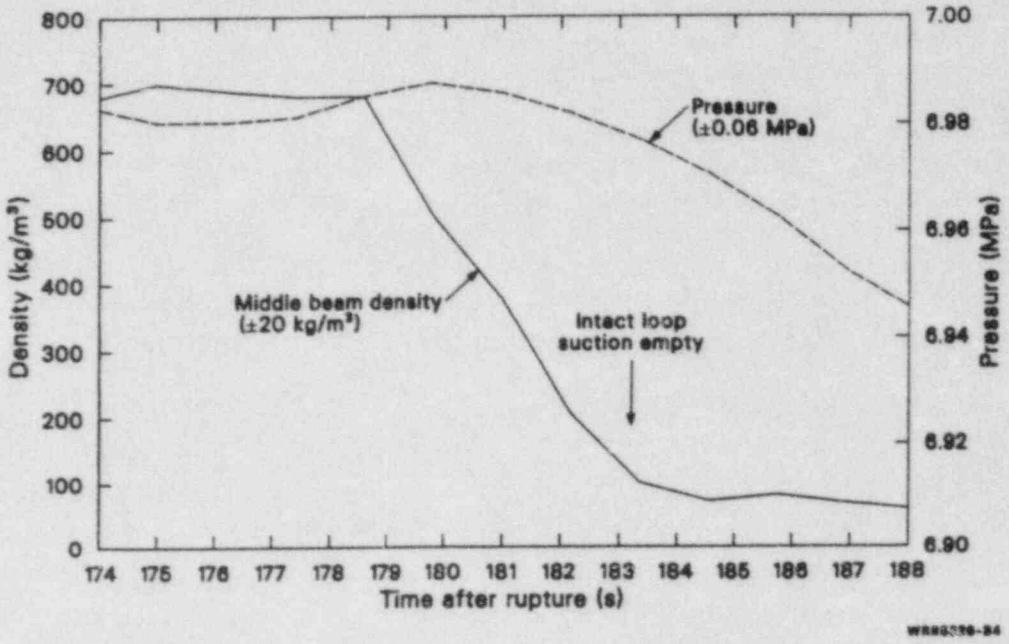

Figure 34. Comparison of broken loop cold leg density (middle beam) and primary pressure during 5% SBLOCA Experiment S-LH-1.

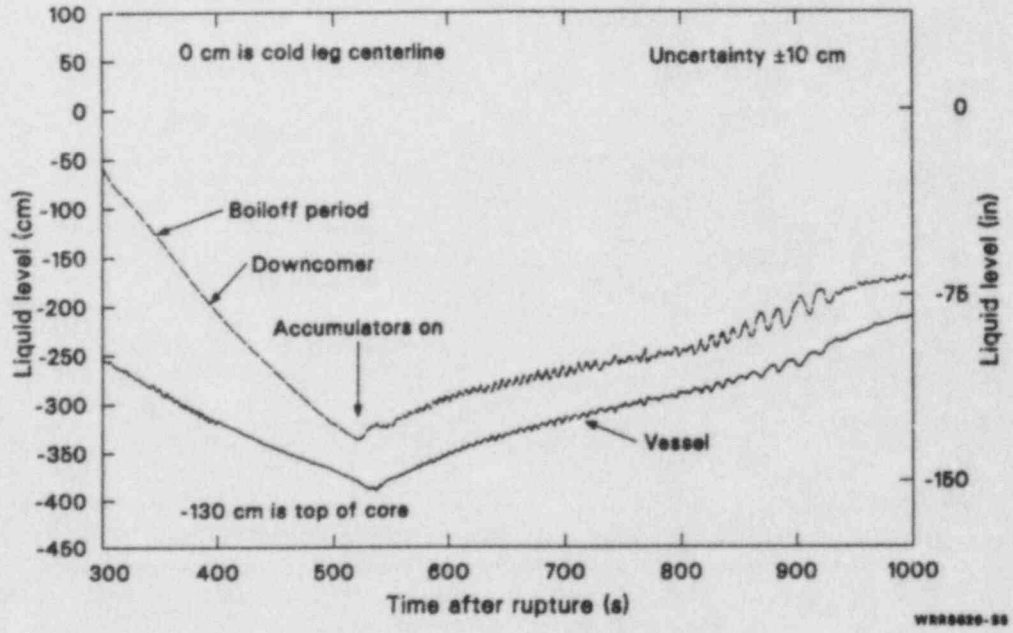

Figure 35. Vessel and downcomer liquid level during 5% SBLOCA Experiment S-LH-1.

into the system. The accumulator flow caused a reflood of hot core structures and heater rods, causing a reduction in the ongoing depressurization due to increased steam production in the core. The experiment was terminated at about 1000 s with a quenched core and an increasing core liquid level. The next section discusses in detail both the core thermal-hydraulic response associated with the first core liquid level depression during the manometric period and the core level depression associated with the boil-off.

Core Thermal-Hydraulic Response

Two major core liquid level depressions caused core heater rod temperature excursions during S-LH-1. The first temperature excursion was associated with the vessel liquid level depression caused by the pump suction seal formation and steam generation in the core described in the previous sections. Following pump suction seal clearing in both loops, the second depression was caused by a simple boil-off of core liquid due to decay heat and continued break flow. As an example, Figure 36 shows the temperature response of a core heater rod at 253 cm (99.6 in.) above the bottom of the heated length, illustrating the core temperature excursions associated with the two core liquid level depressions. The temperature excursion associated with the pump suction seal formation was minor, even though the vessel liquid level was depressed to about the same level as for the second temperature excursion induced by boil-off. This is attributed to the mechanism of core level depression. During the pump suction seal formation, the vessel liquid level was depressed below mid-core for only about 25 s, during the boil-off period, the liquid level was below mid-core much longer (~250 s) at essentially the same core power. The maximum cladding temperatures achieved for any rod position in the Semiscale core were 624 K (663°F) during the pump seal formation period [at the 253-cm (99.6-in.) elevation] and 764 K (915°F) during the boil-off period [at the 228-cm (89-in.) elevation].

Not all rod positions quenched when the intact loop pump suction seal cleared, as shown in Figure 37. The temperature excursion for the 319-cm (125-in.) elevation above the bottom of the core was unaffected by intact loop pump suction seal clearing (at 180 s); however, when the broken loop seal cleared at about 280 s, the additional vessel liquid caused a turnaround in temperature. In addition, multidimensional core temperature excursions were observed during the first level

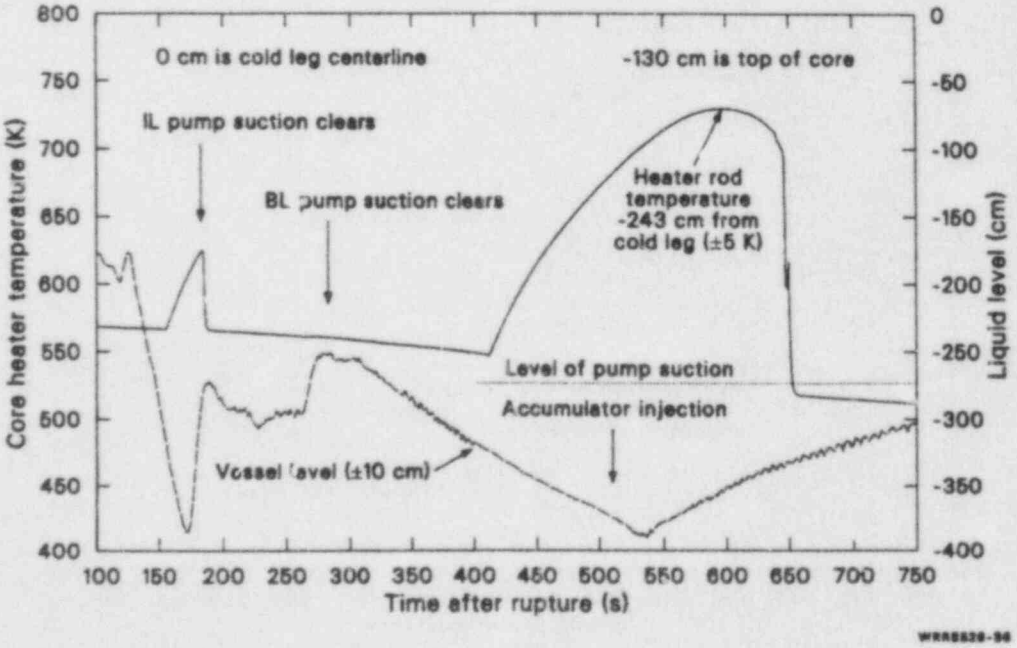

Figure 36. Core heater rod temperature 243 cm (96 in.) below the cold leg and vessel liquid level during 5% SBLOCA Experiment S-LH-1.

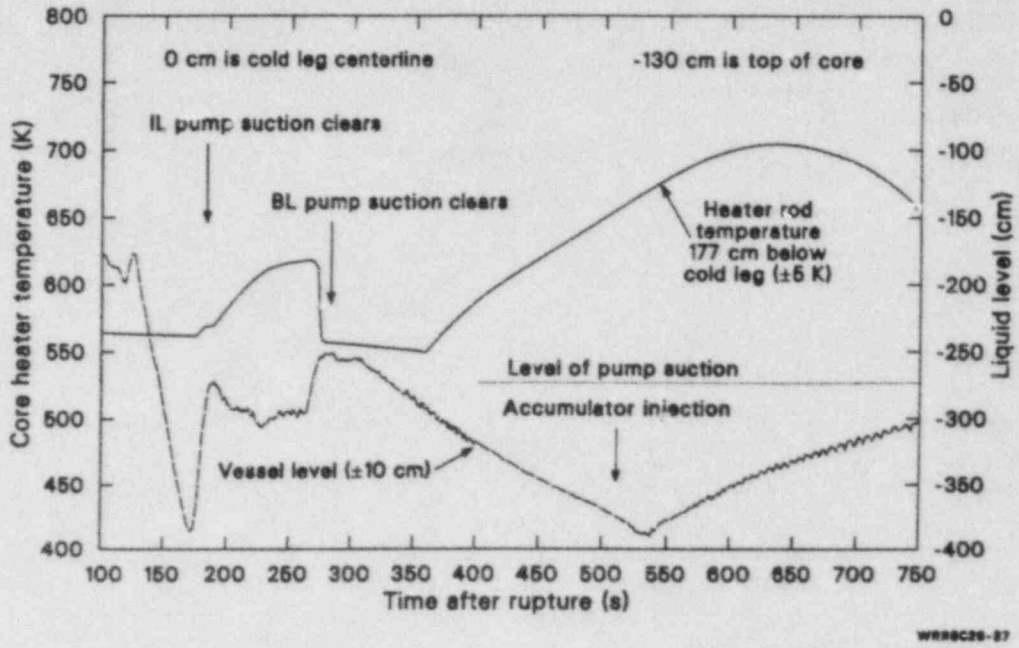

Figure 37. Core heater rod temperature 177 cm (70 in.) below the cold leg and vessel liquid level during 5% SBLOCA Experiment S-LH-1.

depression. At identical elevations, but at different azimuthal locations in the core, some rods showed heat-up while others did not. These multidimensional effects suggest falling films of liquid on the rods. The sequence of core rod heat-up during the boil-off followed an orderly top-down heat-up pattern as fluid boiled off. The boil-off of core liquid was mitigated by accumulator injection starting at about 500 s. The detailed core hydraulic and thermal responses associated with these two level depressions are discussed next.

Core Hydraulic Response. The hydraulics associated with the two core level depressions were found to be dependent on flow rate. Figure 38 shows the core collapsed liquid level[a] and the froth level.[b] Basically, the froth level is the upper limit of a two-phase mixture, above which is steam and below which is a single-phase liquid pool or two-phase mixture. The froth level is a more physical representation of actual hydraulic conditions in the core than the collapsed liquid level, which gives only a relative guide to fluid conditions.

The froth and collapsed liquid levels are nearly the same for the first (rapid) core level depression; however, for the second (slower) depletion, there is a constantly higher froth level than collapsed level. This difference is attributed to the mechanism of mass depletion. With the first depletion, steam created in the core is bound by the space created by the fluid plugs in the pump suction and vessel downcomer and core, with a resultant depression of the core froth level. Following pump suction seal clearing, steam created in the core has a plug-free path to the break, which causes a higher froth level than collapsed liquid level due to boiling and bubble rise.

Using data from the gamma densitometers, void fraction[a] distribution maps for each depression level are presented as Figures 39 and 40, which show a definite axial stratification of void fractions in the core prior to, during, and after the liquid level depressions. This stratification was supported by saturated nucleate boiling and film boiling due to core decay heat (averaging about 50 kW during this period), with the amount of steam bubbles being higher for higher regions of the core (bubble rise).

a. Collapsed liquid level is determined by using a differential pressure (DP) transducer and assumes all the fluid between the DP taps is saturated.

b. The froth level is determined by using the elevation of the densitometer and the time the density showed a sudden drop from two-phase to steam conditions.

a. The void fraction (α) was determined by $\alpha = \rho f - \rho m / \rho f - \rho g$ where ρf = saturated liquid density; ρg = saturated gas density; and ρm = measured average channel density.

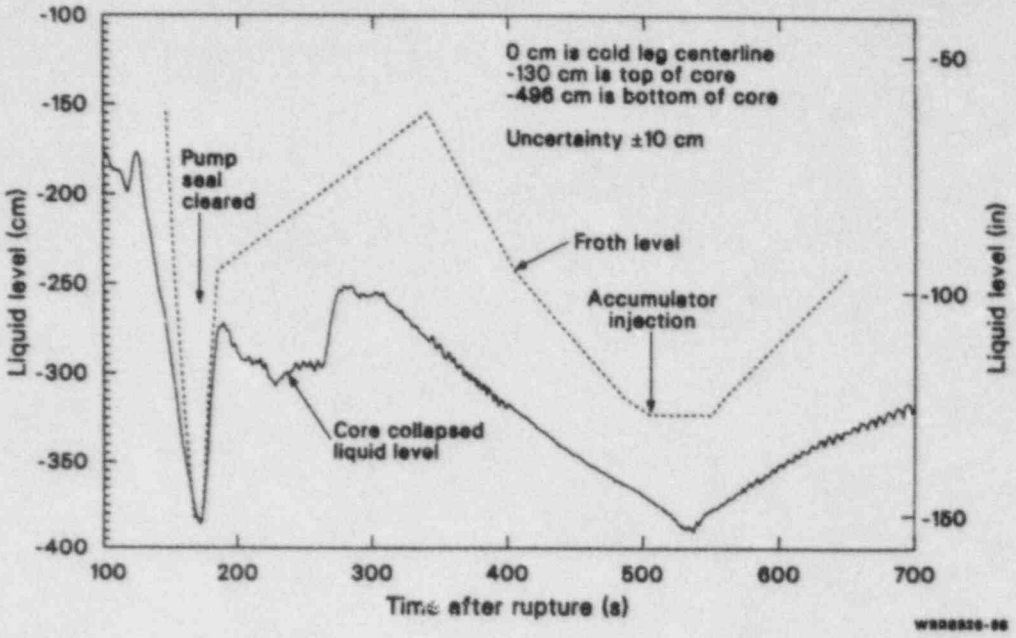

Figure 38. Vessel froth level and collapsed liquid level during 5% SBLOCA Experiment S-LH-1.

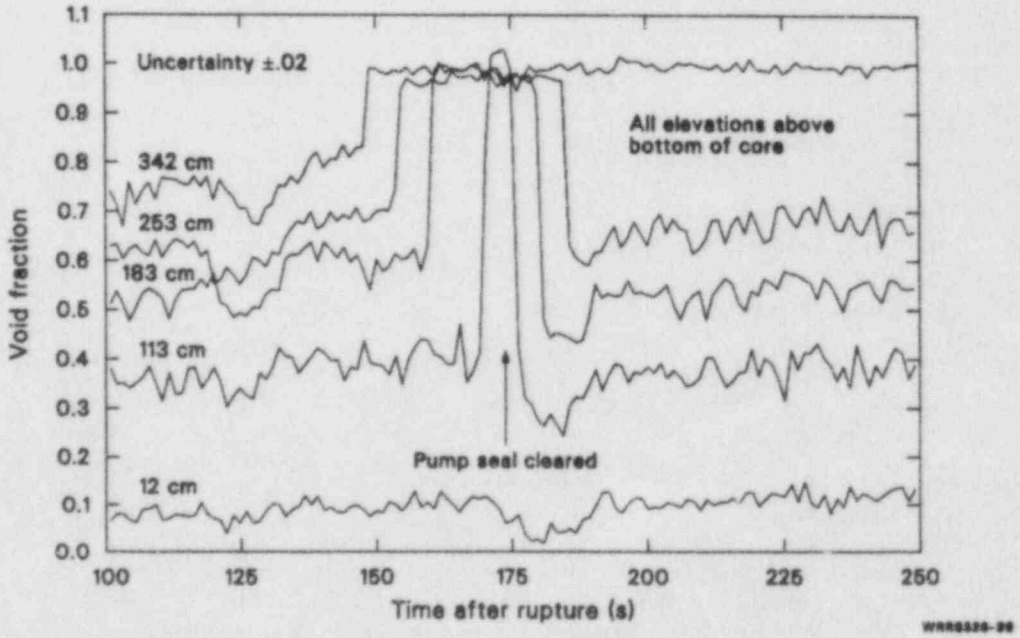

Figure 39. Vessel axial void fraction distribution during the manometric depression of 5% SBLOCA Experiment S-LH-1.

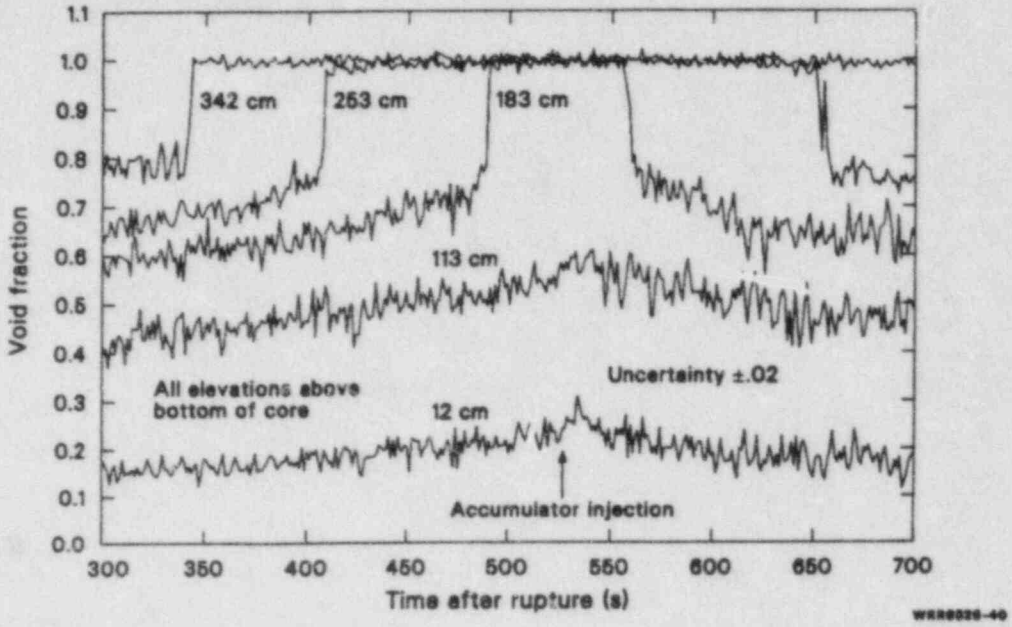

Figure 40. Vessel axial void fraction distribution during core boil-off of 5% SBLOCA Experiment S-LH-1.

Core Thermal Response. Core rod heat-ups were observed during both level depressions. During the first level depression, multidimensional heat-ups occurred; whereas during the second level depression, the heat-up occurred in a uniform top-down manner following the froth level. As an example of the multidimensional nature of the heat-ups during the first level depression, Figure 41 shows the core rod thermocouple response at two different azimuthal positions, but essentially the same axial positions (Rod B2-356; and Rod D2-352, see Figure 2), and the local average void fraction at the same axial position. The void fraction remains 1 (+0; -0.02) throughout the period, indicating passage of the froth level. The thermocouple on Rod B2 shows heat-up (nucleate boiling to forced convection to steam), while the thermocouple on Rod D2 shows no heat-up (nucleate boiling). These thermocouples are within a few centimeters of each other and are both immersed in a steam environment. This behavior suggests falling films of liquid or drops of liquid attached to the rod surface of some rods but not others. With a film of liquid on the rod wall, nucleate boiling would remove decay heat and preclude rod heat-up. Another example of core thermal response during the first level depression and further evidence of the presence of water films or drops on rod surfaces is seen on Figure 42. Two rod positions (D3 + 352; C3 + 352, see Figure 2) at the same elevation (top of the core) but at different azimuthal positions show no heat-up even though the local void fraction shows steam. These multidimensional effects present an impractical challenge to one-dimensional code calculations of core thermal response because of the multidimensional distribution of the positions that show heat-up versus positions that show no heat-up. To adequately calculate this type of behavior, two- or three-dimensional codes would be required.

During the second level depression, the heat-ups for all rod positions are consistent. No heat-ups of a rod position occur until the local void fraction reaches 1 (+0; -0.02). If the rod remains immersed in a froth mixture (void fraction less than 1.0), no heat-up occurs. As an example, Figure 43 shows a mid-core rod thermocouple response (C3 + 181, see Figure 2) and the local void fraction at the same elevation. As the void fraction becomes 1 (+0; -0.02), the heat-up begins (indicating a heat transfer mode change from nucleate boiling to convection to steam). Figure 44 presents two rod thermocouple responses at identical axial positions but different azimuthal locations (B3 + 351; E3 + 351; see Figure 2) and the local void fraction. No multidimensional effects are observed. Both

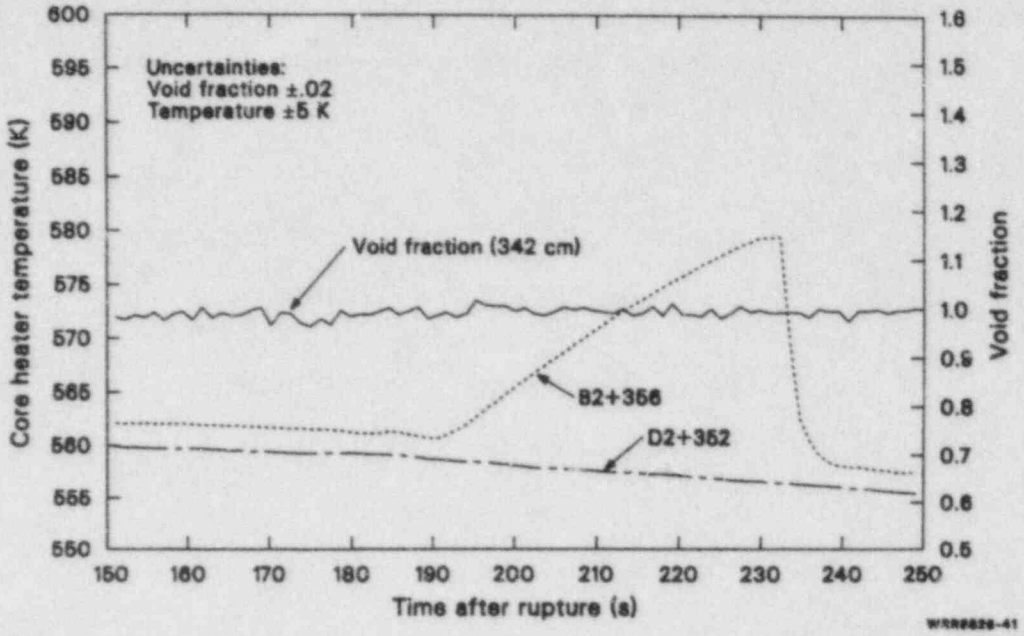

Figure 41. Upper core void fraction and core rod temperature response for two core rod thermocouple positions (with and without heat-up) during the manometric vessel liquid level depression for 5% SBLOCA Experiment S-LH-1.

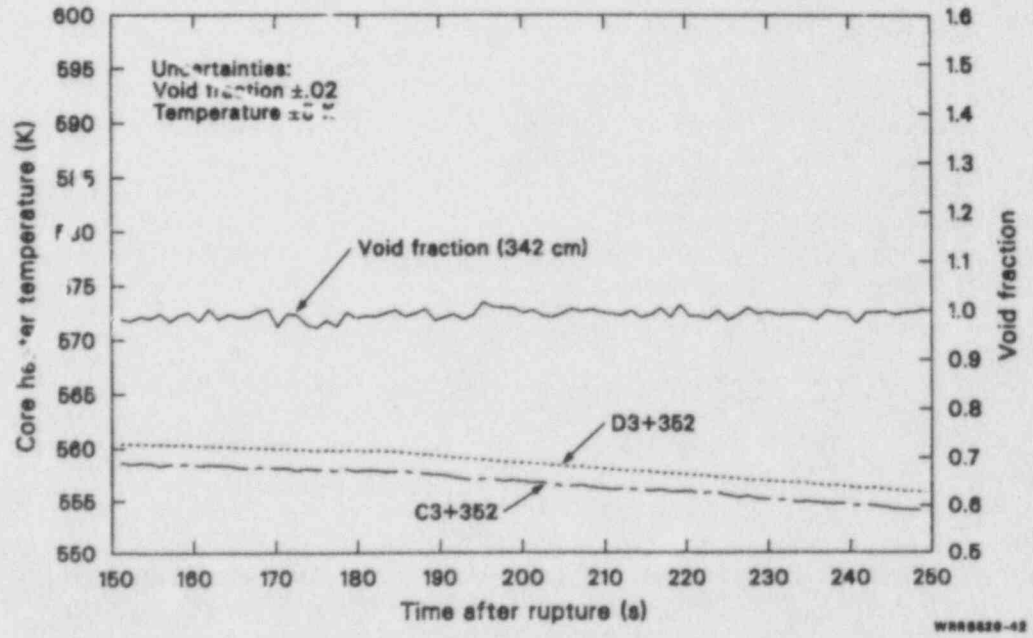

Figure 42. Two upper core thermocouple responses without heat-up and the local average void fraction during the manometric vessel liquid level depression for 5% SBLOCA Experiment S-LH-1.

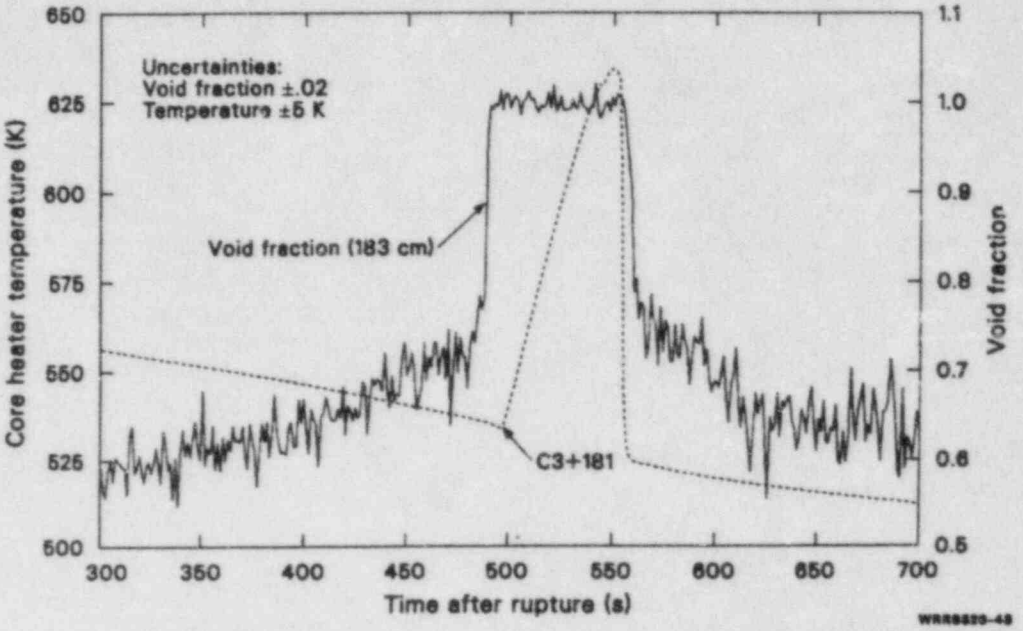

Figure 43. Core heater rod temperature response and local void fraction at mid-core during core boil-off of 5% SBLOCA Experiment S-LH-1.

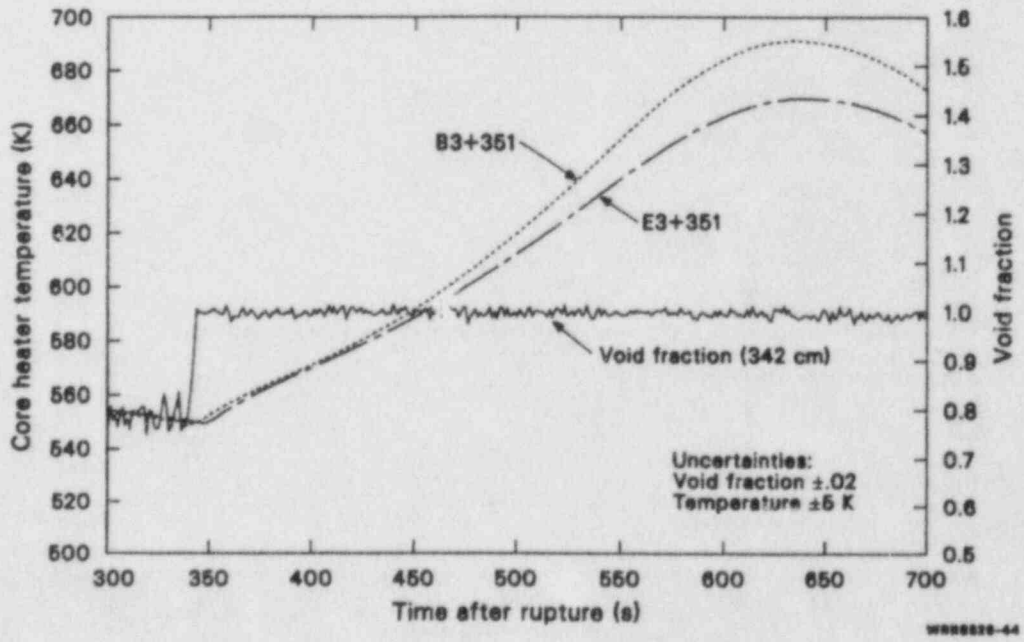

Figure 44. Core heater rod temperature response at two different azimuthal but identical axial positions and the local void fraction during core boil-off for 5% SBLOCA Experiment S-LH-1.

portions show heat-up when the void fraction changes to 1.0. Figure 45 shows a rod thermocouple response for a position immersed in a froth level during the second liquid depletion, indicating no heat-up.

The Semiscale data base described above can be used for assessment and development purposes to improve calculational ability for SBLOCA applications. A total of 54 core rod thermocouples and 5 density measurements at a variety of axial positions in the core are available for this purpose.

Effect of Bypass Flow on Accident Severity

The amount of core bypass flow had a strong effect on 5% SBLOCA severity as measured by core liquid level depressions during the manometric period. Semiscale experiments S-LH-1, with 0.9% of initial core flow bypassed, and S-LH-2, with 3.0% of initial core flow bypassed, approximately covered the range of bypass flow existing in commercial PWRs (0.5% to 4%) and showed that the core liquid level depression during the manometeric depression period was greater for lower bypass flow.

Figure 46 compares the overall system fluid mass inventories for the two cases and shows approximately 10% more mass retained for the higher bypass flow. On an overall basis, however, the same basic phenomena occurred regardless of bypass flow. The primary pressure response for the two transients was essentially identical, as shown in Figure 47. There was a slight variation between S-LH-1 and S-LH-2 primary pressures starting at about 350 s, which was due to a difference in broken loop pump suction seal clearing. The broken loop pump suction seal cleared of fluid during S-LH-1 but not during S-LH-2, thus causing a reduced depressurization rate for S-LH-2. During S-LH-1, after the broken loop pump suction seal cleared at about 280 s, steam generated in the core had basically three paths for pressure relief: (a) through the intact loop, (b) through the bypass line, and (c) through the broken loop. However, in S-LH-2, only two paths existed: (a) the intact loop and (b) the bypass line, which combined to give a more resistant path for steam relief; i.e., there was less ventilation potential for the core-generated steam. As a result, the primary pressure was slightly higher for S-LH-2 after 350 s.

The drain of upper head liquid was considerably enhanced during S-LH-2. Figure 48 compares

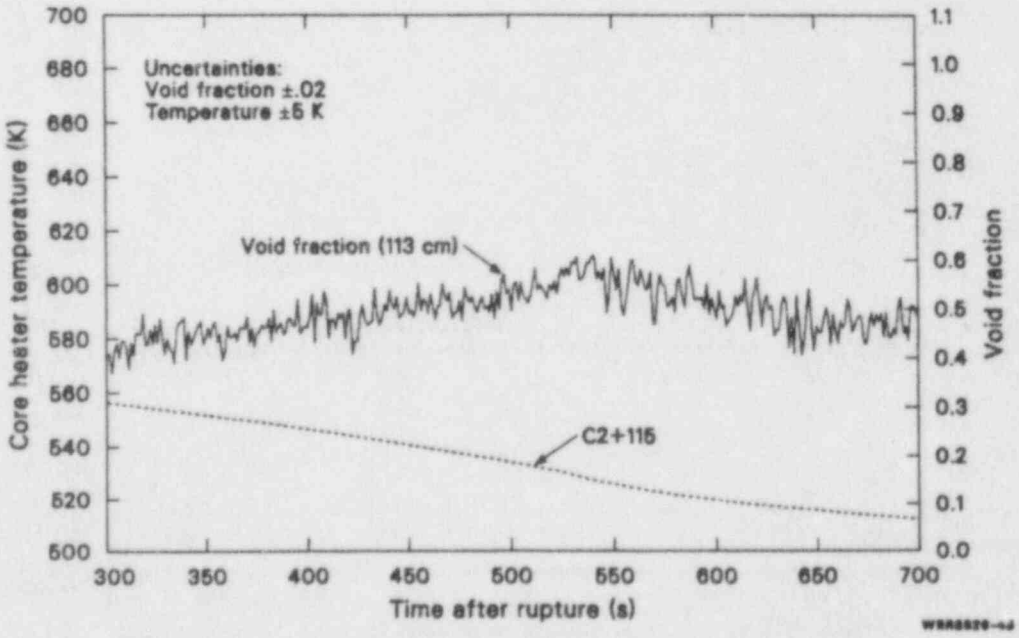

Figure 45. Core rod temperature response and local void fraction in the lower core during core boil-off of 5% SBLOCA Experiment S-LH-1.

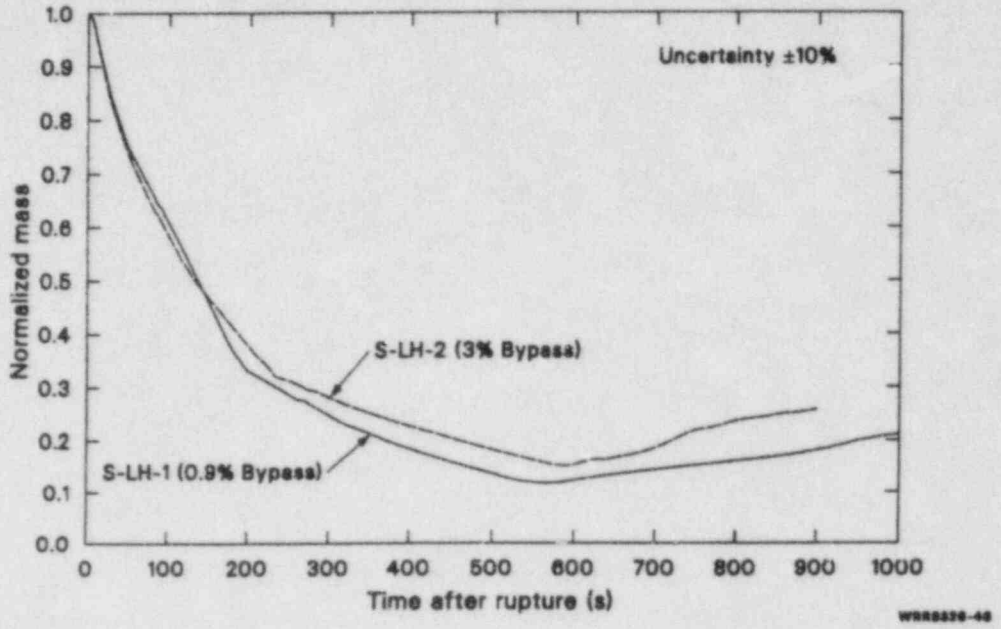

Figure 46. Mass inventory for 5% SBLOCA Experiments S-LH-1 (0.9% bypass flow) and S-LH-2 (3.0% bypass flow).

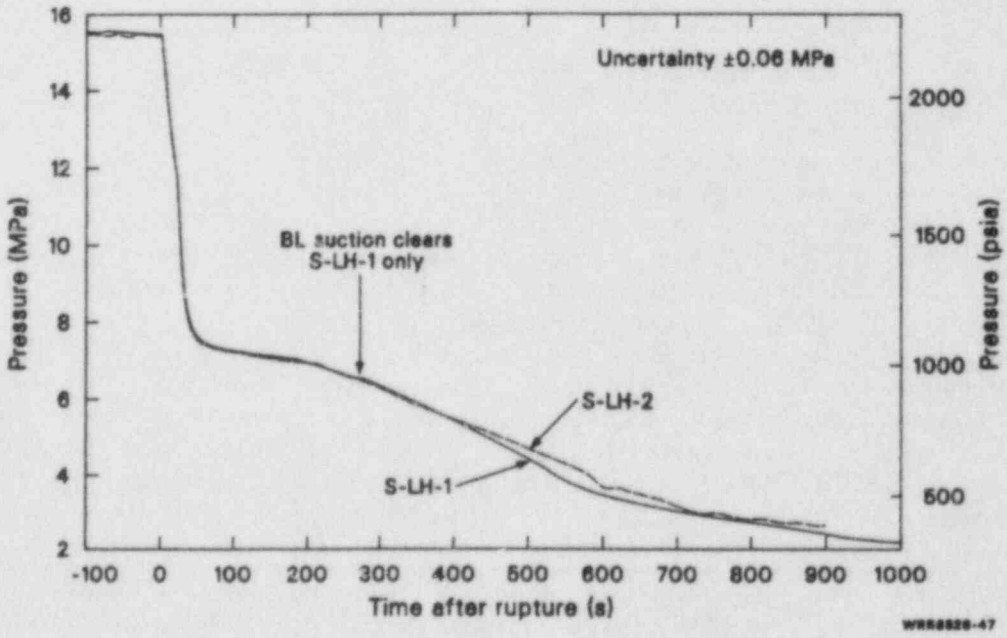

Figure 47. Primary system pressure for 5% SBLOCA Experiments S-LH-1 (0.9% bypass flow) and S-LH-2 (3.0% bypass flow).

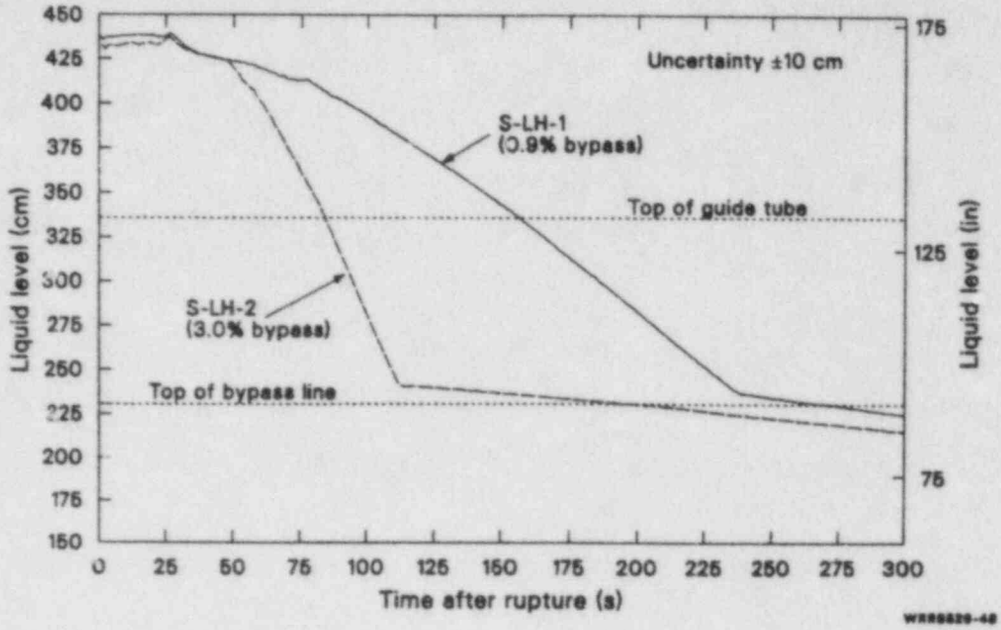

Figure 48. Vessel upper head liquid level for 5% SBLOCA Experiments S-LH-1 (0.9% bypass flow) and S-LH-2 (3.0% bypass flow).

upper head liquid level, showing that the upper head drained to the top level of the bypass line about twice as fast for the 3.0% bypass case as for the 0.9% bypass case. This is attributed to the larger bypass line area for the 3.0% case. Both cases exhibited the same lack of upper head draining until the pressurizer emptied, as discussed in an earlier section. This faster draining for the 3.0% case had a pronounced effect on break flow, as shown on Figure 49. With more steam flow through the bypass line at 110 s (from the upper head to the downcomer and then to the break), the break flow was reduced. This increase in steam upstream of the break is shown on Figure 50, which compares the fluid densities from the top density beam in the broken loop cold leg for S-LH-1 and S-LH-2. When the bypass was cleared for steam flow at about 110 s on S-LH-2, the amount of steam in the top of the cold leg pipe increased, thus increasing steam flow and decreasing break flow.

The drain of the upper head for S-LH-2, the 3.0% bypass flow case, influenced the drain of the steam generator primary U-tubes. There was delayed drain of the primary tubes in the intact loop steam generator for the 3.0% bypass case, as shown on Figure 51. This delay in draining of intact steam generator primary tubes also delayed the intact loop pump seal clearing about 40 s, as shown on Figure 52. During S-LH-2, the draining of the intact loop primary tubes seen on Figure 51 occurred at about 110 s, which corresponded in time to the uncovery of the bypass line in the upper head. Therefore, at 110 s during S-LH-2, the core bypass flow path was open for core steam relief, thus reducing the ongoing flow in the hot leg because steam created in the core could now also travel through the bypass line. This reduction in hot leg flow precipitated the drain of the primary tubes. As mentioned earlier, the broken loop pump suction seal never did clear for the 3.0% bypass case,

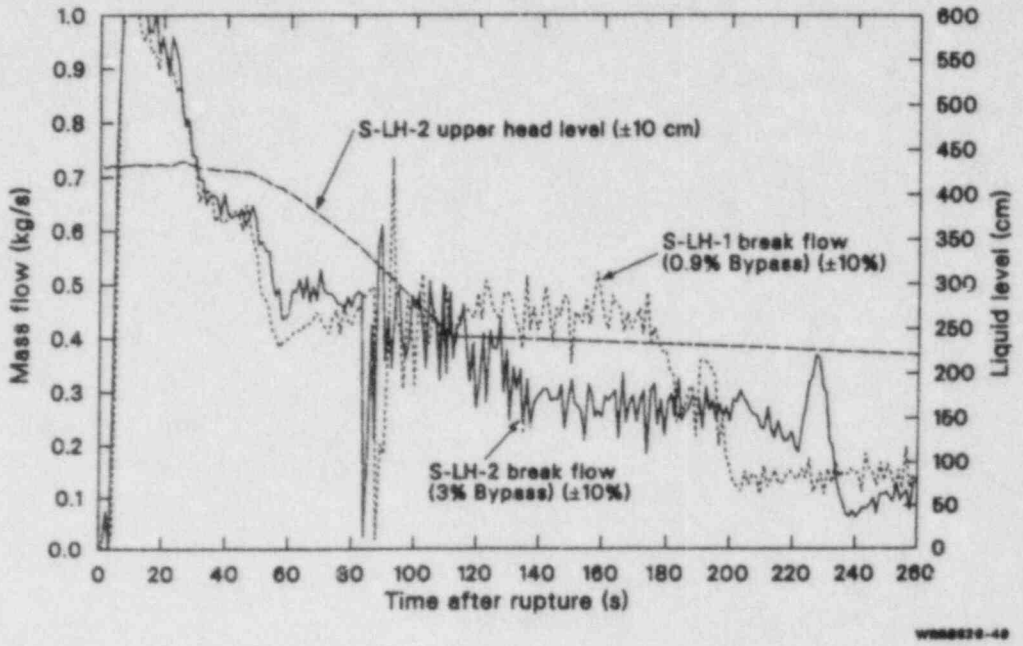

Figure 49. Vessel upper head liquid level and break flow for 5% SBLOCA Experiment S-LH-2 (3.0% bypass flow) and break flow for Experiment S-LH-1 (0.9% bypass flow).

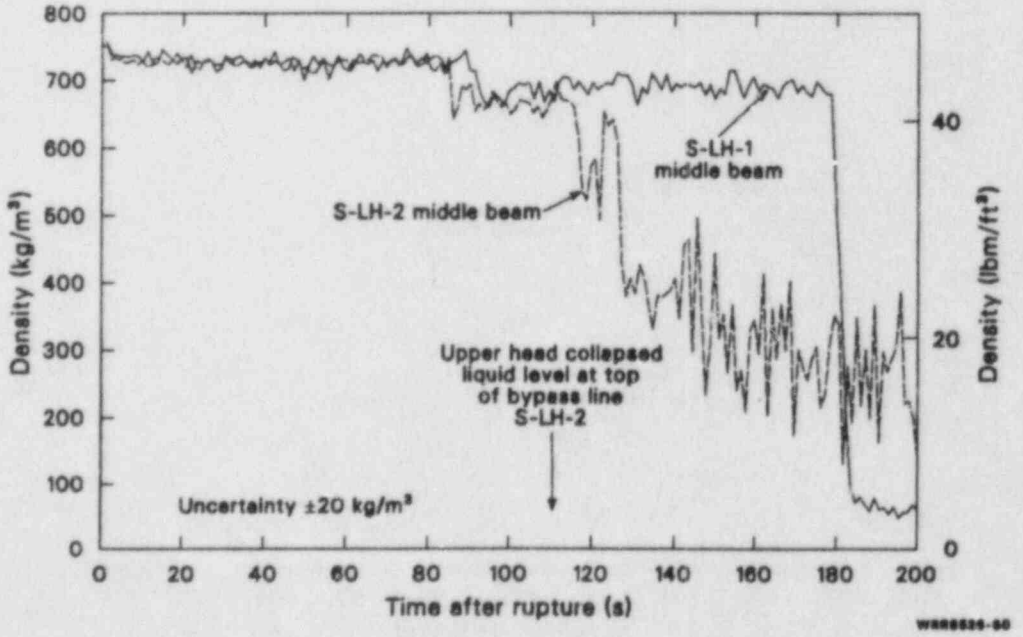

Figure 50. Broken loop cold leg density for 5% SBLOCA Experiments S-LH-1 (0.9% bypass flow) and S-LH-2 (3.0% bypass flow).

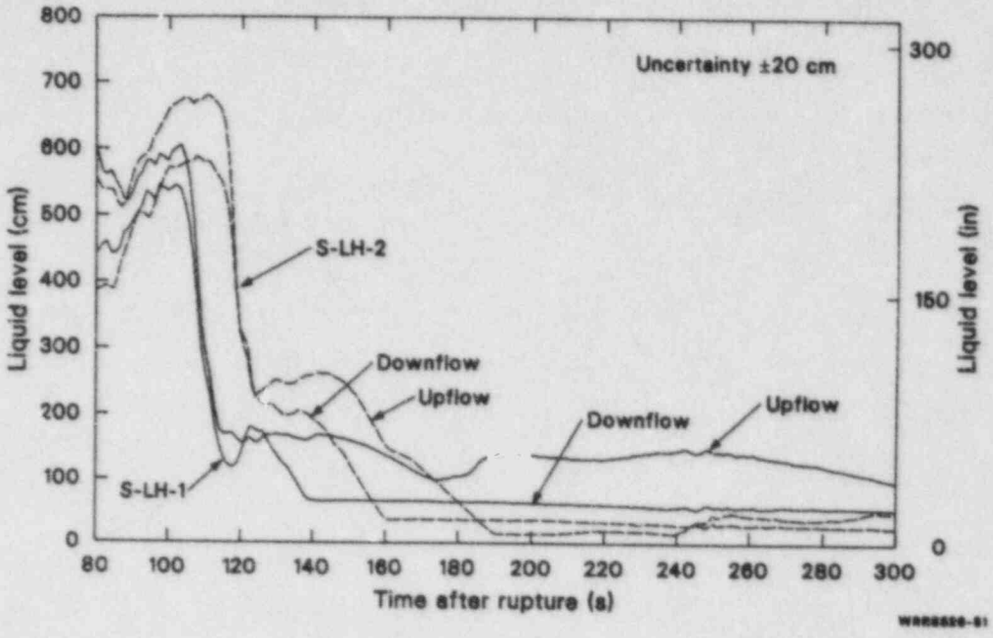

Figure 51. Intact loop steam generator primary U-tube liquid levels for 5% SBLOCA Experiments S-LH-1 (0.9% bypass flow) and S-LH-2 (3.0% bypass flow).

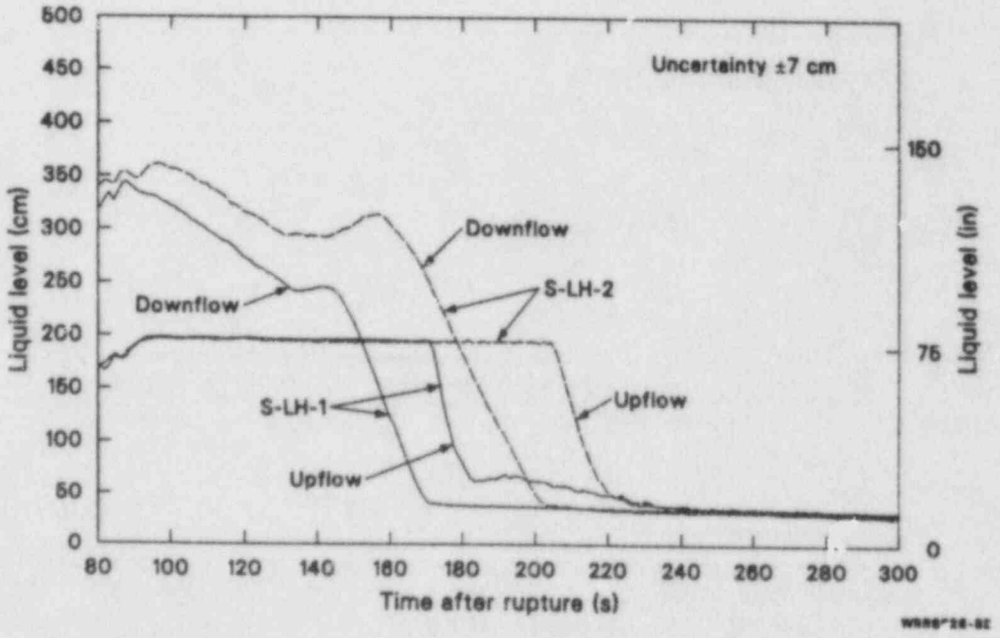

Figure 52. Intact loop pump suction liquid level for 5% SBLOCA Experiments S-LH-1 (0.9% bypass flow) and S-LH-2 (3.0% bypass flow).

as shown on Figure 53. The downflow side is partially cleared of fluid; however, the upflow side remained nearly full. The increased bypass flow was enough to relieve pressure in the vessel which relieved the manometric balance throughout the loop.

In terms of severity, the 3.0% core bypass case resulted in a less severe core liquid level depression than for the 0.9% core bypass case. Figure 54 compares the vessel levels for the 0.9% and 3.0% core bypass cases, showing the same basic level response but with reduced core level depression during the manometric balance period for the 3.0% case. With the increased bypass flow for the 3.0% case and the resulting earlier upper head drain of liquid to the top level of the bypass line, more steam was relieved from the core, causing a general relaxation of the core level depression. The core liquid level depressed only to near the level of the bottom of the suctions [226 cm (90 in.) above the bottom of the core] for the 3.0% case. It is essential to note that the net heads of fluid in the steam generator primary tubes in both the broken and intact loops are similar at the time of minimum core level depression for the high and low bypass flow cases[a] (Figures 55 and 56). In both S-LH-1 and S-LH-2, where *only* the bypass flow was changed, the net head across the steam generator is simply the heads associated with the ongoing reflux mode in each loop. The implication of a similar head across the steam generator tubes, but with an enhanced core level depression for the lower bypass flow case, is that the increased steam relief path and lack of an upper head fluid head alone precluded the additional core level depression seen for the lower bypass flow case.

Unlike the 0.9% core bypass case, no core rod heat-ups were observed during the manometric core liquid depression for the 3.0% core bypass case. Figure 57 compares cladding temperature responses for the 0.9% and 3.0% case; there is no heat-up during the first level depression and a less extensive heat-up during the core boil-off phase for the 3.0% case.

Accumulator flow was different for S-LH-1 and S-LH-2, causing a faster filling of the vessel for S-LH-2 (see Figure 53). During S-LH-2, due to operational differences, no accumulator flow entered the broken loop; however, the intact loop accumulator flow was almost double the specified amount, causing a much faster refill of vessel level for S-LH-2 than S-LH-1. Due to the slightly different depressurization rate shown for S-LH-2, the accumulator pressure set point was not reached until about 575 s (compared to 504 s for S-LH-1). This extra 71 s of core boil-off for S-LH-2 resulted in the vessel liquid level being at about the same level as S-LH-1 when the accumulator finally began to inject (see Figure 54).

a. Previous studies of 5% SBLOCA response with 1.1% (S-UT-8) and 4.0% (S-UT-6) bypass flow claimed that differences in steam generator heads caused the difference in core level. However, based on S-LH-1 and S-LH-2 results, it is suspected that hardware changes and different boundary conditions effected the difference in steam generator heads.

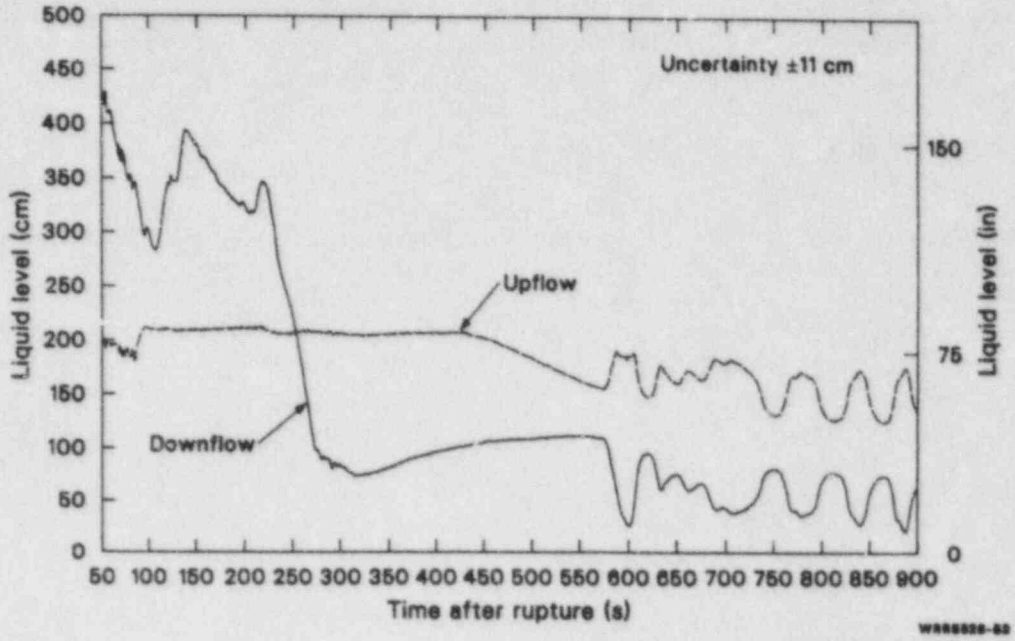

Figure 53. Broken loop pump suction liquid level for 5% SBLOCA Experiment S-LH-2 (3.0% bypass flow).

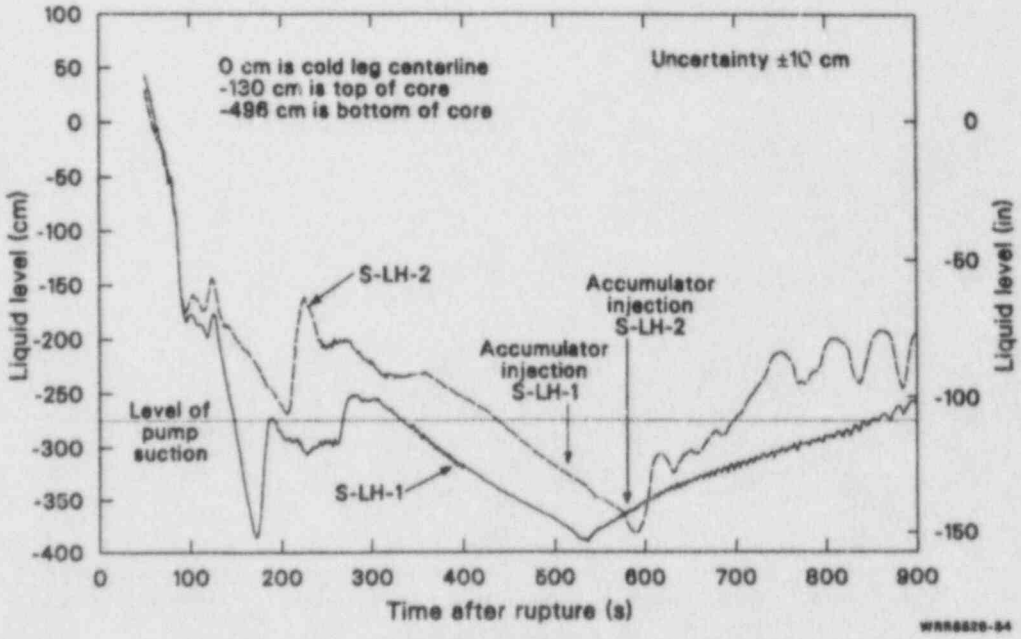

Figure 54. Vessel liquid level for 5% SBLOCA Experiments S-LH-1 (0.9% bypass flow) and S-LH-2 (3.0% bypass flow).

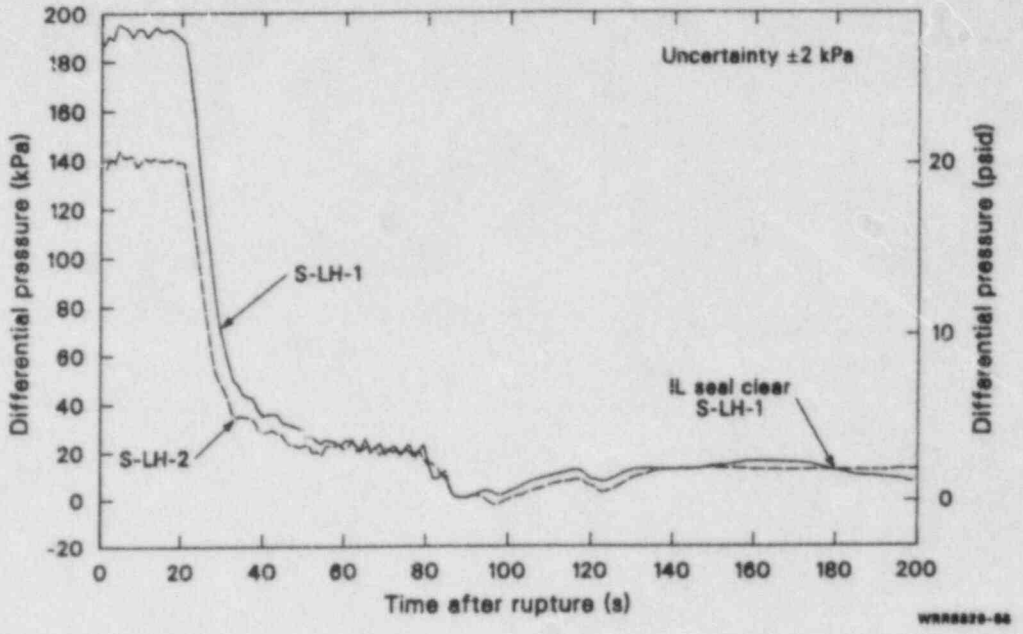

Figure 55. Differential pressure across the broken loop steam generator primary tubes (inlet to outlet) for 5% SBLOCA Experiments S-LH-1 (0.9% bypass flow) and S-LH-2 (3.0% bypass flow).

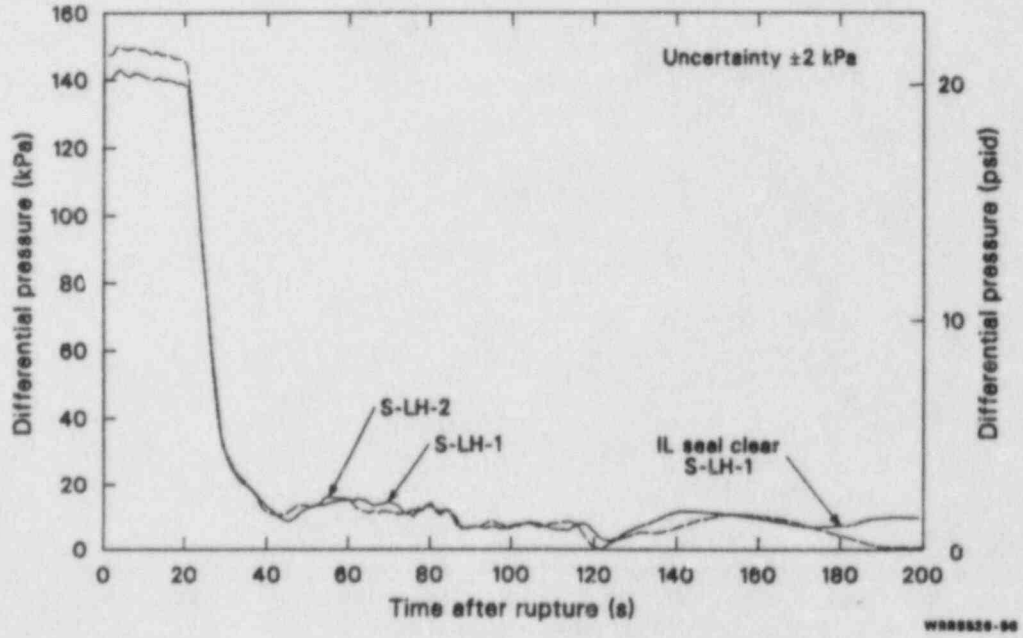

Figure 56. Differential pressure across the intact loop steam generator primary tubes (inlet to outlet) for 5% SBLOCA Experiments S-LH-1 (0.9% bypass flow) and S-LH-2 (3.0% bypass flow).

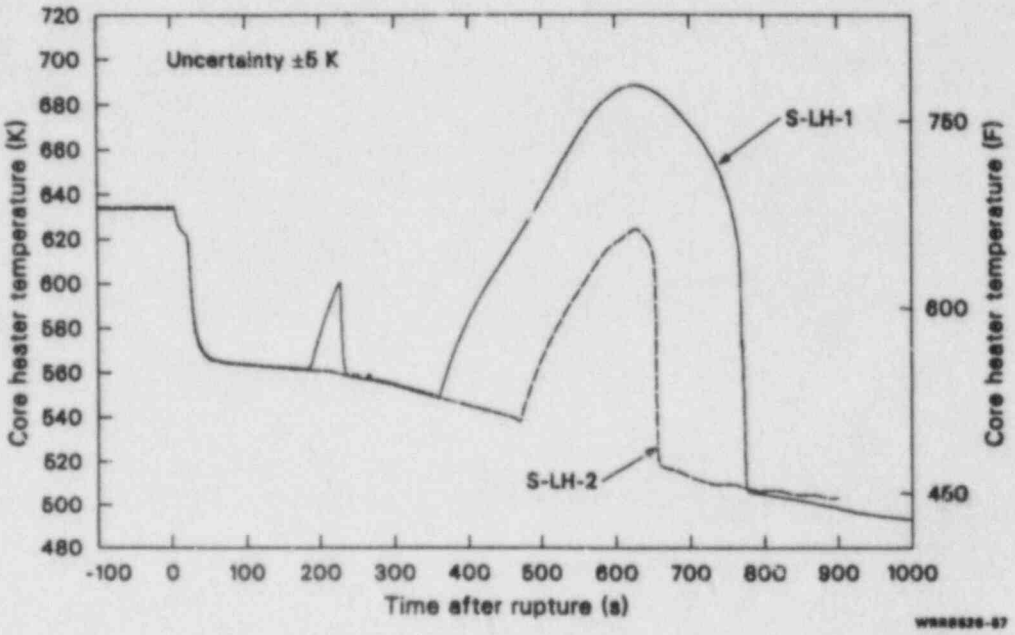

Figure 57. Core heater rod temperature during 5% SBLOCA Experiments S-LH-1 (0.9% bypass flow) and S-LH-2 (3.0% bypass flow).

COMPARISON OF RELAP5 POSTEXPERIMENT CALCULATIONS TO DATA

This section presents a comparison of the postexperiment RELAP5[10] calculated results with S-LH-1 and S-LH-2 experimental data. The adequacy of the Semiscale RELAP5 computer code model for calculating the important thermal-hydraulic responses is discussed. The overall system response, the system fluid mass distribution, and the core response are each discussed separately. Sensitivity calculations as related to the core response are also discussed. The model used in the RELAP5 calculation and the initial and boundary conditions are described in Appendix A. Since experiments S-LH-1 and S-LH-2 were identical except for the bypass flow, most of the discussion will center around S-LH-1. Tables and figures for S-LH-2, corresponding to the ones shown for S-LH-1, are given in Appendix B.

Overall Response

A comparison of primary pressure response data for S-LH-1 and the RELAP5 calculation is shown in Figure 58. Since the calculated pressure agrees very well with the experimental pressure early in time (0 to 40 s), reactor scram, MSIV closure, pump coastdown initiation, and HPIS initiation were all calculated to occur at nearly the same times as they occurred in the experiment (Table 3). However, when the break uncovered (at 185 s in the experiment and 215 s in the calculation, Figure 59) and only steam flowed out the break, RELAP5 calculated a larger depressurization rate than occurred during the experiment. This larger depressurization rate resulted in the activation of the accumulators earlier than in the experiment, thus the boil-off and corresponding heater rod temperature excursions were not calculated.

Basically, primary pressure is an indicator of the energy in the system and is affected by primary-to-secondary heat transfer, fluid-to-primary-piping heat transfer, and energy carried out of the system by the break flow. Since the pressure (Figure 58), density (Figure 59), and fluid mass flow (Figure 60) at the break are approximately the same as in the experiment when the break uncovers, the calculated primary system depressurization should be the same as in the experiment; but it is not. This result points to a problem in RELAP5, as the fluid mass flow out of the system is calculated correctly while the associated energy out of the system is too large. The primary-to-secondary heat transfer or the fluid-to-primary-piping heat transfer or the energy associated with the break flow is being improperly calculated by RELAP5.

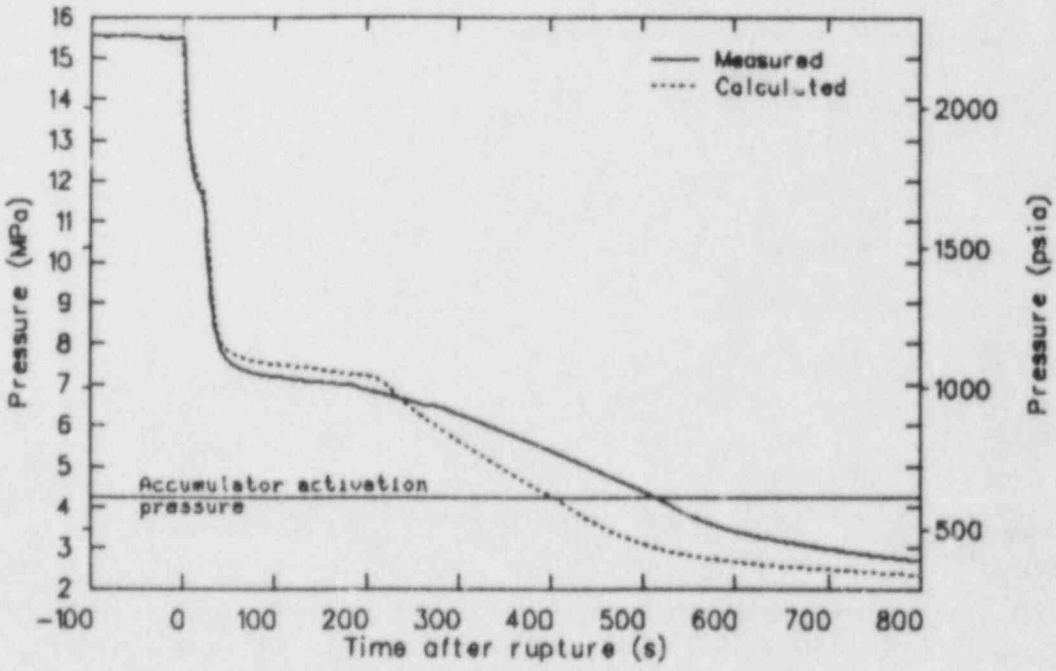

Figure 58. Comparison of measured (S-LH-1) and calculated (RELAP5) primary system pressures.

Table 3. Comparison of calculated and measured sequence of events for S-LH-1.

Event	Time (s)	
	Measured	RELAP5
Break opened	0.5	0.0
Pressurizer at 12.6 MPa (1827 p.ia)	14.67	16.50
Core scram	19.57	21.15
Pump coastdown initiated		
Intact loop	21.35	21.25
Broken loop	20.76	20.90
Feedwater off		
Intact loop	19.67	21.50
Broken loop	19.00	21.50
MSIV closure		
Intact loop	22.0	23.85
Broken loop	22.0	23.85
HPIS initiated		
Intact loop	41.60	42.85
Broken loop	40.98	42.85
Pressurizer emptied	33.9	35.0
Minimum core liquid level reached[a]	172.6	180.0
Break uncovered	184.6	213.8
Intact loop pump suction cleared	171.4	184.0
Broken loop pump suction cleared	262.3	178.0
Accumulator flow initiated		
Intact loop	503.8	401.1
Broken loop	501.4	401.1

a. Minimum measured level was -386 cm (-152 in.), and minimum calculated level was -483 cm (-190 in.).

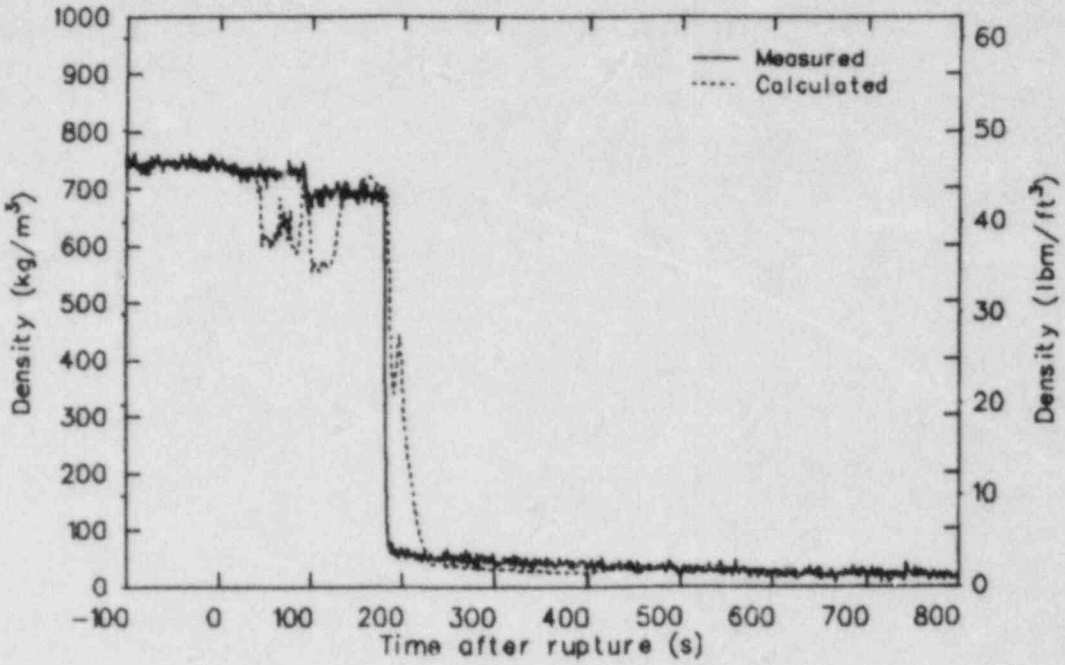

Figure 59. Comparison of measured (S-LH-1) and calculated (RELAP5) upstream break densities.

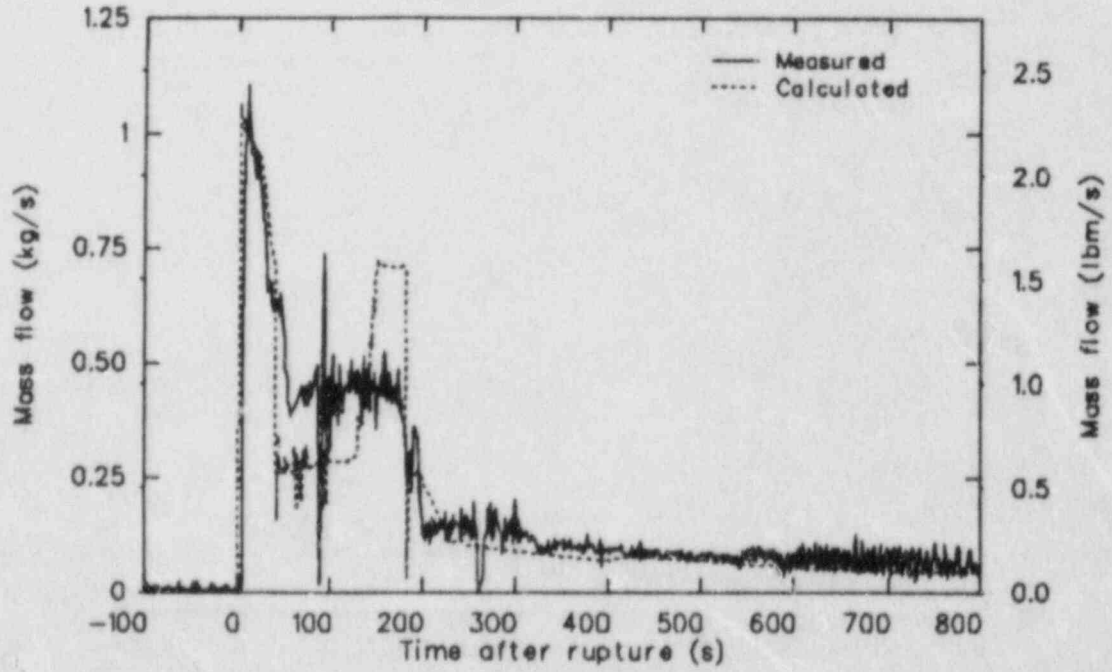

Figure 60. Comparison of measured (S-LH-1) and calculated (RELAP5) break mass flow rates.

System Mass Distribution

RELAP5 calculated the system to drain in much the same way as was observed in the experiment. First, the pressurizer emptied (Figure 61); then the upper head began to drain (Figure 62). The fluid mass flow out of the pressurizer was lower than the break flow (Figure 63), so liquid was removed from the reactor vessel as soon as the break was opened.

The calculated initial drain rate of the upper head was larger than was observed in the experiment. Different loss coefficients were tried in the guide tube to adjust the upper head drain rate using the upper head drain rates for both S-LH-1 and S-LH-2 as the boundary conditions; the loss factors used in these calculations were a compromise between the two drains. It is, however, important to note that in both the experiments and the RELAP5 calculations the upper head level was above the top of the bypass line in S-LH-1 and below the top of the bypass line in S-LH-2 (Figure 64) when the minimum core liquid level was reached. The minimum core liquid level depends on when a steam path is established from the core through the upper head and bypass line to the downcomer. If this steam path is established early in the transient, the core liquid level will not fall below the level of the pump suctions.

As the pressurizer emptied, the primary system depressurized rapidly and became saturated. Vapor was formed in the core, and bubbles became entrained in the fluid. The pumps forced this two-phase mixture around the loops and out the break. When the two-phase mixture reached the break (at 45 s in the experiment and 40 s in the calculation), the break flow (Figure 65) dropped significantly. Although RELAP5 used the horizontal stratification model to account for vapor pull-through and liquid entrainment, the calculated break flow was 65% of the observed break flow during the two-phase flow period (40 to 130 s).

The two-phase forced circulation when the pumps were running was correctly calculated by RELAP5. After the pumps stopped, differences appeared between the observed and calculated flow in the loops. Although the type of flow was correctly calculated for both loops, significant differences in the duration and the effect these flows had on the transient resulted.

When the pumps stopped at 90 s, two-phase natural circulation became established in the intact loop in both the experiment and the calculation. In the experiment, this allowed all of the decay heat to be dissipated in the intact loop, allowing the broken loop U-tubes to drain (Figure 66) until reflux became established (110 s). With reflux established, the broken loop could then remove the

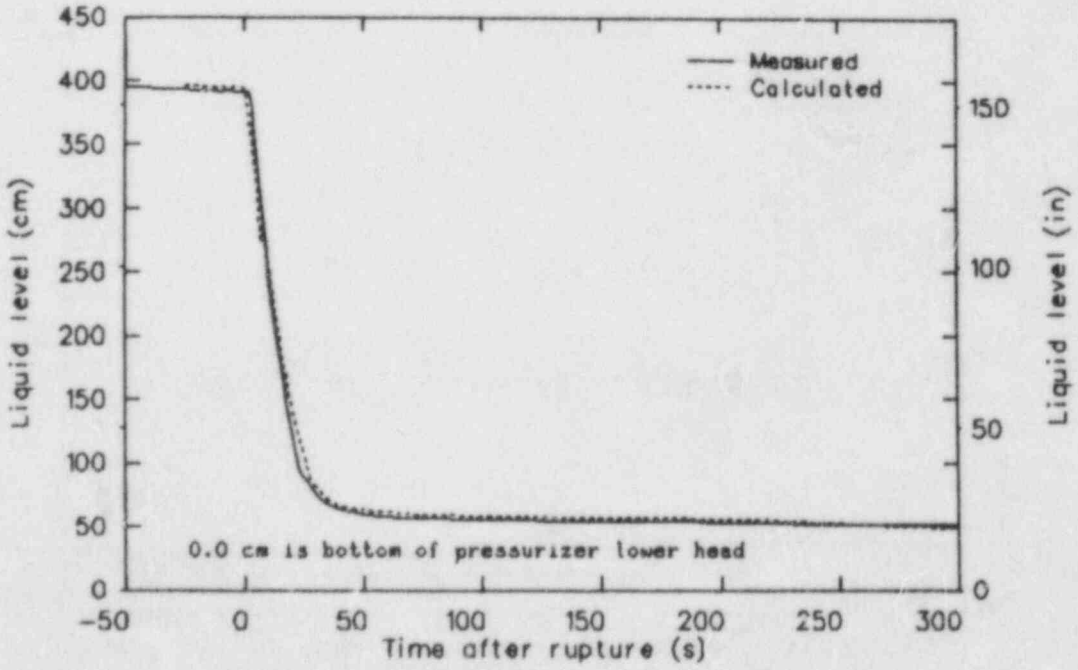

Figure 61. Comparison of measured (S-LH-1) and calculated (RELAP5) pressurizer collapsed liquid levels.

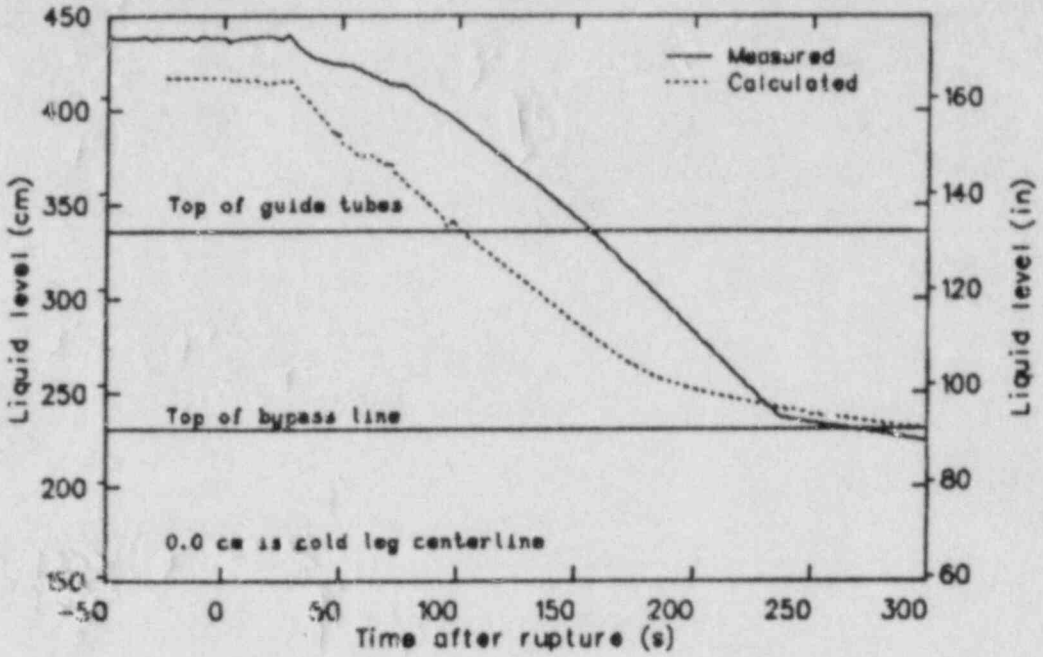

Figure 62. Comparison of measured (S-LH-1) and calculated (RELAP5) upper head collapsed liquid levels.

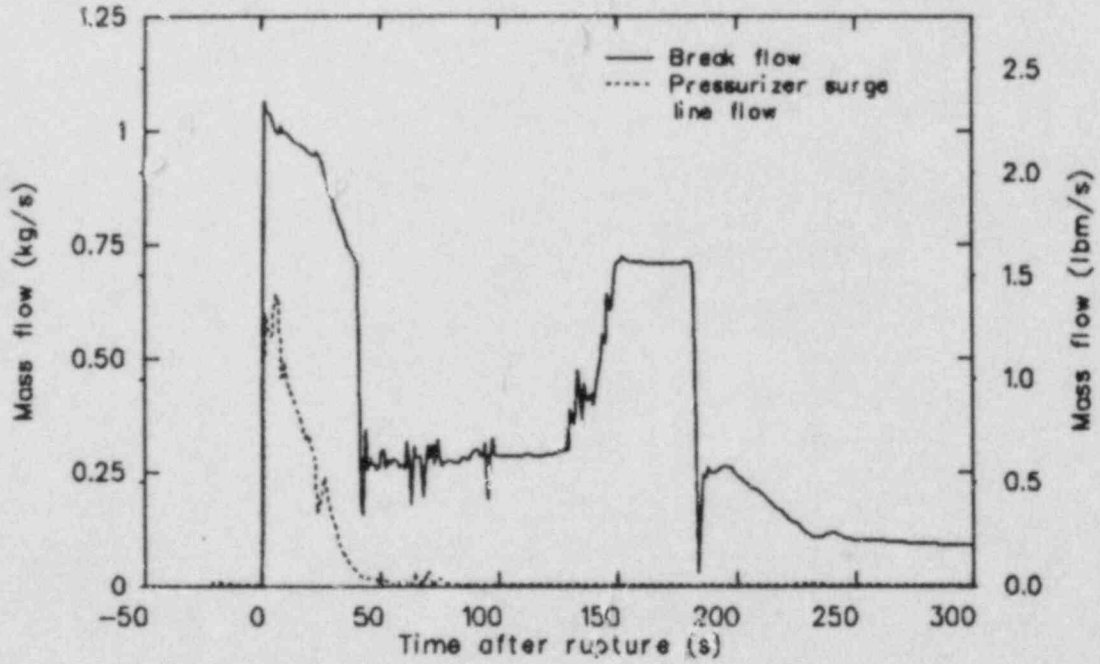

Figure 63. Comparison of calculated (RELAP5) break and pressurizer surge line mass flow rates.

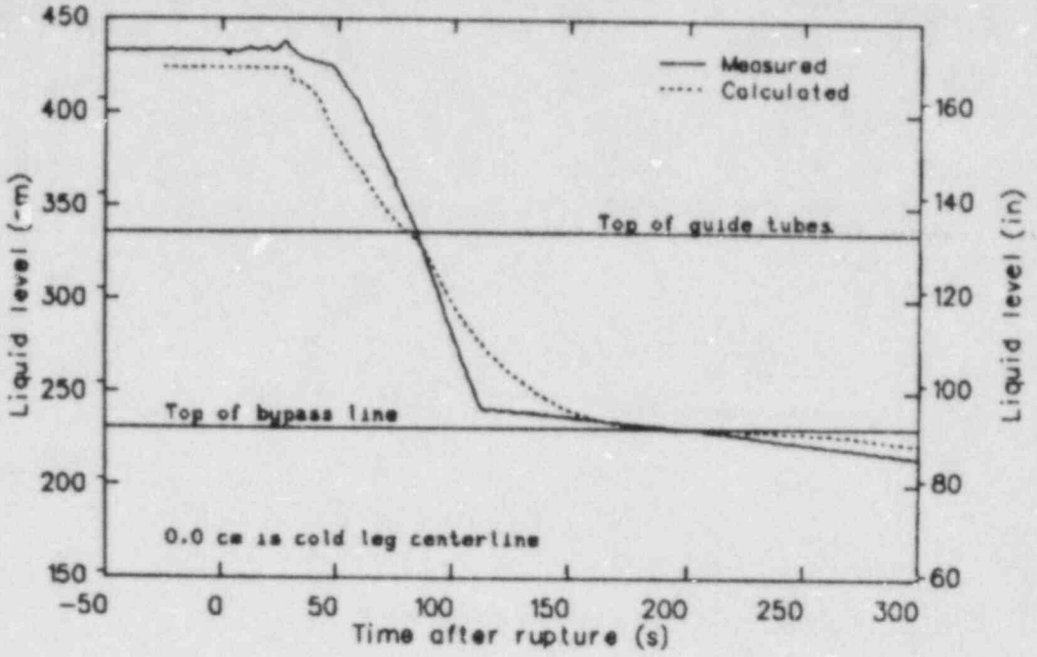

Figure 64. Comparison of measured (S-LH-2) and calculated (RELAP5) upper head collapsed liquid levels.

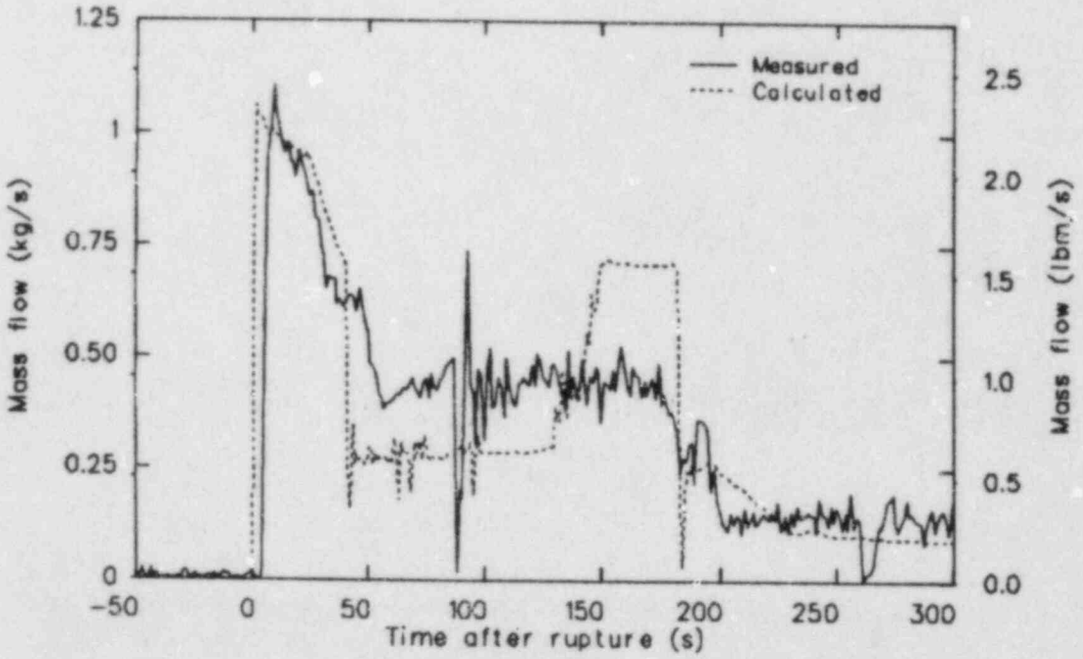

Figure 65. Comparison of measured (S-LH-1) and calculated (RELAP5) break mass flow rates during core level depression.

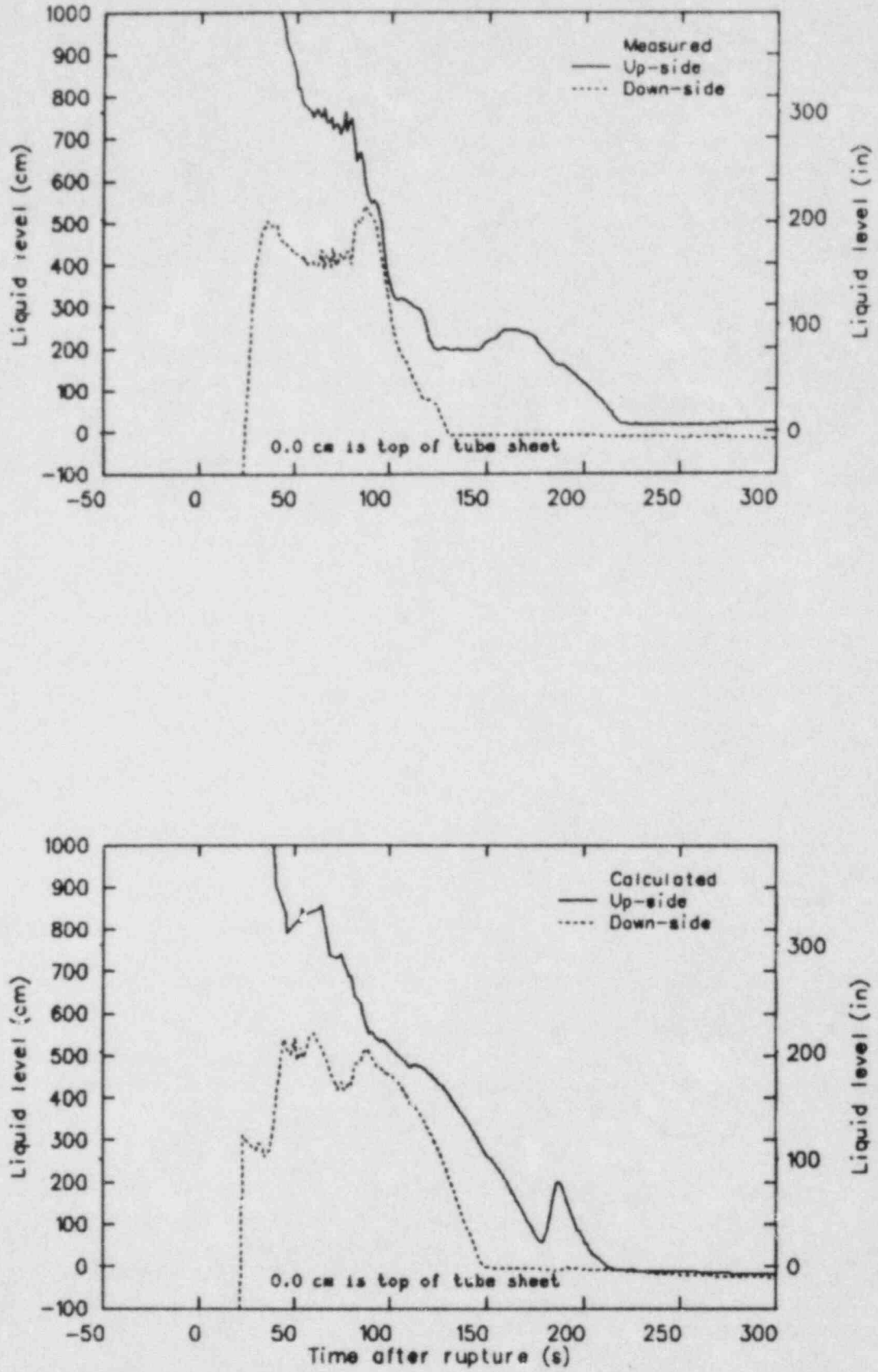

Figure 66. Comparison of measured (S-LH-1) and calculated (RELAP5) broken loop U-tube collapsed liquid levels.

decay heat, allowing the intact loop U-tubes to drain (Figure 67). The reflux in the broken loop U-tubes could not remove all the decay heat, so reflux was also established in the intact loop U-tubes by 120 s. During reflux, steam continued to condense on the upflow side of the U-tubes while the downflow sides drained. This condensate caused a manometric imbalance across the U-tubes which resulted in the core liquid level being depressed.

In the calculation, reflux[a] was established in the broken loop steam generator U-tube before the pumps stopped (Figure 68). This caused the intact loop U-tubes to drain down approximately 1.0 m (3.3 ft), as opposed to the 4.5 meters (14.8 ft) in the experiment. The intact loop upside U-tube drain then slowed as reflux became established; and a quasi-steady state in the core resulted, with the upper head draining and maintaining the core level at approximately 175 cm (69 in.) (Figure 69). When reflux was fully established in the intact loop U-tube at 130 s, the core level was depressed in the calculation for the same reasons as in the experiment. Since it is the differential pressure across the steam generator U-tubes that results in the core liquid level depression, no important phenomena were missed by not calculating the early drains in the U-tubes. However, with a higher calculated U-tube liquid level, less fluid was available to the core, contributing to a more severe calculated core level depression, although the calculated rate of depression was correct. More significant, however, is that RELAP5 did not calculate a heater rod temperature excursion (Figure 70) with this more severe depression.

The core liquid level depression was alleviated by the clearing of the pump suctions in both the experiment and the calculation (Figures 71 and 72). RELAP5, however, calculated the pump suctions to clear at the same time; while in the experiment, the broken loop pump suction cleared 80 s after the intact loop.[b] The more symmetrical draining of the intact and broken loop U-tubes in the calculation caused this difference in pump suction clearing. As a result of clearing both pump suctions at the same time, the core recovered to a higher liquid level in the calculation (Figure 69). When the broken loop pump suction did clear in the experiment, the core liquid level rose to the level calculated by RELAP5. Therefore, when boil-off began at 300 s, not only had the same amount of fluid mass been lost through the break (Figure 73) and added by HPIS (Figure 74) in both the experiment and calculation, but the mass was distributed throughout the primary system in the same way.

When the pumps were running, the fluid that flowed out the break came from the broken loop cold leg. However, when the pumps stopped at 90 s, the flow reversed; and the fluid that flowed out the break came from the intact loop cold leg in both the experiment and the calculation. Because the intact loop was in two-phase natural circulation, the break flow was also two-phase. However, when the intact loop went into reflux in the calculation (130 s), the break flow became single-phase liquid. This resulted because all the steam that flowed into the intact loop steam generator U-tube was condensed on the upside of the U-tubes, creating stagnation at the top of the U-tube. The vapor on the down-side of the U-tube then reversed and by buoyant forces flowed up the down-side of the U-tube. As a result, single-phase liquid was left in the intact loop pump suction and cold leg to flow out the break until the pump suction cleared. This did not happen in the experiment, but the increased break flow due to single-phase liquid allowed the calculation to catch up with the total amount of mass that was observed to flow out the break.

The clearing of the intact loop pump suction also resulted in break uncovery. When the break uncovers, vapor flows out the break, increasing volumetric break flow and primary coolant system depressurization rate (Figure 58). The depressurization rate as a result of break uncovery was larger in the RELAP5 calculation than was observed in the experiment. The steam that flowed out the break was calculated to be at nearly the same pressure, density, and flow rate as the experiment, which should have resulted in the same depressurization rate if primary-to-secondary heat transfer and fluid-to-primary piping heat transfer were identical to the experiment. Since these heat transfer parameters were unavailable in the experiment, it is unclear what caused the larger depressurization rate. As a result of the larger depressurization rate, the accumulator pressure set point was reached much earlier in the calculation than in the experiment. This allowed liquid from the accumulators to

a. Reflux is evidenced in RELAP5 when liquid downflow occurs against vapor upflow in the presence of condensing vapor.

b. In S-LH-2, the broken loop pump suction did not clear in either the experiment or the calculation.

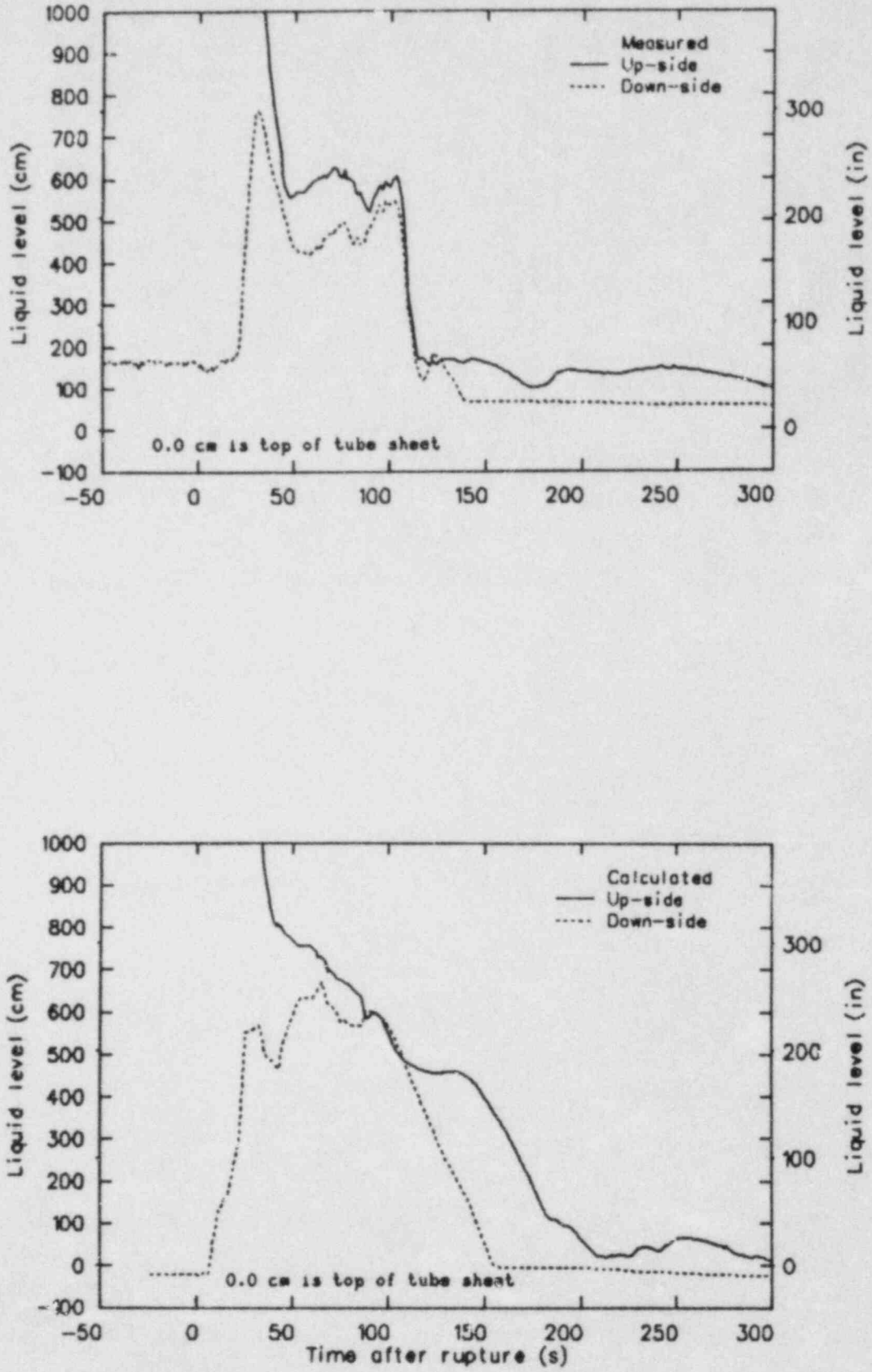

Figure 67. Comparison of measured (S-LH-1) and calculated (RELAP5) intact loop U-tube collapsed liquid levels.

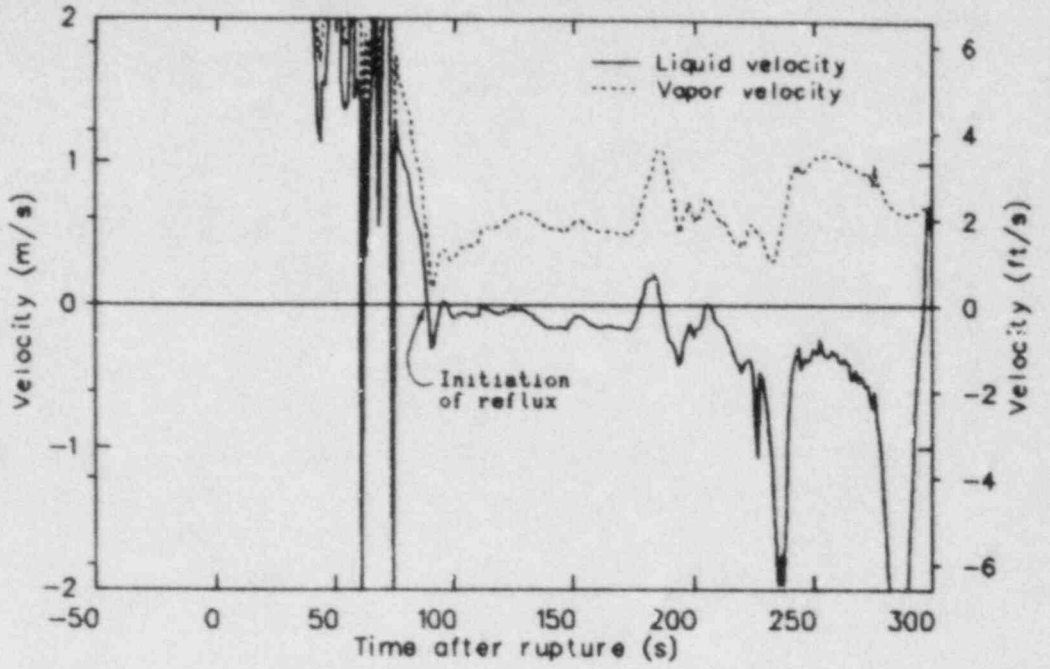

Figure 68. Calculated (RELAP5) liquid and vapor velocities at the broken loop steam generator inlet.

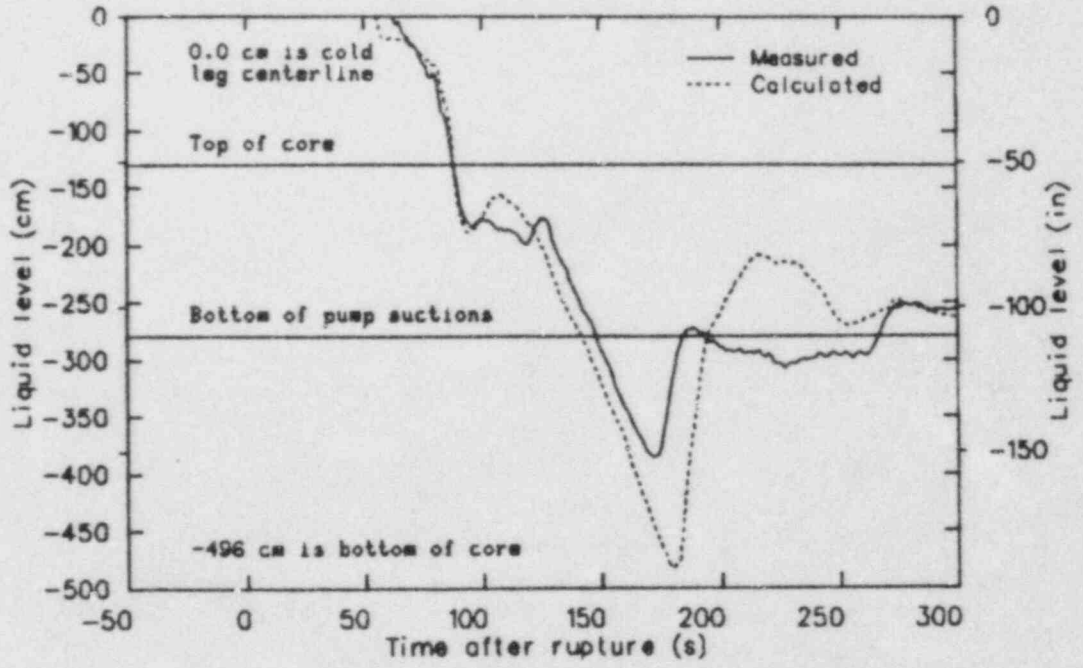

Figure 69. Comparison of measured (S-LH-1) and calculated (RELAP5) vessel collapsed liquid levels.

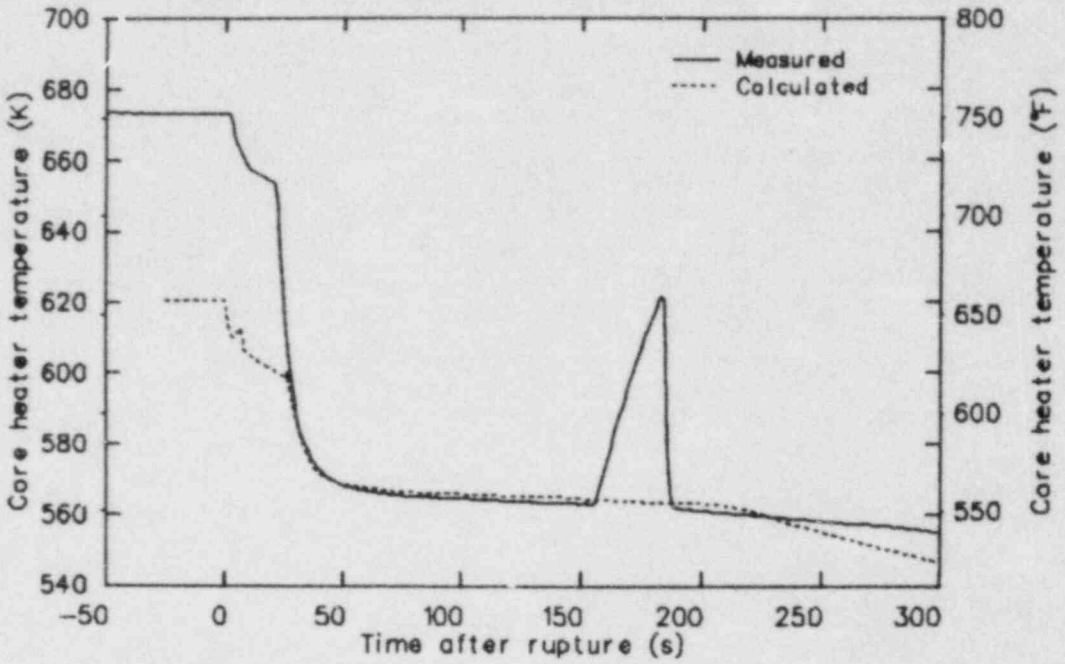

Figure 70. Comparison of measured (S-LH-1) and calculated (RELAP5) maximum core heater rod temperatures.

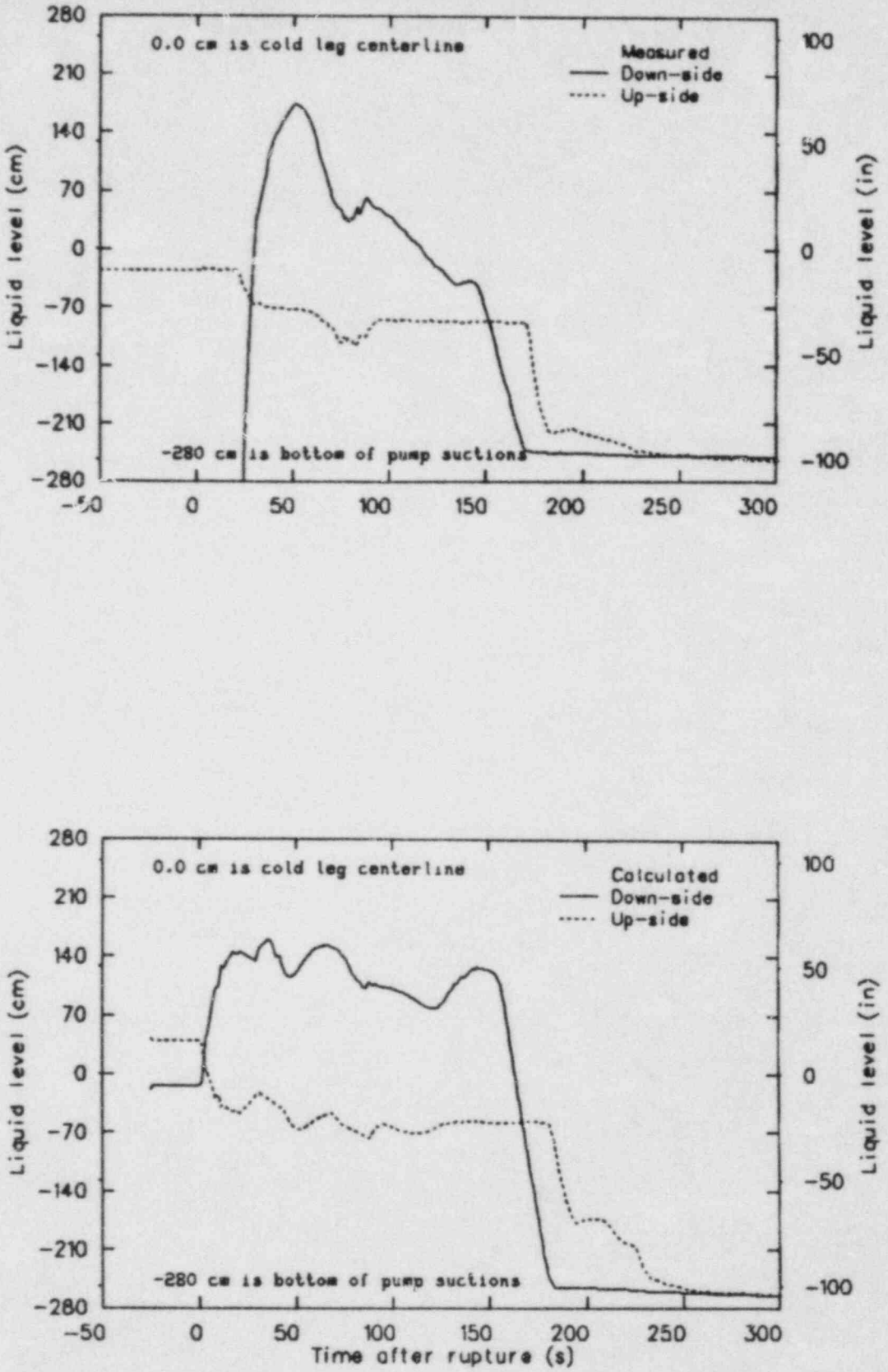

Figure 71. Comparison of measured (S-LH-1) and calculated (RELAP5) intact loop pump suction collapsed liquid levels.

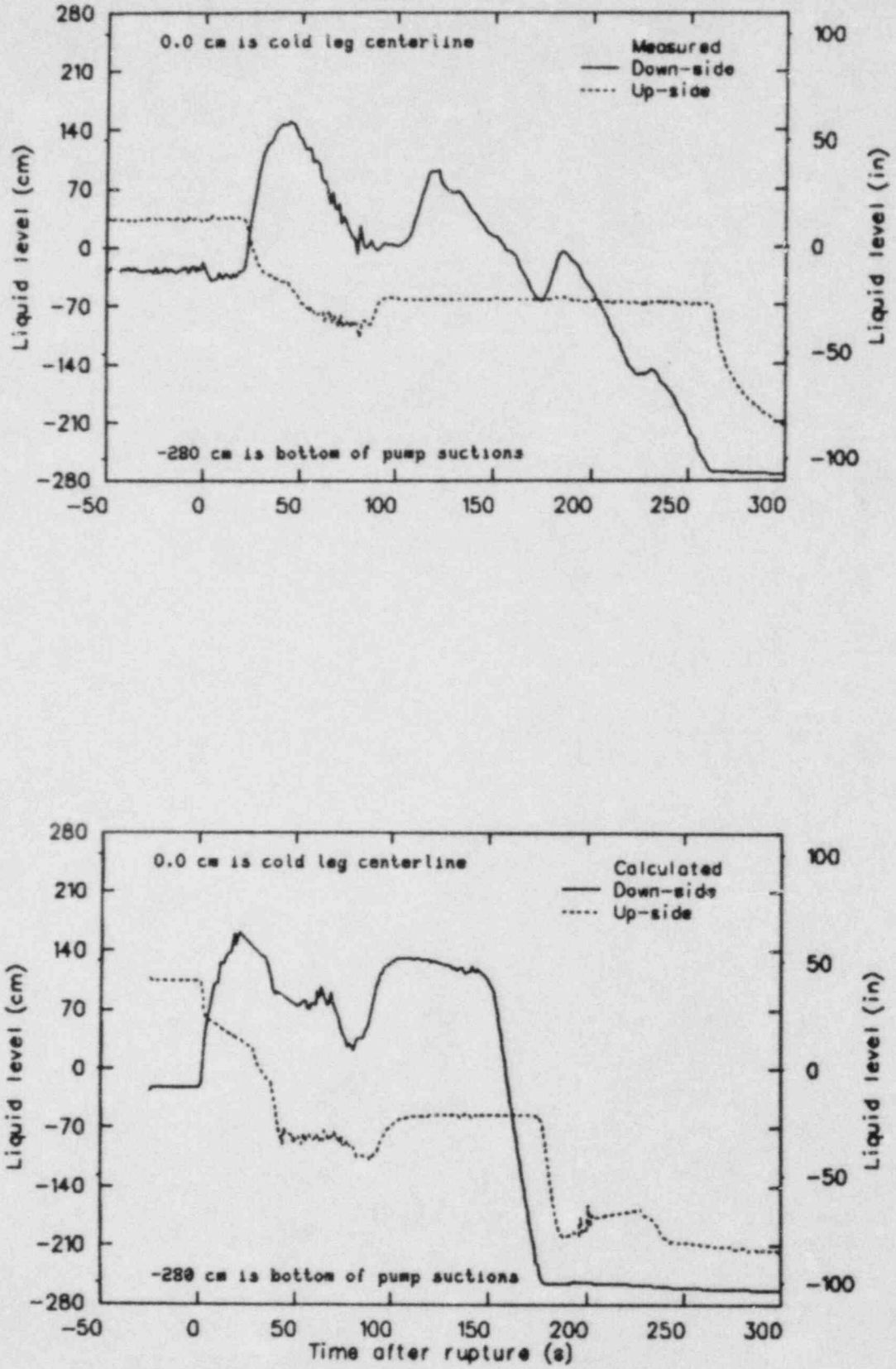

Figure 72. Comparison of measured (S-LH-1) and calculated (RELAP5) broken loop pump suction collapsed liquid levels.

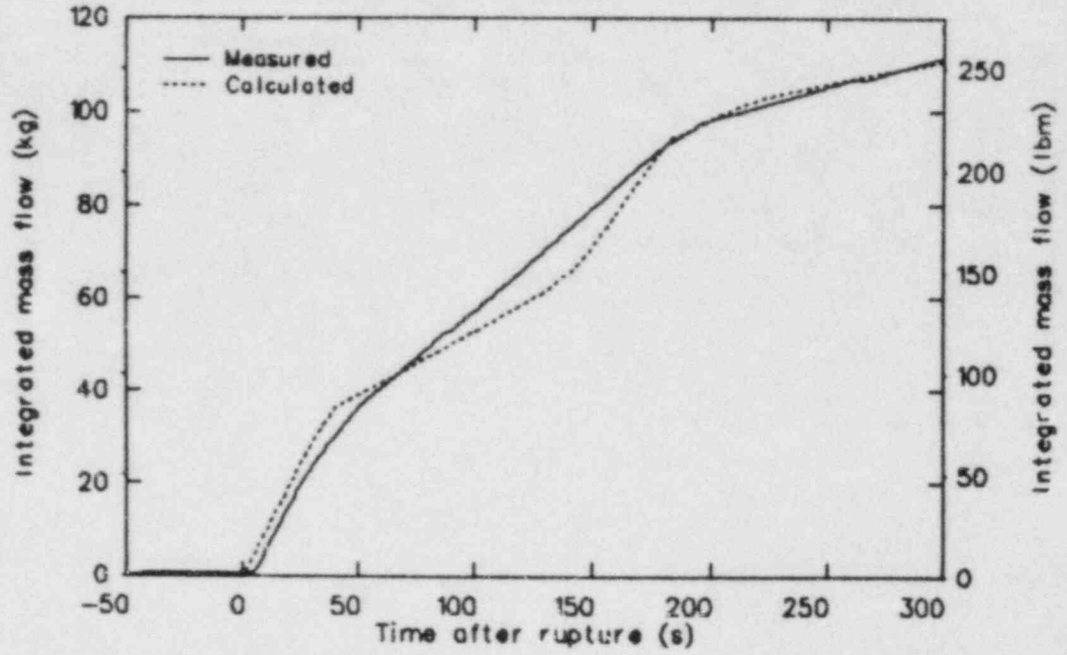

Figure 73. Comparison of measured (S-LH-1) and calculated (RELAP5) integrated break mass flow rates.

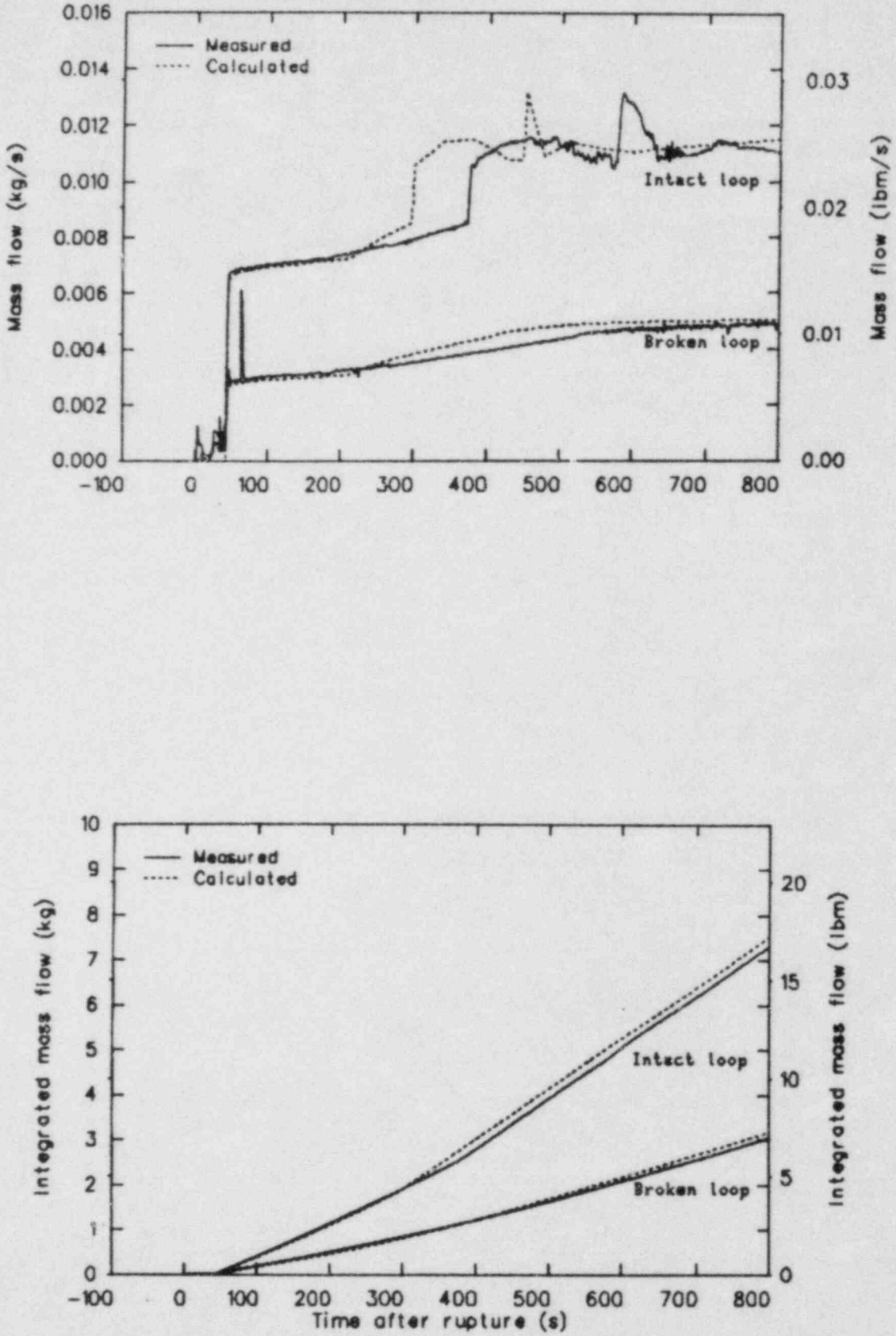

Figure 74. Comparison of measured (S-LH-1) and calculated (RELAP5) HPIS mass flow rates.

flood the core and prevented the boil-off (Figure 75) and subsequent heat-up observed in the experiment (Figure 76). Prior to accumulator injection, RELAP5 calculated a slower boil-off in the core than was observed in the experiment. This was the result of the calculated steam flow out the break being lower than the measured flow (Figure 60). With the exception of the core, the system fluid mass distribution was accurately calculated. More fluid mass was calculated to remain in the core than was observed during the experiment. In the experiment, this additional mass flowed out the break in a higher-than-calculated break flow. After the accumulator set point was reached in the calculation, there was a large difference in the mass in the primary system between experiment and calculation. As a result, there is little value in code-to-data comparisons after this point.

Core Response

In S-LH-1, the core liquid level was depressed below the level of the pump suctions in both the experiment and the RELAP5 calculation. In the experiment, this depression produced heat-ups in the upper portions of the core that were both two- and three-dimensional in nature, as not all the rods had heat-ups at a given elevation and some rods had heat-ups at higher elevations after the heat-ups at lower elevations on other rods were quenched. Although this type of multidimensional behavior is beyond the capabilities of a one-dimensional code such as RELAP5, the calculated core liquid level depression was much more severe than the observed depression and should have produced a heat-up. In previous calculations of other experiments, RELAP5 calculated heat-ups to occur when the core level was as low as levels reached in this calculation (Figure 77). These calculations, however, were done with RELAP5/MOD1 and MOD1.5, not MOD2.

The calculated depression voided 95% of the core, reaching a level of -483 cm (-190 in.).[a] This should have been more than sufficient to produce a heat-up, but did not. RELAP5 calculated almost no axial density variation in the core, while the experiment showed a large density gradient (Figure 78) especially in the upper part of the core. RELAP5, then, calculated a two-phase mixture of almost uniform density to exist throughout the entire core region between 140 and 185 s, while the

a. The top of the core is at -130 cm (-51 in.), and the bottom of the core is at -496 cm (-195 in.).

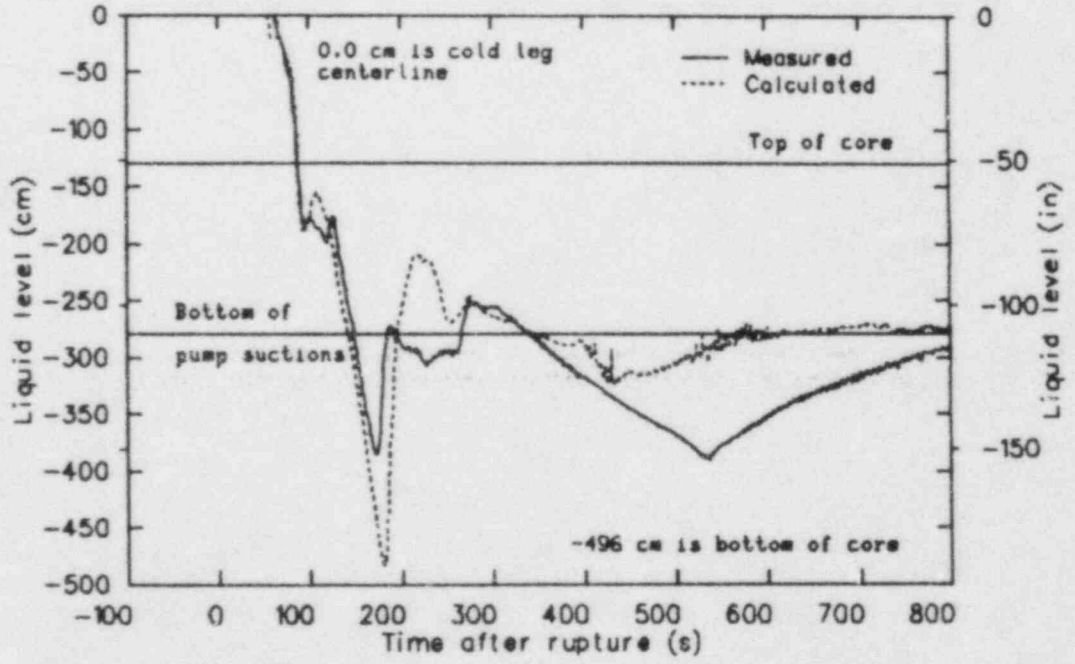

Figure 75. Comparison of measured (S-LH-1) and calculated (RELAP5) vessel collapsed liquid levels.

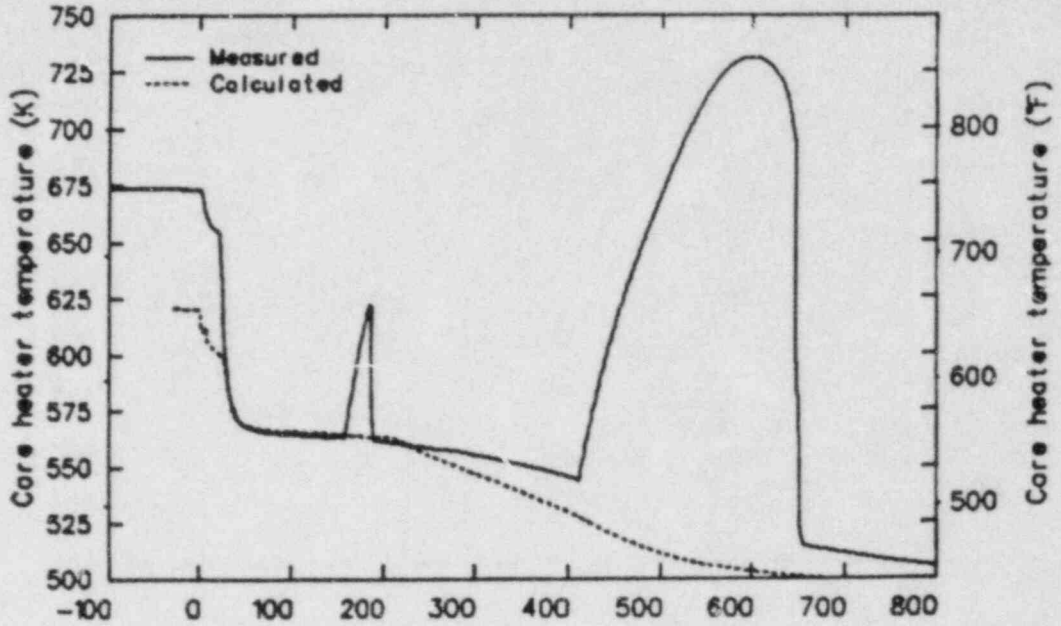

Figure 76. Comparison of measured (S-LH-1) and calculated (RELAP5) maximum core heater rod temperatures.

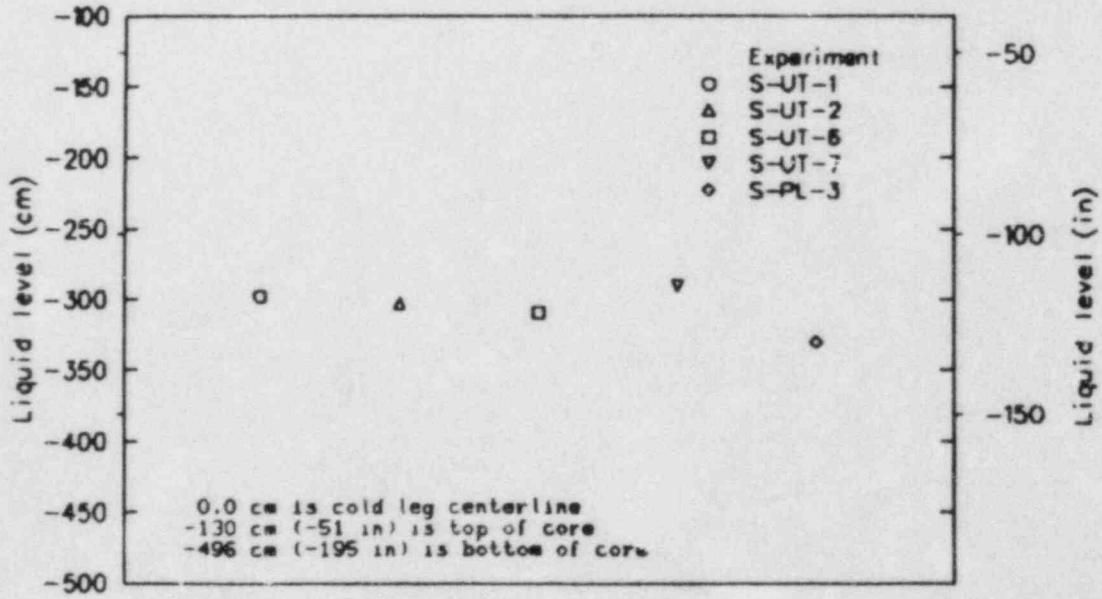

Figure 77. Typical vessel collapsed liquid levels at which RELAP5 calculated a heater rod temperature excursion in Semiscale.

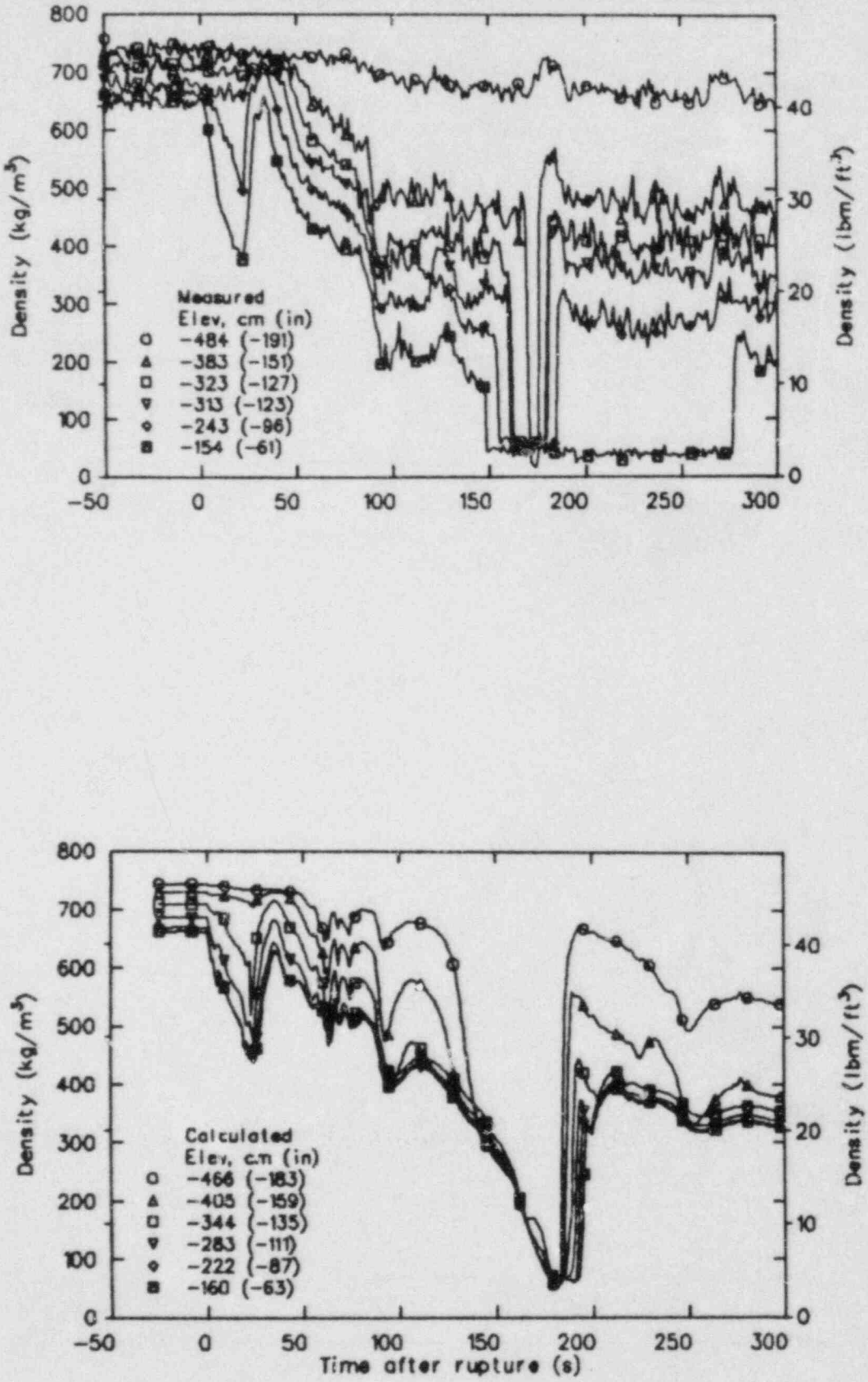

Figure 78. Comparison of measured (S-LH-1) and calculated (RELAP5) core densities (no updates to RELAP5).

experiment showed a highly stratified core. This caused RELAP5 to calculate saturated nucleate boiling in every section of the core, so no heat-up was produced by calculating a core with uniform density. The vertical stratification model in RELAP5 was not operative, as it requires the difference between the void fractions in two adjacent vertical volumes to be greater than 0.50.[10] The nonstratification of the two-phase mixture appears to be caused by too much interfacial drag on the upward moving bubbles, which prevents the liquid from pooling in the lower core regions. Saturated nucleate boiling remained the mode of heat transfer, because a void fraction of 0.9999[a] is required for dryout and single-phase vapor convection. While this void fraction is realistic for a highly localized condition, it may be too high for a discrete volume model like RELAP5 which assumes that the entire volume is at the same thermodynamic state.

To examine the effects of interfacial drag and dryout criterion, two updates to RELAP5 were written. The first arbitrarily set the interfacial drag terms in the core to one-tenth of their calculated values, and the other lowered the void fraction for dryout to 0.94.

The interfacial drag update did cause the core to stratify (Figure 79), although not as much as observed in the experiment. The heat transfer in the lower part of the core changed to subcooled nucleate boiling, while the rest of the core remained in saturated nucleate boiling. The maximum void fraction for any individual volume in the core was 0.991, so no heat-up was calculated. A small heat-up was calculated with the dryout criterion update (Figure 80). The upper portions of the core went into single-phase vapor convection, as the maximum void fraction reached 0.959, lower than without the update. The calculated core level depression was slightly less severe using either update than with no updates (Figure 81).

When the two updates were combined, the calculated core liquid level depression was no more severe than was observed in the experiment (Figure 82). Yet a heat-up, similar to those observed in top portions of the core, was calculated (Figure 83). This heat-up began at -305 cm (-120 in.), almost the same level as in the experiment [-320 cm (-126 in.)]. The less severe core liquid level depression calculated with the updates is not really surprising. The core was more stratified (Figure 85) and so was cooled by subcooled nucleate boiling at the bottom, saturated nucleate boiling in the middle, and single-phase vapor convection at the top. As a result of the single-phase vapor convection, the total vapor generation rate in the core was reduced. With less vapor from the core, the buildup of liquid due to reflux on the upside of the U-tubes was reduced; so the core liquid level depression was correspondingly reduced.

A Comparison of S-LH-1 and S-LH-2

Basically the same phenomena were calculated for both S-LH-1 and S-LH-2. Reflux was established in both loops, leading to a manometric imbalance across the U-tubes. While this imbalance produced a core liquid level depression below the bottom of the pump suctions in S-LH-1, it did not in S-LH-2. The only major initial difference in the two experiments was the core bypass flow rate. This larger flow rate, and therefore larger flow area, enabled the upper head to drain faster in S-LH-2 than in S-LH-1 (Figure 85). A flow path between the core and the break via the guide tube, upper head, and bypass line was thus established earlier in S-LH-2 than in S-LH-1. This flow path allowed steam from the core to flow to the downcomer and out the break so the manometric imbalance across the U-tubes did not result in a core liquid level depression. The calculated core liquid level response (Figure 86) was the same until the flow path through the upper head was established. The U-tube level responses (Figures 87 and 88) were also similar. The upstream break density (Figure 89), however, was not. The only thing that can account for this is the flow through the bypass line. It is therefore the smaller initial bypass flow that resulted in the core liquid level depression calculated in S-LH-1 and not in S-LH-2. This effect was evidenced in both the test and the calculations.

a. Although the core was 95% voided, the maximum void fraction for any volume was 0.984.

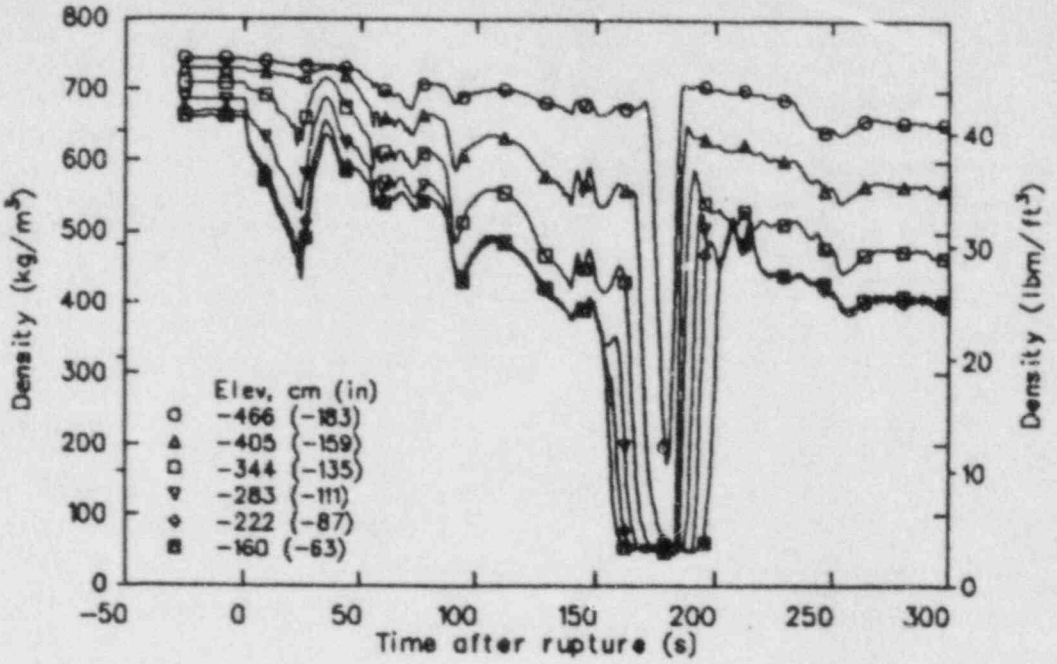

Figure 79. Calculated core densities for S-LH-1 with interfacial drag update to RELAP5.

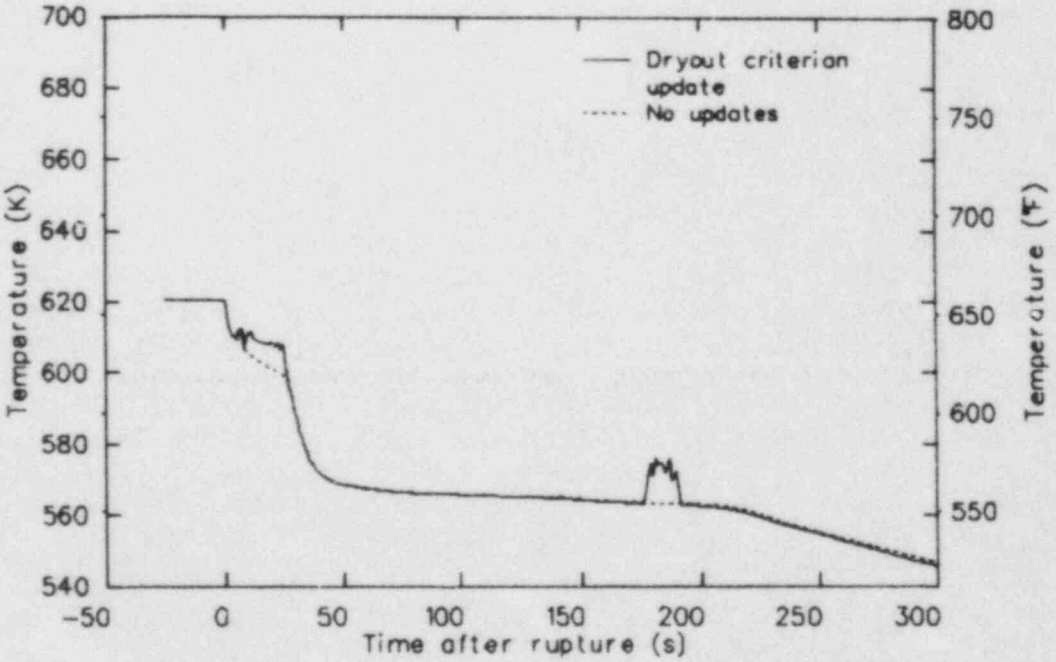

Figure 80. Comparison of calculated maximum rod temperatures for S-LH-1 with and without dryout criterion update to RELAP5.

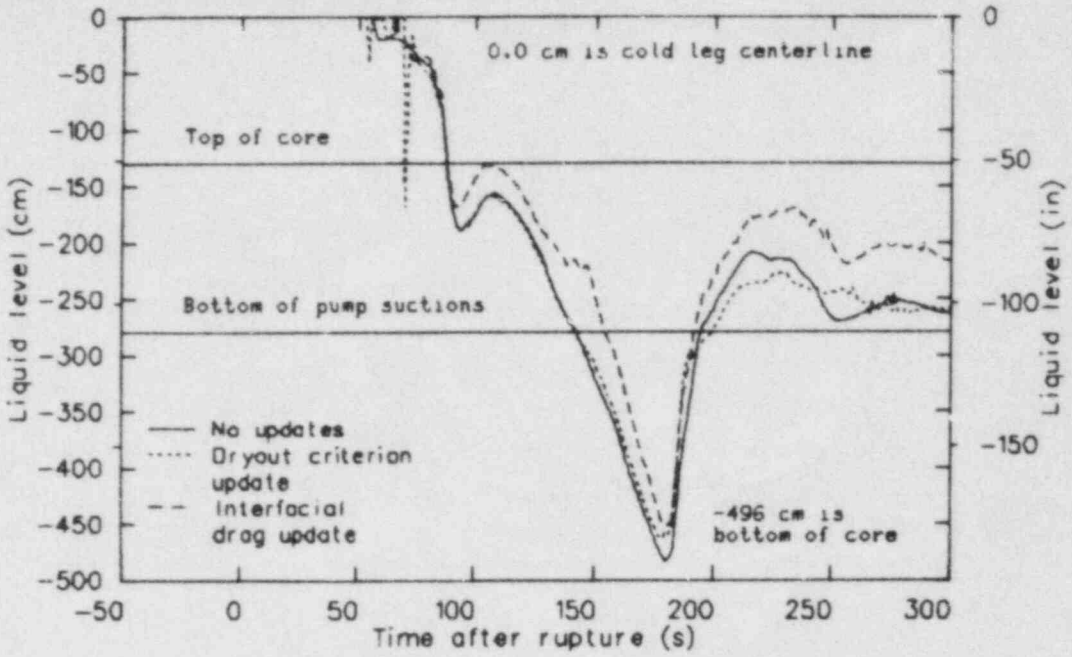

Figure 81. Comparison of calculated vessel collapsed liquid levels with and without updates.

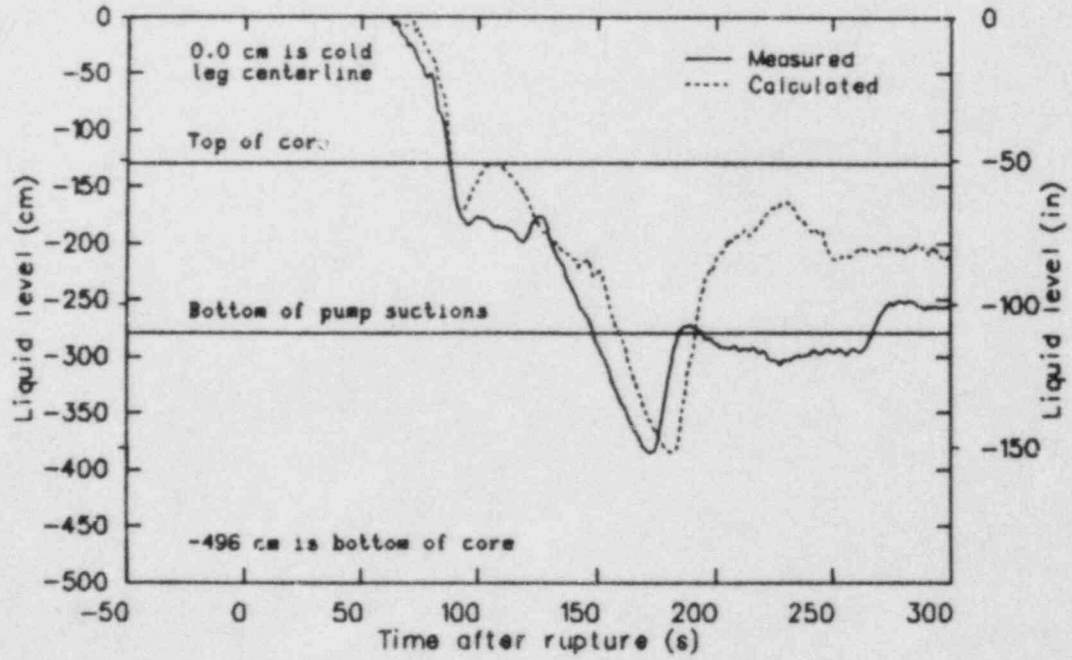

Figure 82. Comparison of calculated (RELAP5) and measured (S-LH-1) vessel collapsed liquid levels with interfacial drag and dryout criterion updates.

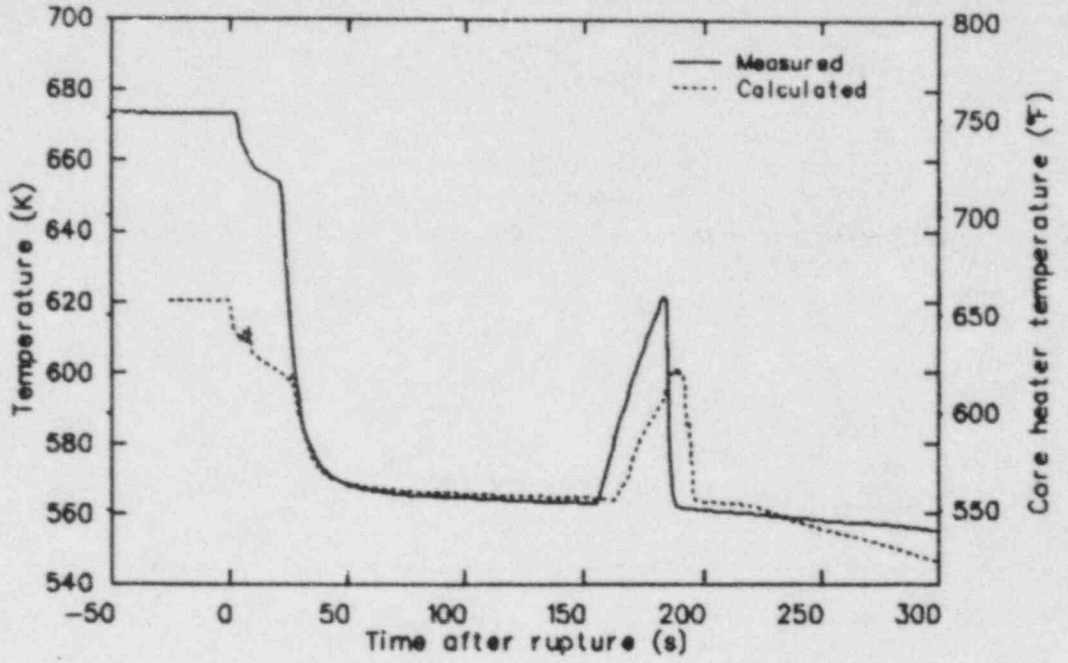

Figure 83. Comparison of calculated (RELAP5) and measured (S-LH-1) maximum heater rod temperatures with interfacial drag and dryout criterion updates.

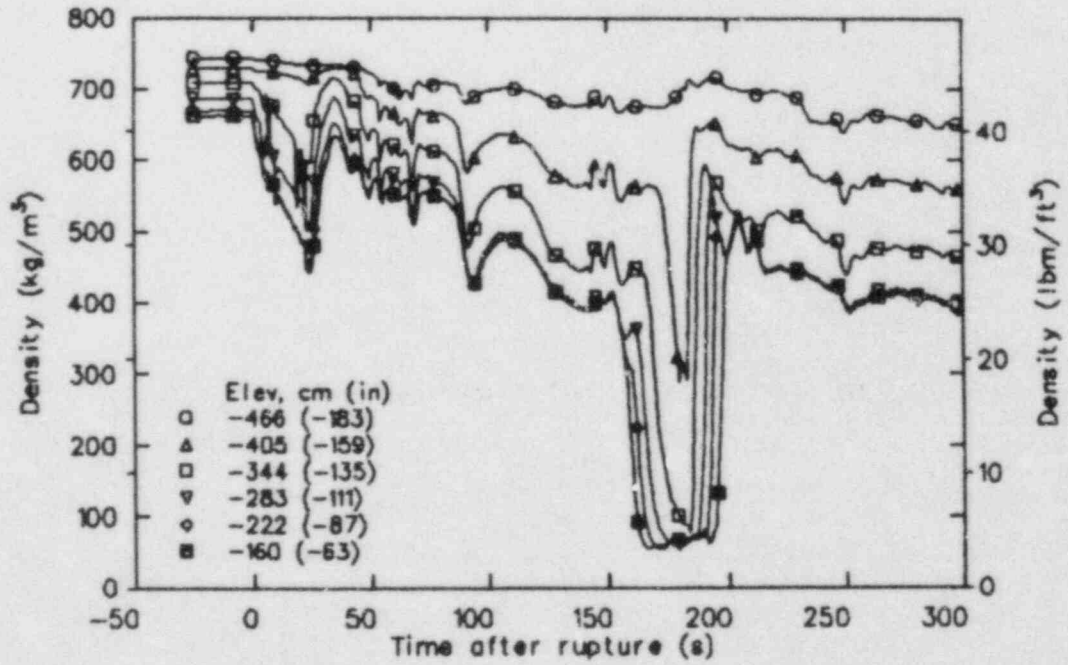

Figure 84. Calculated core densities for S-LH-1 with interfacial drag and dryout criterion updates to RELAP5.

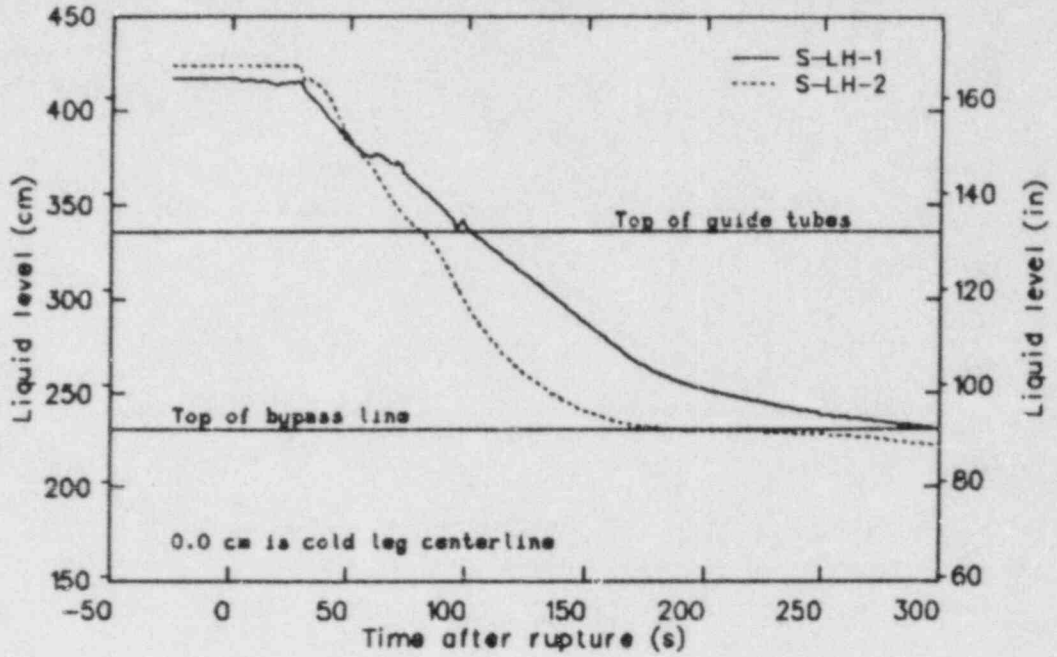

Figure 85. Comparison of calculated (RELAP5) upper head collapsed liquid levels for Experiments S-LH-1 and S-LH-2.

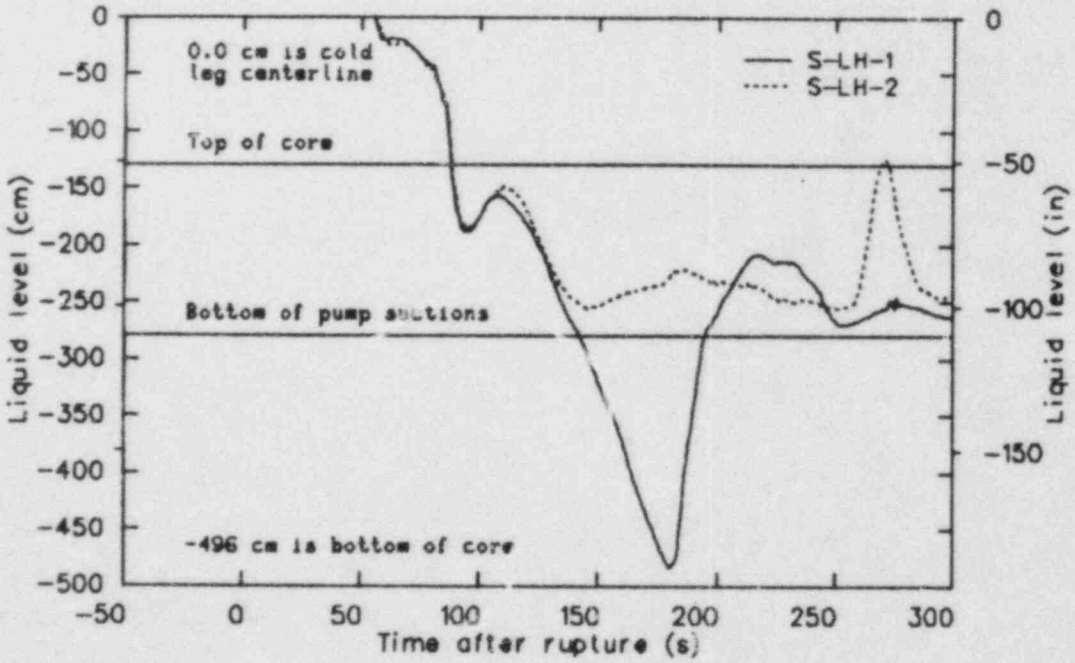

Figure 86. Comparison of calculated (RELAP5) vessel collapsed liquid levels for Experiments S-LH-1 and S-LH-2.

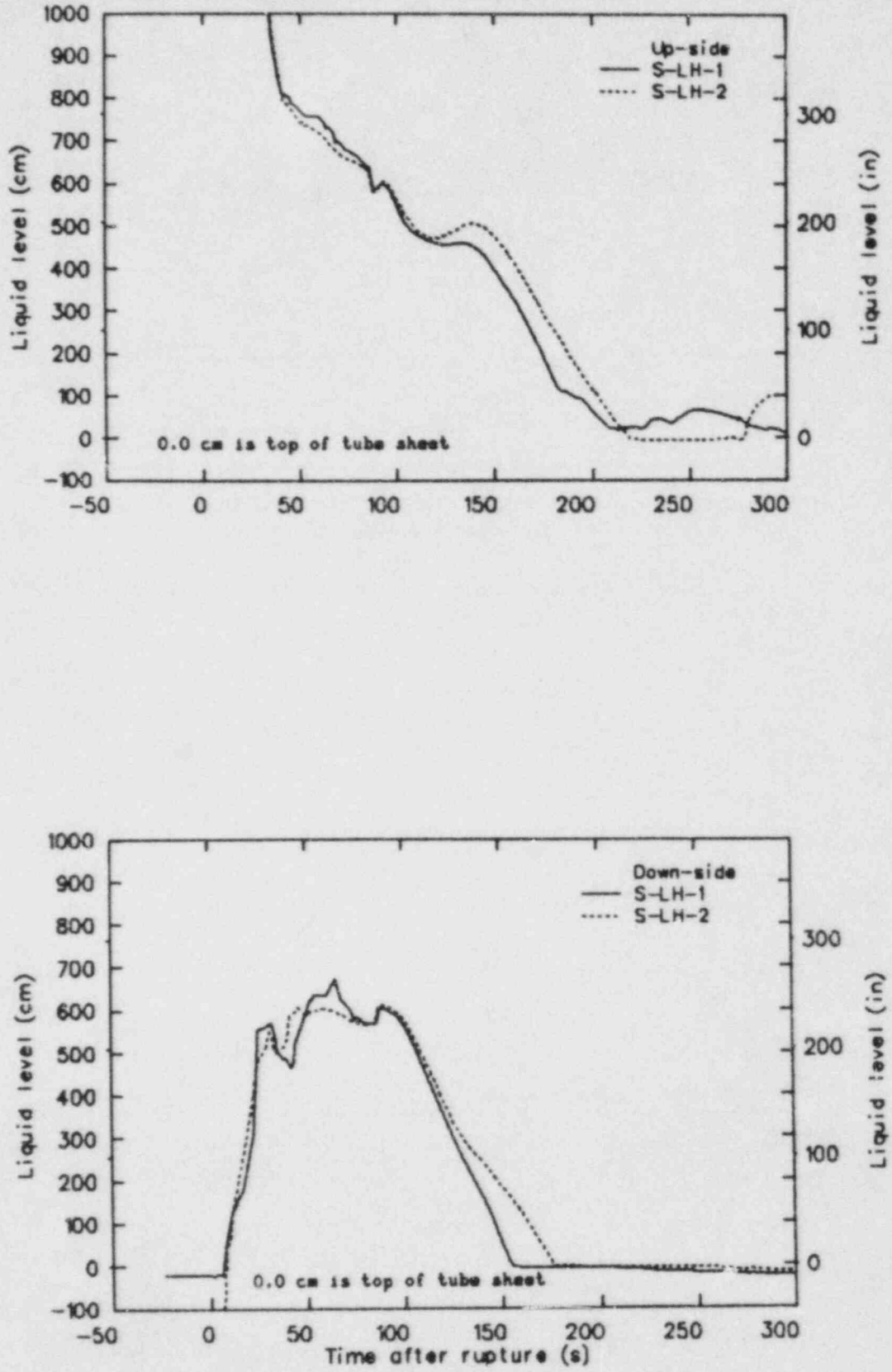

Figure 87. Comparison of calculated (RELAP5) intact loop U-tube collapsed liquid levels for Experiments S-LH-1 and S-LH-2.

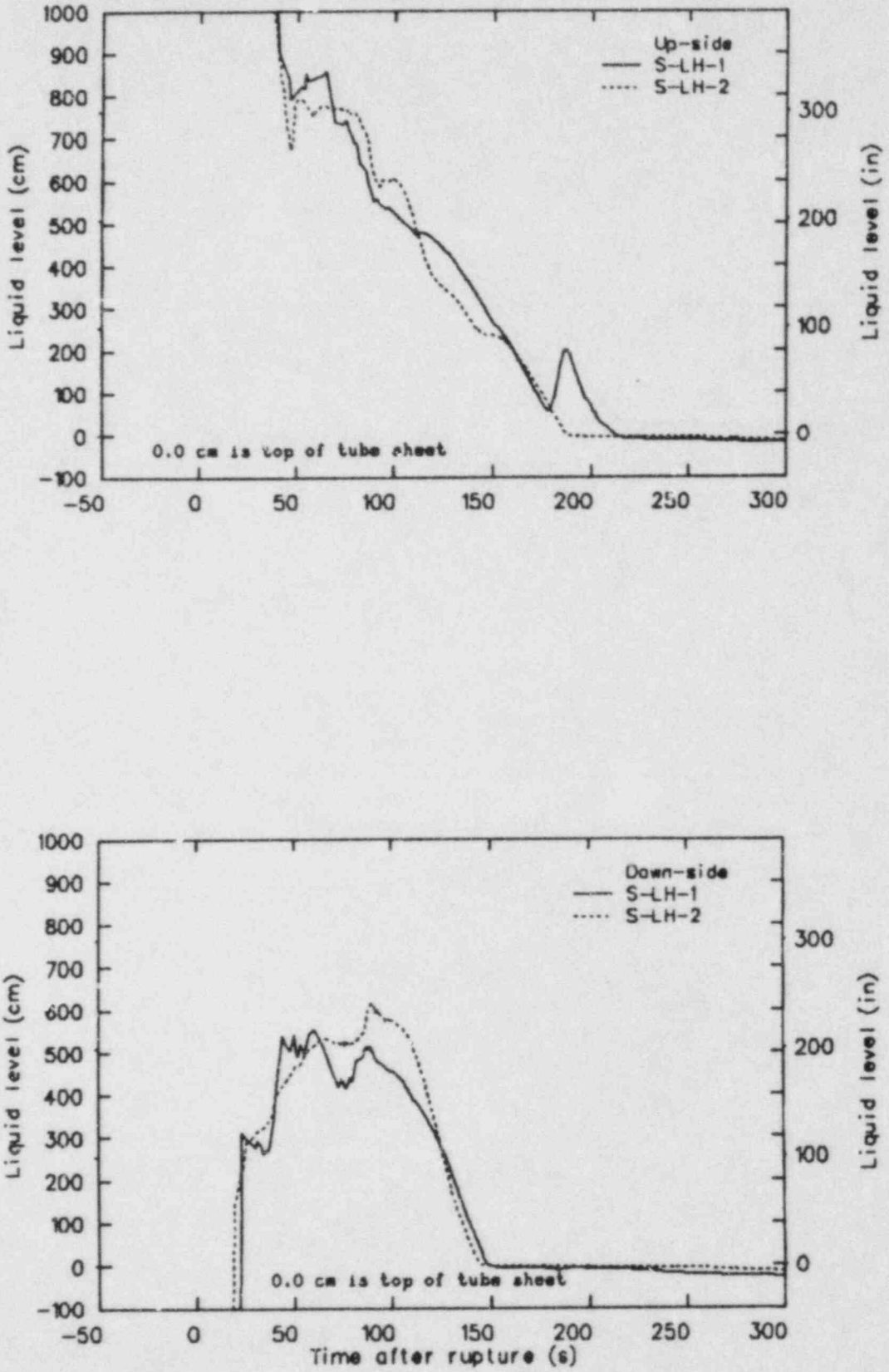

Figure 88. Comparison of calculated (RELAP5) broken loop U-tube collapsed liquid levels for Experiments S-LH-1 and S-LH-2.

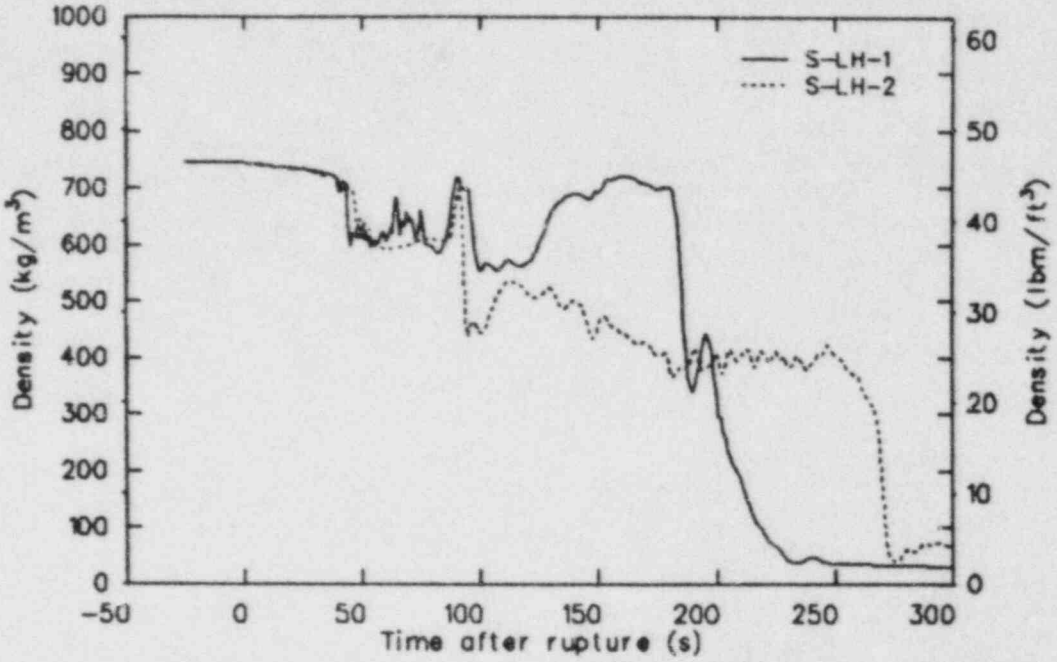

Figure 89. Comparison of calculated (RELAP5) upstream break densities for Experiments S-LH-1 and S-LH-2.

CONCLUSIONS

The following conclusions have been drawn based on analyses of S-LH-1 and S-LH-2 data and comparison of RELAP5 postexperiment calculations with data.

1. Two distinct core liquid level depressions occur during a 5% SBLOCA. One, of relatively fast duration (~25 s), is induced by the formation of pump suction liquid seals that support a manometric balance of heads between steam generated in the core and liquid heads in the loop. The other vessel liquid level depression (about 250 s duration) is caused by a long-term boil-off of core liquid prior to accumulator injection.

2. For the 0.9% core bypass flow case, it was possible to depress the core liquid level below the level associated with the bottom of the pump suctions. During the first rapid vessel liquid level depression, the core liquid level was depressed to within 110 cm (43 in.) of the core bottom, which is 100 cm (39 in.) below the level associated with the suctions. This was possible because of the distribution of fluid heads in the loop, most notably fluid heads above the cold leg elevation. The net amount of vessel liquid level depression below the pump suction elevation can be determined by adding or subtracting heads, depending on the tendency of a vertical section to push down or up on core level.

3. What has previously been referred to as "hold-up" in the primary U-tubes following U-tube drain is simply the signature differential head response across the primary U-tubes during the ongoing reflux process. The upflow side of the primary U-tubes shows a higher head of fluid than the downflow side. The head of fluid cannot be envisioned as a liquid plug; rather, the head represents both a frictional drop and liquid gravity head combined.

4. If the primary pumps are running (even at reduced speed), examining collapsed liquid levels in vertical components using differential pressure cells can lead to considerable error. A coastdown of the pump from 20% of initial speed to zero speed resulted in as much as 130 cm (51 in.) change in the calculated collapsed liquid level in the vessel and primary steam generator U-tubes.

5. As primary fluid mass exited the system, the various components drained in a complicated manner dictated by flashing, hydraulic resistance, pump operation, and the transition from forced to natural circulation flow. The pressurizer drained first, as flashing fluid pushed the liquid out. For the 0.9% core bypass case, the upper head drained very slowly out the bypass line throughout the blowdown, as fluid remained subcooled there longer. The vessel upper plenum and upper core drained next, due to the continuing 3-to-1 flow split between the intact and broken loop hot legs, but with break flow diverted out of the system and not returned to the vessel via the broken loop cold leg. Following pump coastdown to zero speed, the primary U-tubes drained. The broken loop U-tubes drained first as the intact loop flow underwent a transition to two-phase natural circulation. Following broken loop U-tube drain, the reflux mode was established in the broken loop and the intact loop drained. Following the drain of the U-tubes, liquid was collected in the pump suction piping which led to a manometric depression of U-tube levels and core levels. As the manometric depression continued, fluid in the pump suctions of both loops depleted, leaving the remaining fluid in the system centered in the vessel and downcomer at which point boil-off of core fluid occurred.

6. During the manometric balance period for the 0.9% core bypass case, first the intact loop pump suction seal clears of fluid, followed by the broken loop. This is attributed to the 9-to-1 hydraulic resistance split between the broken and intact loops. With a 9-to-1 resistance split following pump coastdown, break flow will be supplied from the less resistive intact loop suction before the more resistive broken loop suction. It is hypothesized that the broken loop of a symmetrical four-loop PWR would clear first, based on proximity to the break.

7. The core axial void fraction distribution is stratified during both core liquid level depressions associated with SBLOCAs. In the Semiscale experiments, the stratification is supported by boiling in the core due to core decay heat. The stratification is rate-independent and occurs both for rapid depletions (such as the first 25-s depression) and for slow boil-offs (250-s duration).

8. During the first, rapid, core liquid level depression induced manometrically, core rod heat-ups occurred in a multidimensional manner. These multidimensional heat-ups suggest falling films or drops of liquid on some rods but not on others. During passage of a froth level, rods at different azimuthal but identical axial positions show completely different behavior, i.e., one position shows heat-up while the other shows no heat-up.

9. During the second core liquid level depression associated with core boil-off, core rod heat-up proceeded in a uniform manner regardless of azimuthal position. If the froth level passed a rod position, that position demonstrated a heat-up. For an identical match of axial position for void fraction and rod temperature (both axially and azimuthally), heat-up does not occur until the local average void fraction equals 1 (+0; -0.02).

10. Comparison of otherwise identical 5% SBLOCA's with 3.0% and 0.9% initial core bypass flow showed that the upper head liquid drained faster with a higher bypass flow, allowing earlier clearing of the bypass line for steam relief. This enhanced steam relief path resulted in a less severe core level depression [110 cm (43 in.) from the core bottom for the 0.9% case, and 226 cm (90 in.) from the core bottom for the 3.0% case]. During the manometric core liquid level depression, there were no core rod heat-ups for the 3.0% case; however, there were minor core rod heat-ups for the 0.9% case.

11. RELAP5 calculations indicate that the core liquid level depression in S-LH-1 was caused by the reflux induced buildup of liquid on the upside of the steam generator U-tubes. RELAP5 calculates both the liquid and vapor velocities in a countercurrent manner suggestive of reflux.

12. To correctly calculate thermal-hydraulic response in the core, an improvement in the interfacial drag determination or a modification of the criteria for using the vertical stratification model is needed. During the core liquid level depression in S-LH-1, RELAP5 calculated almost no density variation throughout the core while the experiment showed a large density gradient. A highly stratified core was observed; RELAP5 calculated an almost homogeneous core.

13. The void fraction of 0.9999 required for dryout seems reasonable for localized conditions. However, its applicability in RELAP5 (which uses discrete volumes and assumes that the entire volume is at the same thermodynamic state) is questionable. It is strongly recommended that the dryout criterion be reexamined with the help of appropriate separate-effects experimental data.

14. Improvements in modeling of break flow, primary-to-secondary heat transfer, and fluid-to-piping heat transfer would result in a better calculation of primary pressure response and thus improve the timing of events and code-to-data comparisons. RELAP5 did not calculate enough liquid entrainment from the horizontal stratification model for the two-phase flow out the break.

15. RELAP5 correctly calculates the effect of lower bypass flow on core liquid level depression during the manometric balance period. RELAP5 calculated an identical reflux-induced liquid buildup in the steam generator U-tubes for high and low bypass flow cases (as occurred during S-LH-1 and S-LH-2) but also showed an enhanced core level depression for lower bypass flow, indicating that steam relief in the bypass line alone accounted for the difference in core level depression for the two bypass flow cases.

Data from the two 5% SBLOCA experiments are available for code development and assessment.

REFERENCES

1. M. T. Leonard, J. L. Perryman, and G. W. Johnson, "The Influence of Liquid Hold-up in Steam Generator U-tubes on Small Break Severity," ASME reprint 83-WA-NE-2.

2. M. T. Leonard, *Vessel Coolant Mass Depletion During a Small Break LOCA*, EGG-SEMI-6010, September 1982.

3. G. G. Loomis, "Semiscale Liquid Holdup Investigations: A Comparison of Results from Small Break LOCA Tests Performed in the Semiscale Mod-2A and Mod-2C Facilities," *13th Annual Water Reactor Research Information Meeting, Gaithersburg, Maryland, October 22-25, 1985.*

4. W. W. Tingle, *Experiment Operating Specifications for Semiscale Mod-2A 5% Break Experiment S-UT-8*, EGG-SEMI-5685, December 1981.

5. W. W. Tingle, *Test Data Report on Westinghouse Reactor Vessel Level Indicating System Performance during Semiscale Test S-UT-8*, EGG-SEMI-5827, March 1982.

6. J. M. Cozzuol, C. M. Kullberg, *Quick Look Report for Semiscale Mod-2A Test S-UT-6*, EGG-SEMI-5441, May 1981.

7. G. G. Loomis, *Summary of Semiscale Small Break Loss-of-Coolant Accident Experiments (1979 to 1985)*, NUREG/CR-4393, EGG-2419, September 1985.

8. G. G. Loomis, *Experimental Operating Specifications for Semiscale Mod-2C 5% Small Break Loss-of-Coolant Experiment S-LH-1*, EGG-SEMI-6813, February 1985.

9. G. G. Loomis, K. Soda, *Results of the Semiscale Mod-2A Natural Circulation Experiments*, NUREG/CR-2335, EGG-2200, September 1982.

10. V. Ransom et al., *RELAP5/MOD2 Code Manual*, EGG-SAAM-6377, April 1984.

APPENDIX A

RELAP5 MODEL DESCRIPTION

APPENDIX A

RELAP5 MODEL DESCRIPTION

RELAP5/MOD-2[A-1] is an advanced, one-dimensional system analysis computer code developed at the INEL for the U.S. Nuclear Regulatory Commission, Office of Reactor Safety Research (USNRC-RSR). It uses a full six-equation, two-fluid, nonequilibrium and nonhomogeneous hydrodynamic model for transient simulation of two-phase system behavior. Component models are included to describe the processes that occur during the heat-up and blowdown of a PWR. Cycle 36.02 of RELAP5/MOD-2 was used for the analyses presented in this report.

The Semiscale Mod-2C system RELAP5 model is represented by the nodalization diagram in Figure A-1. This model consists of 181 hydrodynamic volumes and 256 heat structures. All volume parameters are calculated with nonequilibrium code models. Steam generator secondaries, ECC injection, system environmental heat loss, and both vessel and piping external heaters are modelled in detail. The core axial power profile (Figure A-2) (a chopped cosine curve) is modelled in twelve consecutive heat structures over six 2-ft-long axial hydrodynamic volumes.

The upper head region (Figure A-3) is nodalized to allow junctions at the elevations of the top of the control rod guide tube, core bypass line and support columns, and at the elevation of the holes in the guide tube below the upper core support plate. Although the support columns (C182) are plugged, a small leak path exists to them from the upper head (C192). This leak path is simulated by adding a large loss factor at this junction. A loss factor was also added at the junction simulating the holes in the guide tube (C184), which allows venting of the upper plenum (C164). This loss factor was determined from the drain rates seen in experiments S-LH-1 and S-LH-2. In addition to changing the orifice size in the core bypass line (C181), the loss factor at this junction was also modified to obtain the initial core bypass flow rate.

Discharge coefficients are applied to the RELAP5 critical flow model at the break. One coefficient (CD1) is applied for single-phase (subcooled) critical flow, and another (CD2) is used for two-phase flow as the pressure upstream of the throat approaches saturation. These coefficients are an empirical correction to the critical flow rate to account for the multidimensional effects of boundary layer detachment at the orifice throat. These coefficients were determined by calculation comparison to data: the calculated break flow rate was directly compared to experiment data. For the best results, CD1 and CD2 were both equal to 0.90.

These discharge coefficients resulted in very good agreement in the break mass flow. However, when the break mass flow consisted of only steam, too large a primary system depressurization rate was calculated. Also, when the break mass flow was adjusted by the horizontal stratification model for vapor pull-through or liquid entrainment, too little break mass flow was calculated. The break mass flow was calculated correctly only when the break mass flow was single-phase (either liquid or vapor).

The initial conditions calculated by RELAP5, with few exceptions, compared well with the measured initial conditions (Tables A-1 and A-2). To achieve the desired primary cold leg temperatures, the steam generator secondary pressures were adjusted and consequently do not match the data. Also, the secondary masses are lower to achieve stable operation of the steam generators by RELAP5.

The piping external heaters were modelled mechanistically in RELAP5, and the measured power was input as a boundary condition. The external heaters on the vessel and downcomer were turned off as the vessel voided. RELAP5 modelled this control system as a function of the voiding and not as a function of time. The total measured power to the vessel external heaters as a function of time was, however, input as a boundary condition. The external heaters on the pressurizer were not powered for these experiments.

The experiment core power and normalized pump coastdown speeds were also input as boundary conditions. Safety injection system flow rates were input as closely to the same functions of pressure as could be calculated from the experimental data. Also, the upper head drain rate was used to determine loss coefficients in the guide tube.

These calculations were done on a CDC Cyber 176 computer. The important run statistics are given in Table A-3.

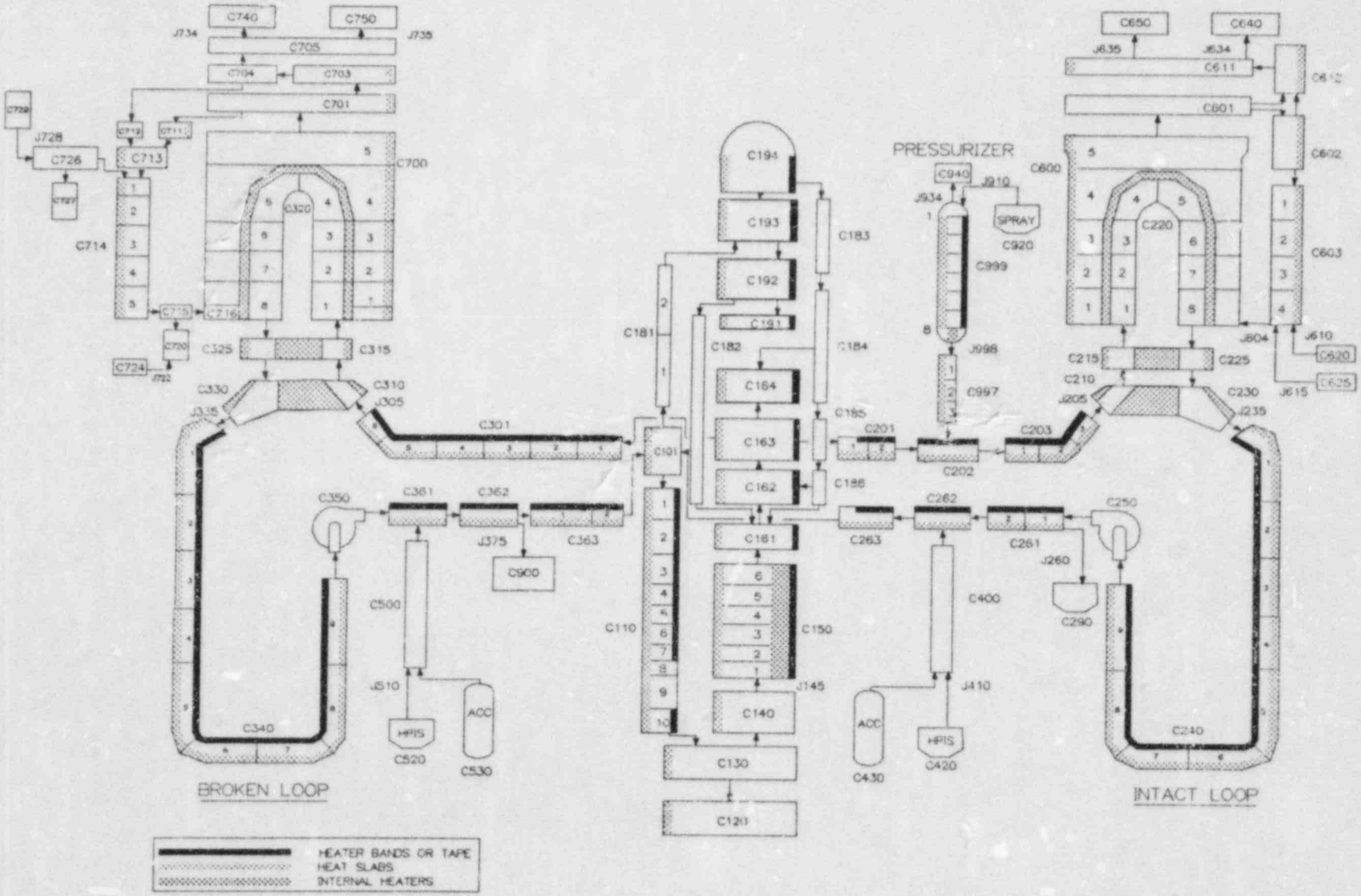

Figure A-1. Nodalization diagram for RELAP5 calculations.

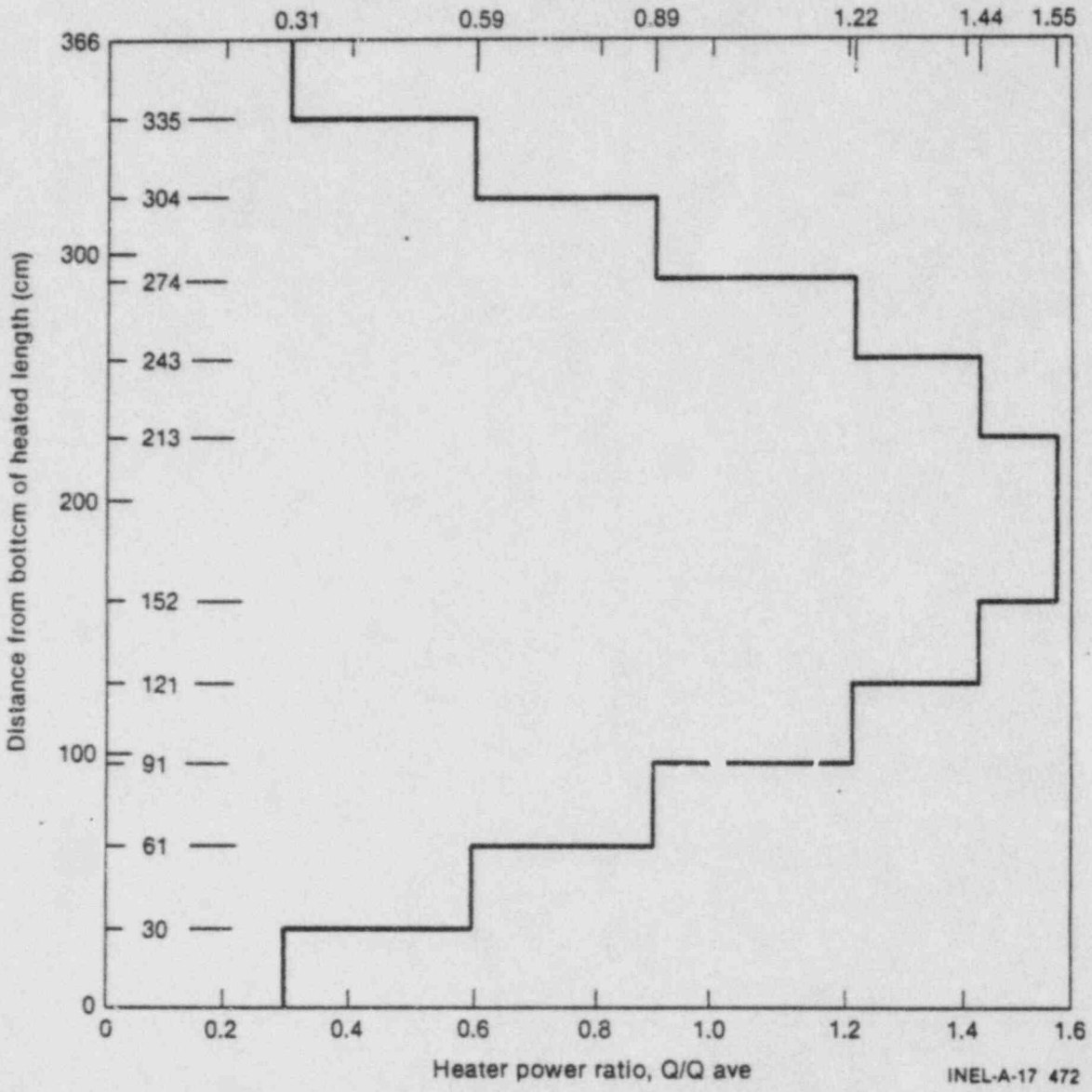

Figure A-2. Axial core power profile.

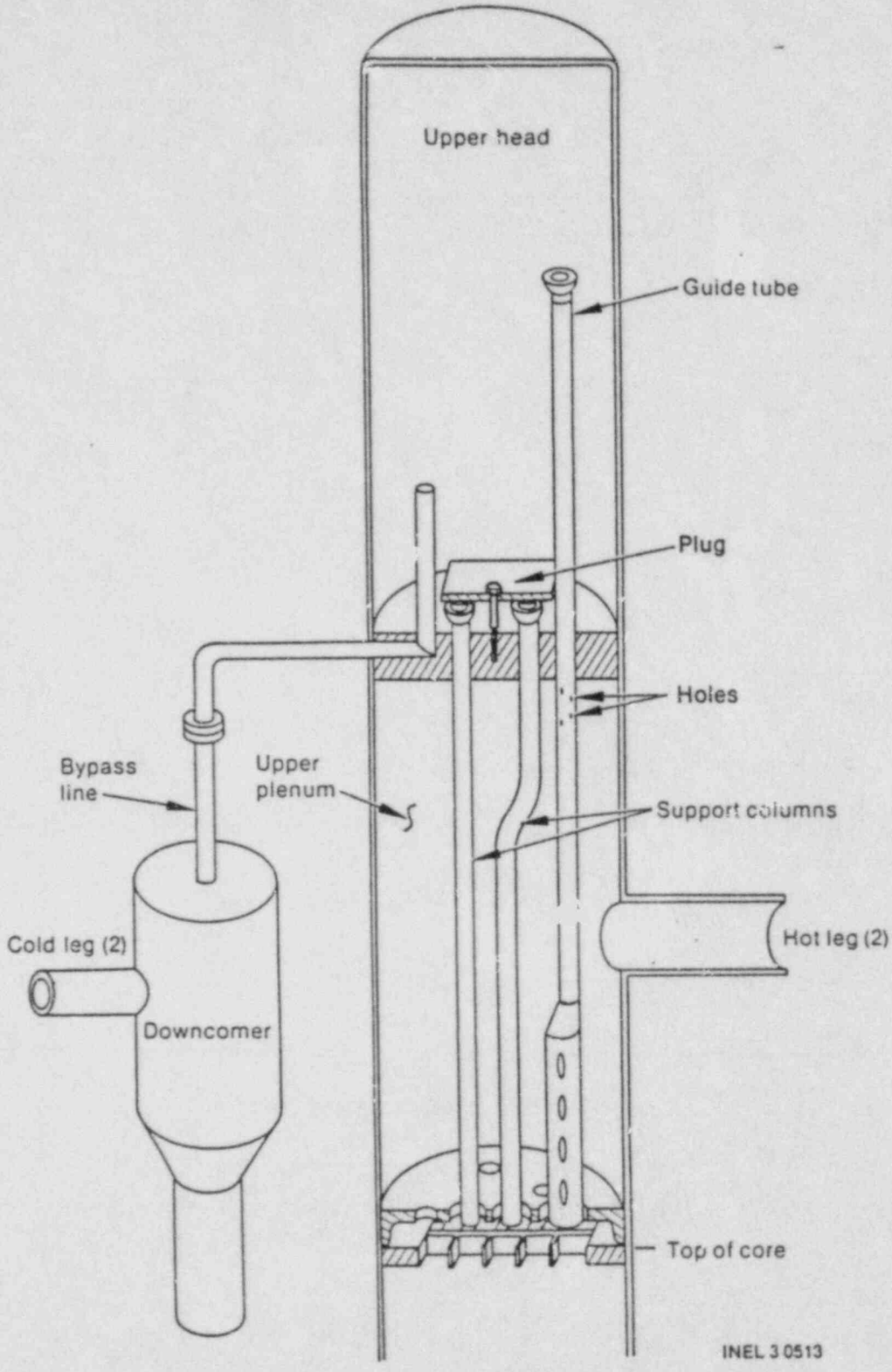

Figure A-3. Vessel upper head configuration for Experiments S-LH-1 and S-LH-2.

Table A-1. Comparison of calculated and measured initial conditions for S-LH-1.

Parameter	Measured	RELAP5
Pressurizer pressure, MPa (psia)	15.47 (2243.7)	15.45 (2240.3)
Core power, (kW)	2014.75	2014.75
Core ΔT, K (°F)	37.65 (67.8)	37.36 (67.2)
Pressurizer liquid level, cm (in.) (collapsed level above bottom)	395 (155.5)	394.1 (155.2)
Cold leg fluid temperature, K (°F)		
Intact loop	562.12 (552.1)	561.52 (551.1)
Broken loop	564.05 (555.6)	564.44 (556.3)
Primary flow rates, kg/s (lbm/s)		
Intact loop	7.13 (15.7)	7.11 (15.7)
Broken loop	2.35 (5.2)	2.34 (5.2)
Initial bypass flow (% of total core flow)	0.9	0.94
Leak rate, kg/s (lbm/s)	0.002 (0.004)	0.0 (0.0)
S. G. secondary pressures, MPa (psia)		
Intact loop	5.72 (829.6)	5.91 (857.1)[a]
Broken loop	6.08 (881.8)	5.91 (858.0)[a]
S. G. secondary side mass, kg (lb)		
Intact loop	191 (421.0)	169.8 (374.4)[b]
Broken loop	43 (94.8)	35.0 (77.1)[b]

a. Adjusted to obtain primary side conditions.

b. Approaching limit of stable operation of steam generators by RELAP5.

Table A-2. Comparison of calculated and measured initial conditions for S-LH-2

Parameter	Measured	RELAP5
Pressurizer pressure, MPa (psia)	15.42 (2236.5)	15.40 (2233.6)
Core power, (kW)	2007.09	2007.09
Core ΔT, K (°F)	37.17 (66.9)	37.60
Pressurizer liquid level, cm (in.) (collapsed level above bottom)	393 (154.7)	391.3 (154.1)
Cold leg fluid temperature, K (°F)		
Intact loop	561.94 (551.8)	561.88 (551.7)
Broken loop	564.35 (556.2)	564.00 (555.5)
Primary flow rates, kg/s (lbm/s)		
Intact loop	7.37 (16.2)	7.35 (16.2)
Broken loop	1.99 (4.4)	2.18 (4.8)
Initial bypass flow (% of total core flow)	3.0	3.00
Leak rate, kg/s (lbm/s)	0.002 (0.004)	0.0 (0.0)
S. G. secondary pressures, MPa (psia)		
Intact loop	5.70 (826.7)	5.91 (857.1)[a]
Broken loop	5.95 (863.8)	6.01 (871.9)[a]
S. G. secondary side mass, kg (lb)		
Intact loop	191 (421.0)	169.9 (374.5)[b]
Broken loop	48.2 (106.3)	35.0 (77.1)[b]

a. Adjusted to obtain primary side conditions.

b. Approaching limit of stable operation of steam generators by RELAP5.

Table A-3. RELAP5 run statistics for Experiments S-LH-1 and S-LH-2

	S-LH-1	S-LH-2
Real time (s)	800.1	800.1
Hydrodynamic volumes	181	181
Heat structures	256	256
Time steps during transient time	16734	16169
CPU time (s)	5914.06	5708.21
CPU/real time ratio	7.39	7.13
CPU time per real time per hydrodynamic volume (x 10)	0.408	0.394
CPU time per real time per time step per hydrodynamic volume (x 10^6)	2.440	2.438
CPU time per time step per hydrodynamic volume (x 10^3)	1.953	1.950

Reference

A-1. V. Ransom et al., *RELAP5/MOD2 Code Manual*, EGG-SAAM-6377, April 1984.

APPENDIX B

COMPARISON OF POSTEXPERIMENT RELAP5 CALCULATIONS TO S-LH-2 DATA

APPENDIX B

COMPARISON OF POSTEXPERIMENT RELAP5 CALCULATIONS TO S-LH-2 DATA

This Appendix contains the RELAP5 calculation-to-data comparisons for Experiment S-LH-2. Table B-1 and Figures B-1 through B-18 correspond to those shown in the text tor Experiment S-LH-1.

Table B-1. Comparison of calculated and measured sequence of events for S-LH-2.

Event	Time (s) Measured	RELAP5
Break opened	0.3	0.0
Pressurizer at 12.6 MPa (1827 psia)	15.91	16.40
Core scram	19.57	21.05
Pump coastdown initiated		
Intact loop	20.65	21.45
Broken loop	20.65	22.15
Feedwater off		
Intact loop	19.60	19.40
Broken loop	19.00	19.40
MSIV closure		
Intact loop	20.0	21.85
Broken loop	19.5	21.35
HPIS initiated		
Intact loop	41.6	42.35
Broken loop	41.6	42.35
Pressurizer emptied	34.8	37.0
Minimum core liquid level reached[a]	204.35	146.0
Break uncovered	214.1	270.2
Intact loop pump suction cleared	205.4	253.0
Broken loop pump suction cleared	Did not clear	Did not clear
Accumulator flow initiated		
Intact loop	575.0	467.1
Broken loop	Not initiated	Not initiated

a. Minimum measured level was -269 cm (-106 in.), and minimum calculated level was -255 cm (-100 in.).

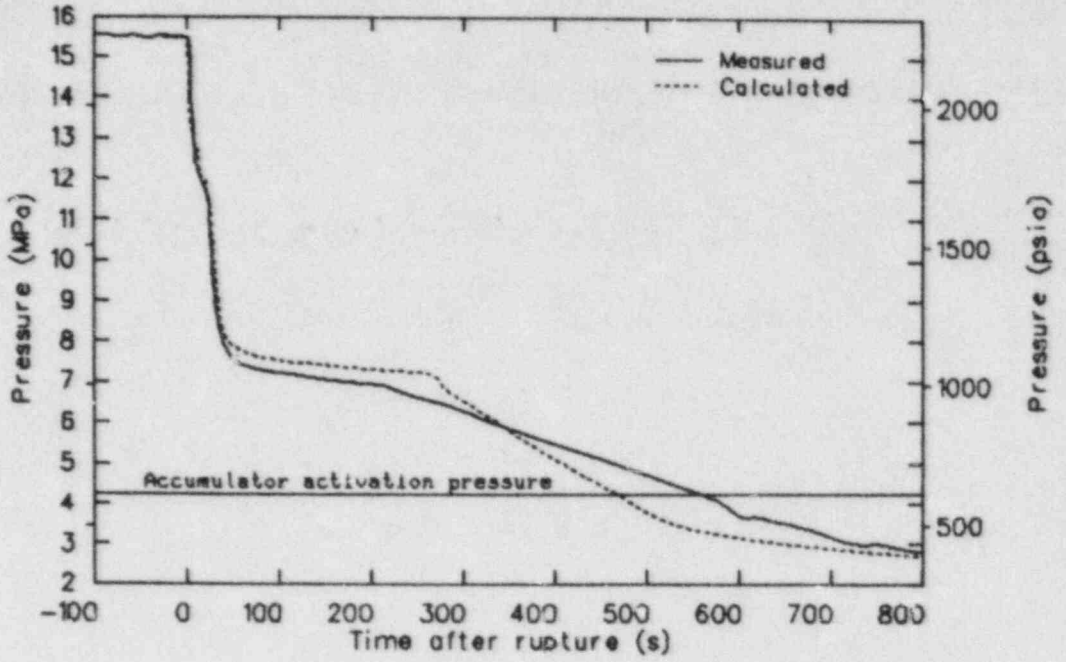

Figure B-1. Comparison of measured (S-LH-2) and calculated (RELAP5) primary system pressures.

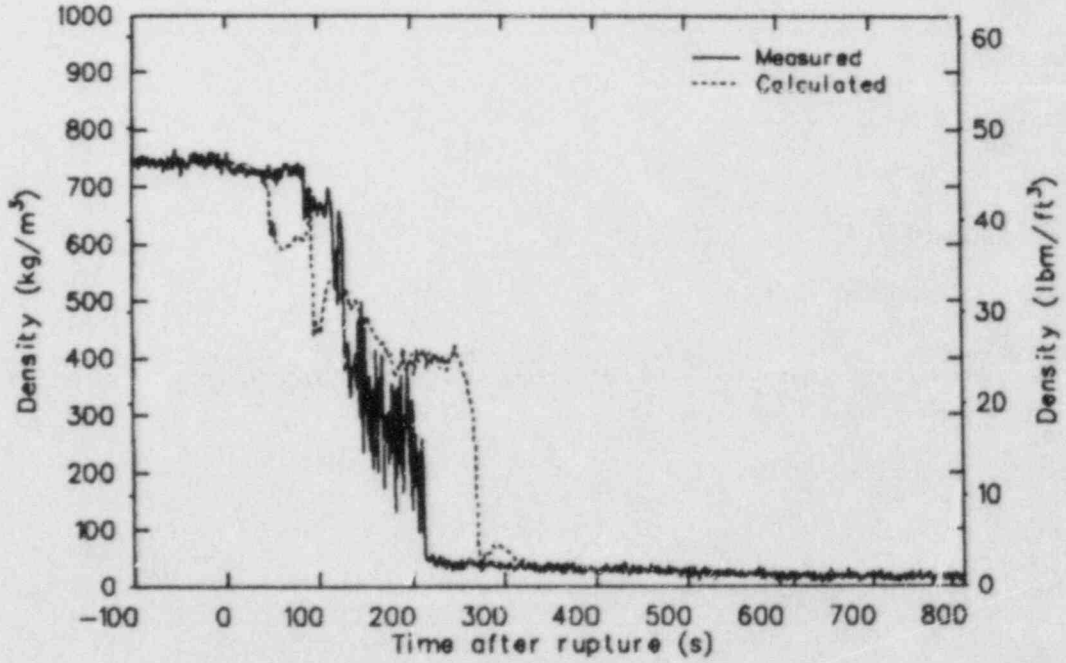

Figure B-2. Comparison of measured (S-LH-2) and calculated (RELAP5) upstream break densities.

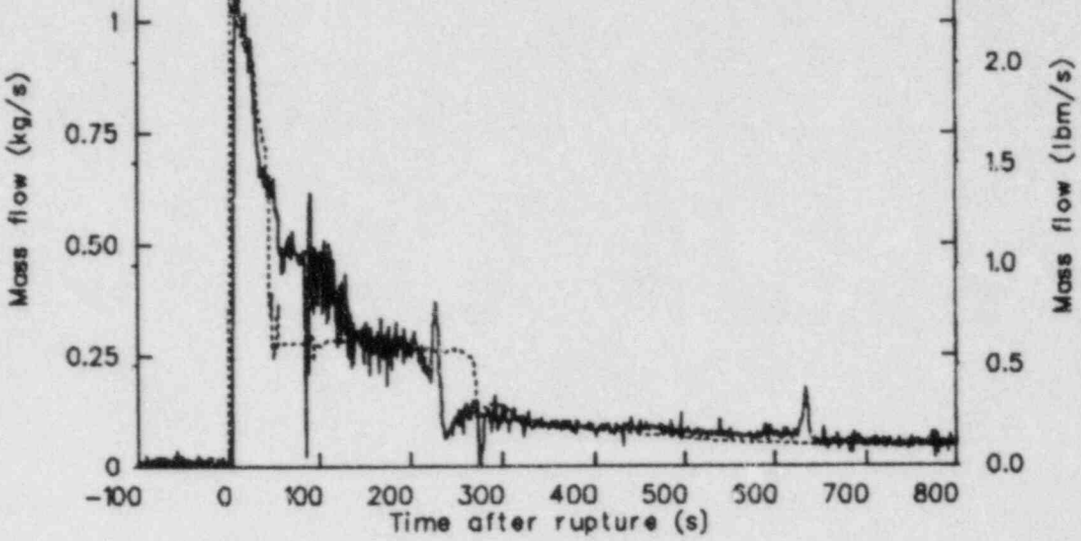

Figure B-3. Comparison of measured (S-LH-2) and calculated (RELAP5) break mass flow rates.

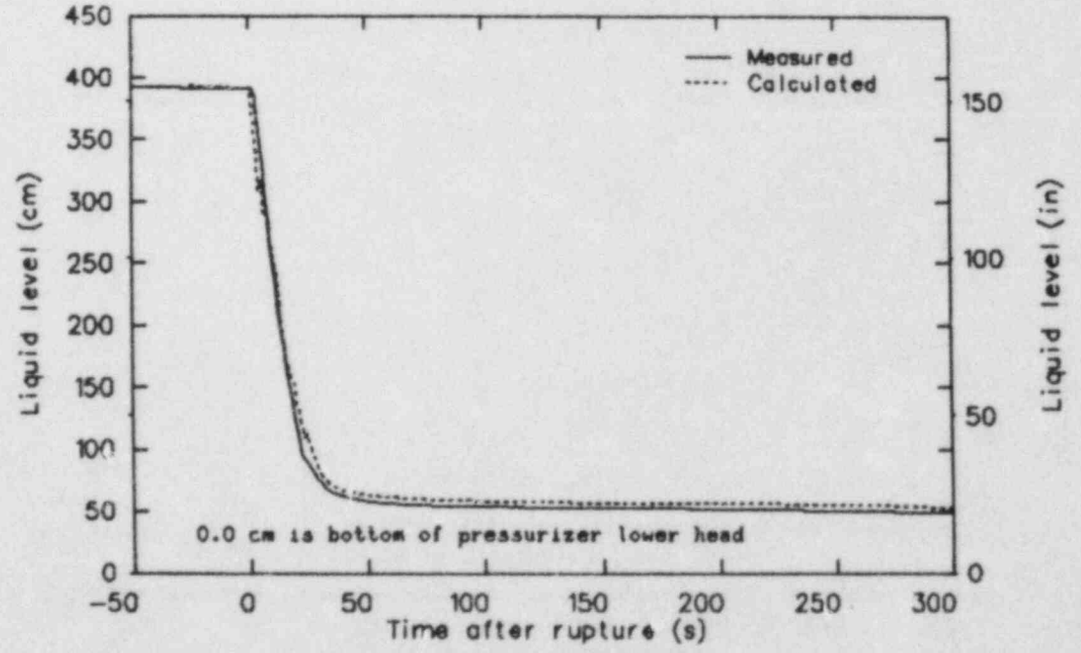

Figure B-4. Comparison of measured (S-LH-2) and calculated (RELAP5) pressurizer collapsed liquid levels.

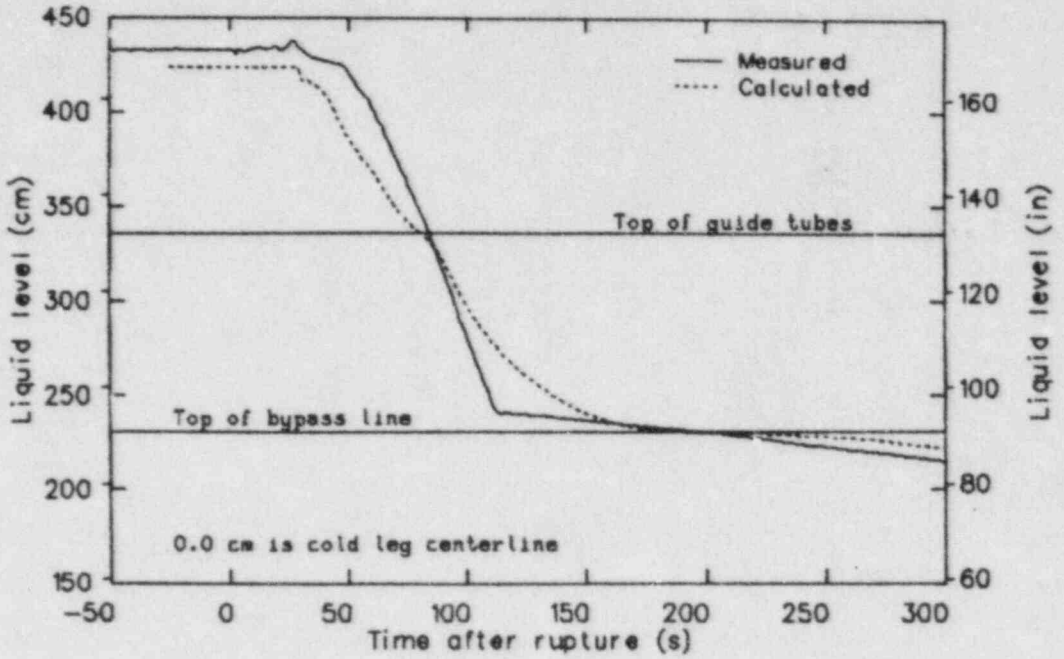

Figure B-5. Comparison of measured (S-LH-2) and calculated (RELAP5) upper head collapsed liquid level

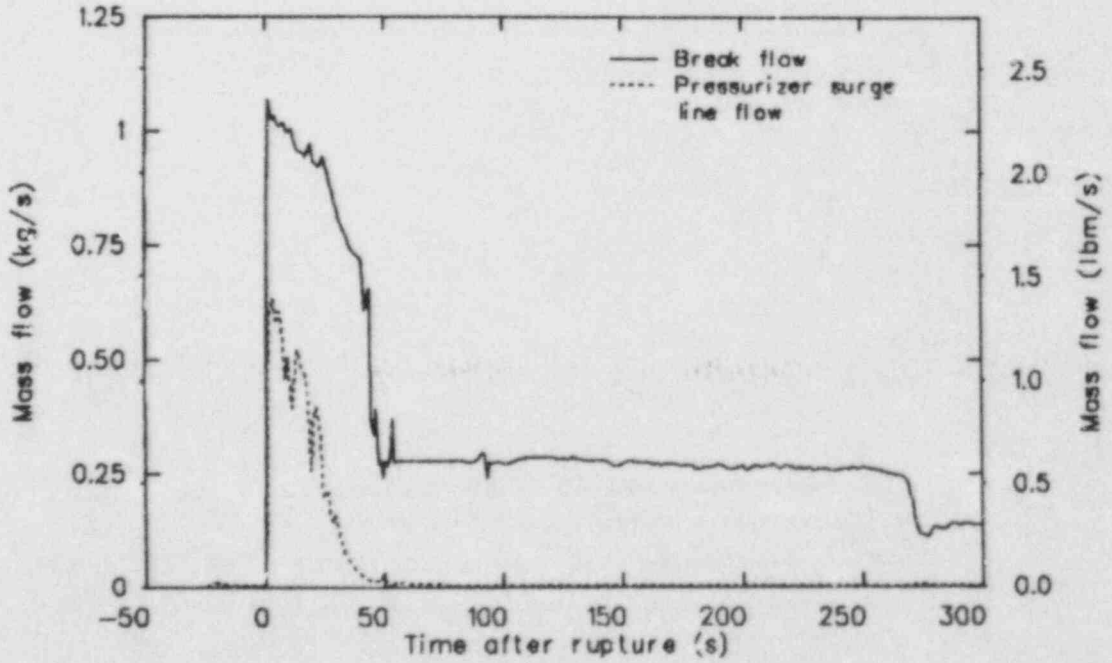

Figure B-6. Comparison of calculated (RELAP5) break and pressurizer surge line mass flow rates.

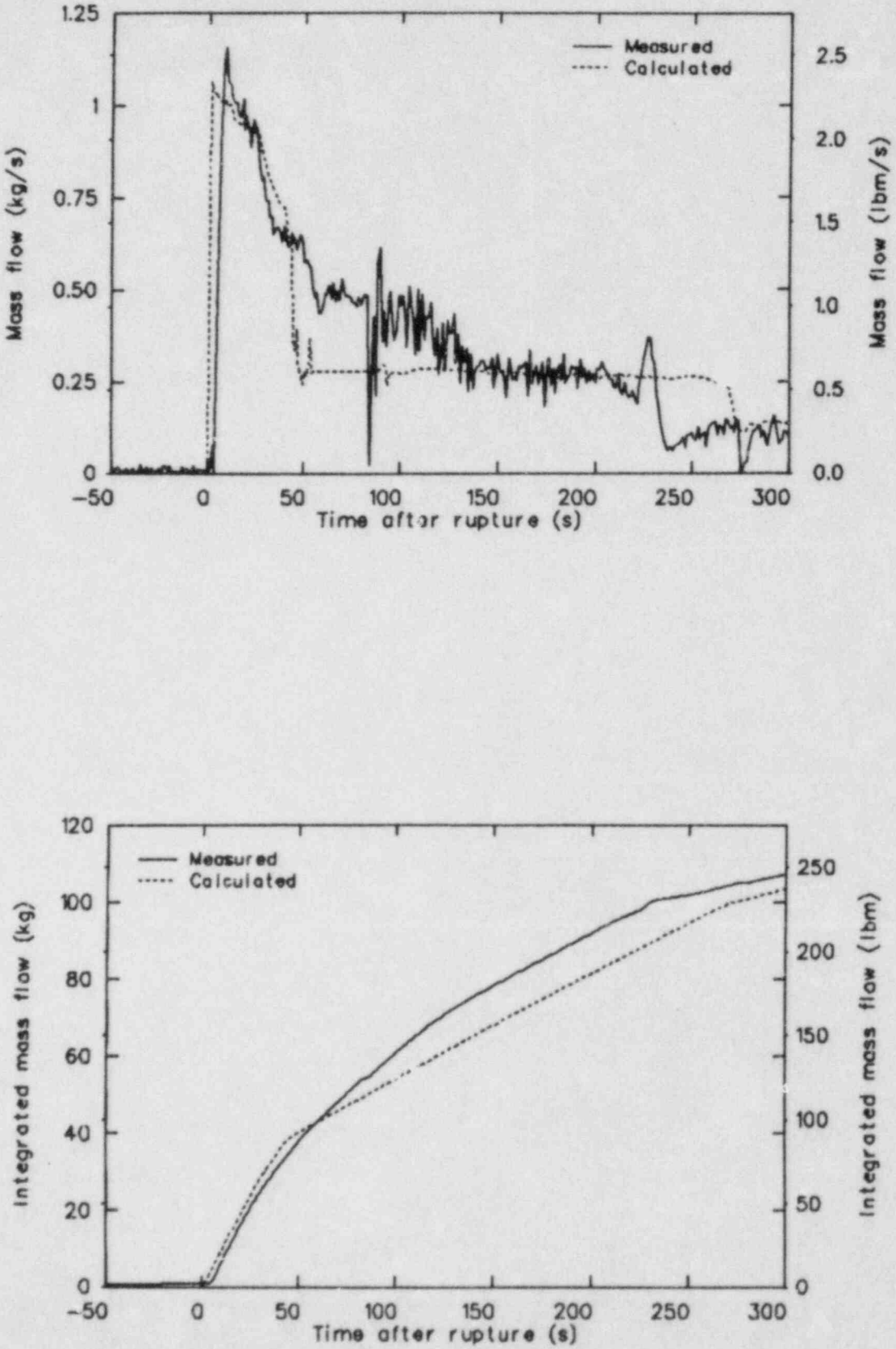

Figure B-7. Comparison of measured (S-LH-2) and calculated (RELAP5) break mass flow rates during core level depression.

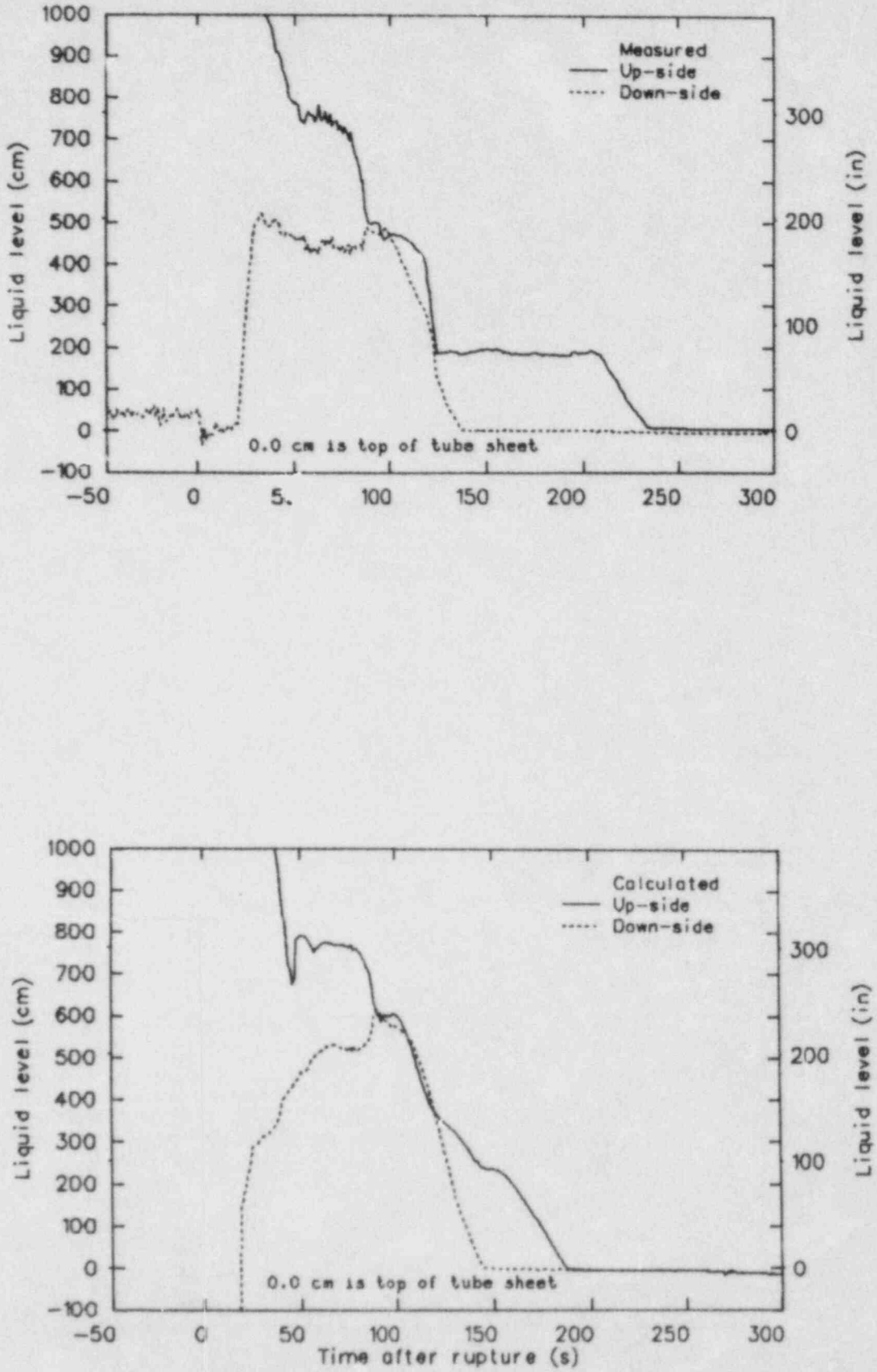

Figure B-8. Comparison of measured (S-LH-2) and calculated (RELAP5) broken loop U-tube collapsed liquid levels.

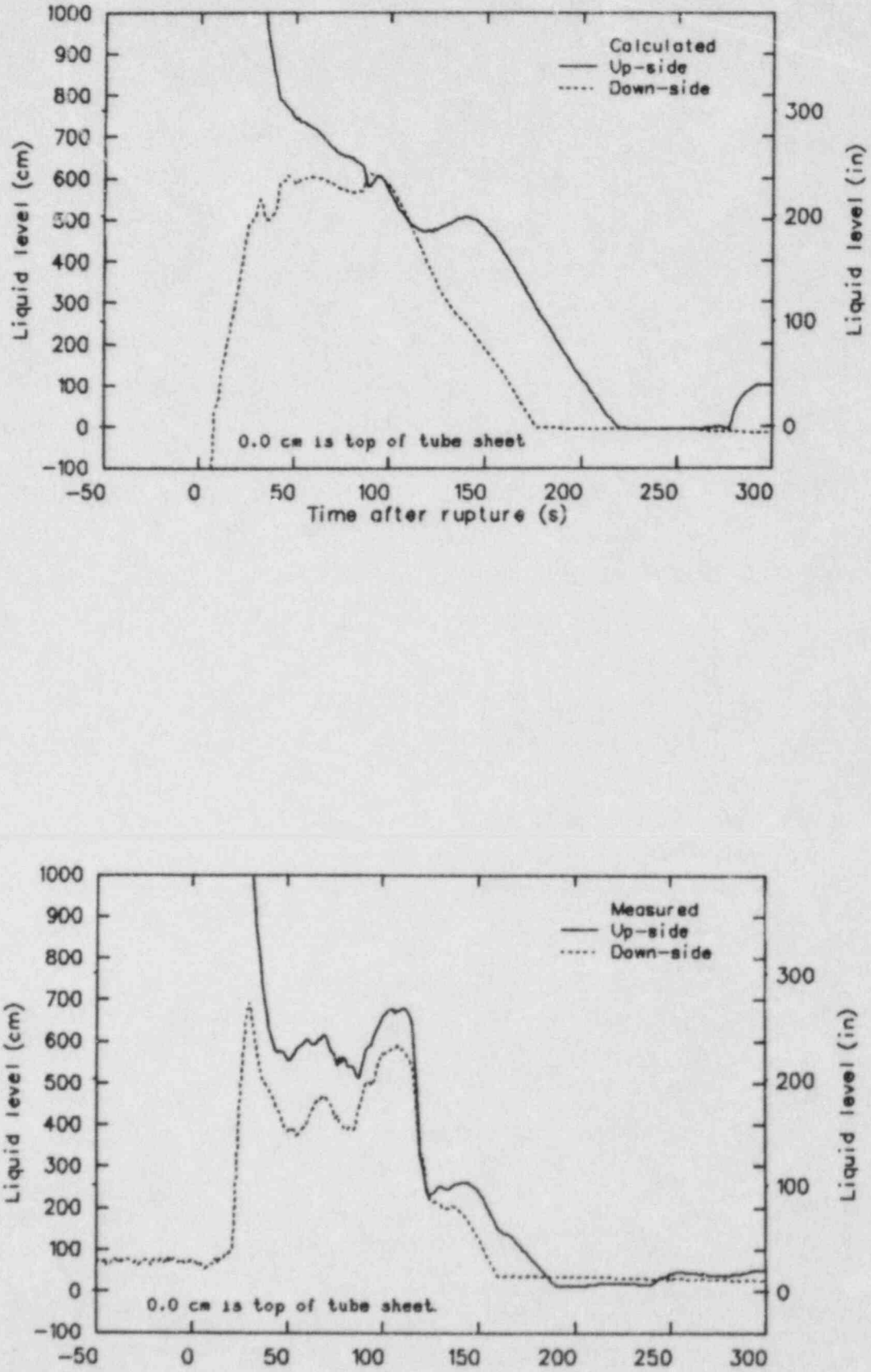

Figure B-9. Comparison of measured (S-LH-2) and calculated (RELAP5) intact loop U-tube collapsed liquid levels.

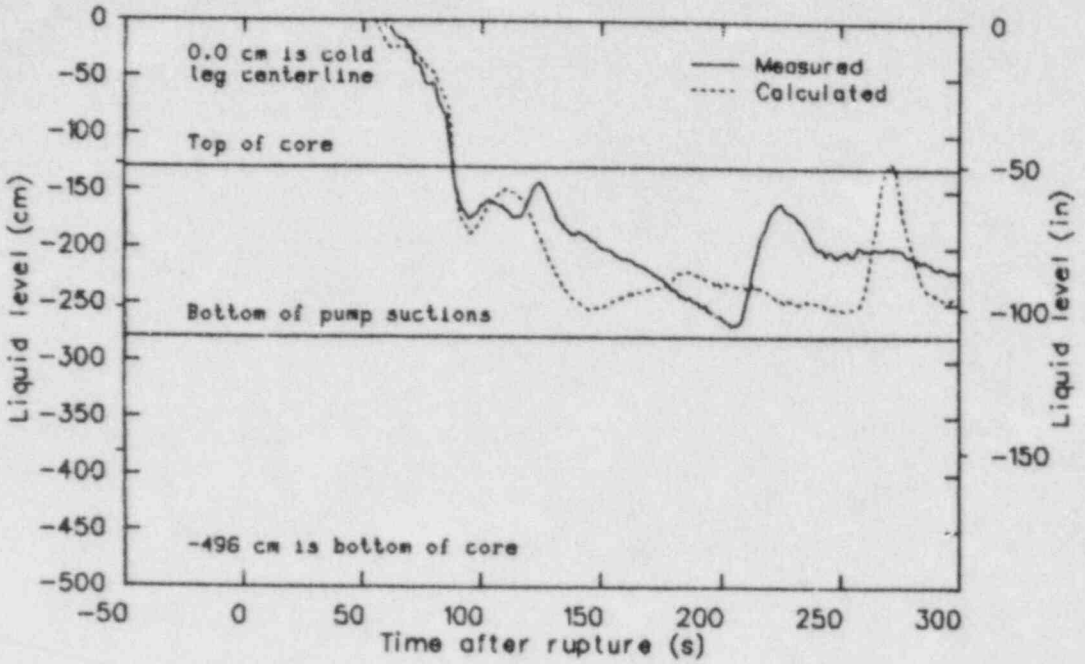

Figure B-10. Comparison of measured (S-LH-2) and calculated (RELAP5, vessel collapsed liquid levels.

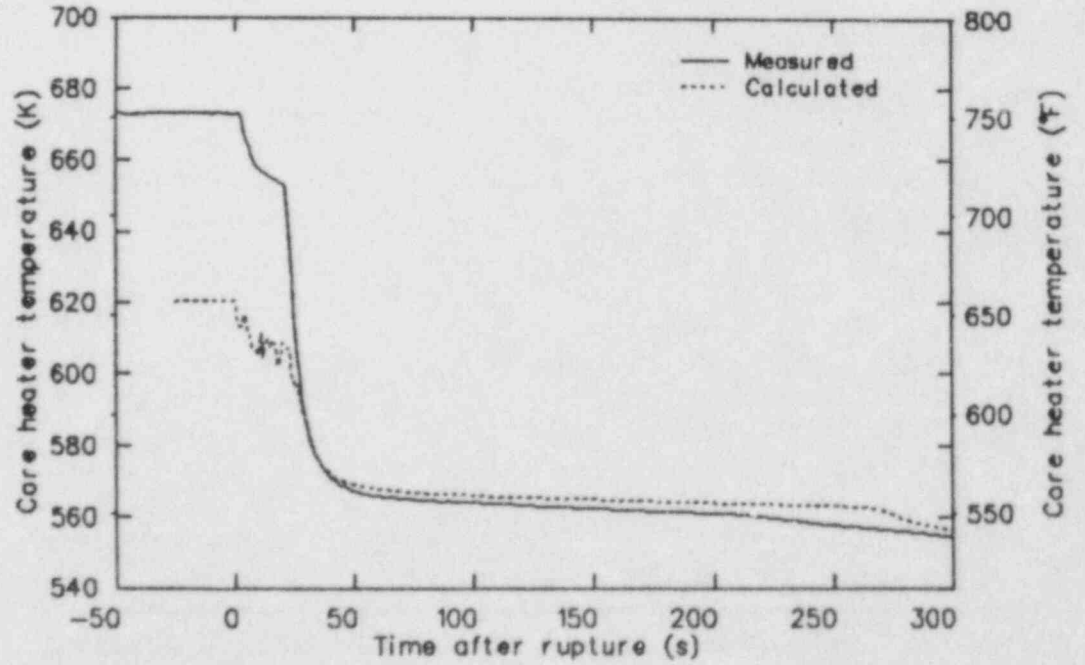

Figure B-11. Comparison of measured (S-LH-2) and calculated (RELAP5) maximum core heater rod temperatures.

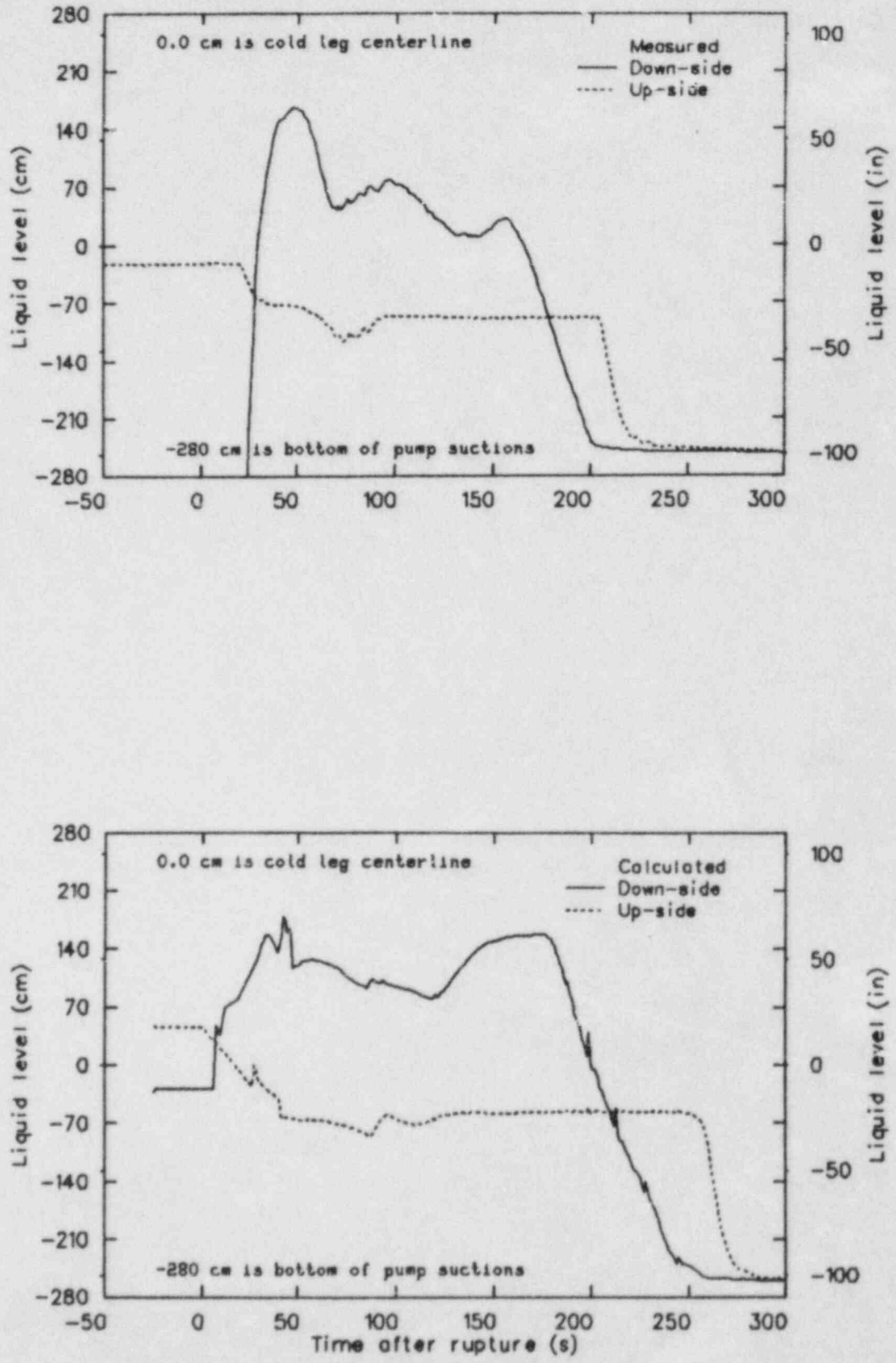

Figure B-12. Comparison of measured (S-LH-2) and calculated (RELAP5) intact loop pump suction collapsed liquid levels.

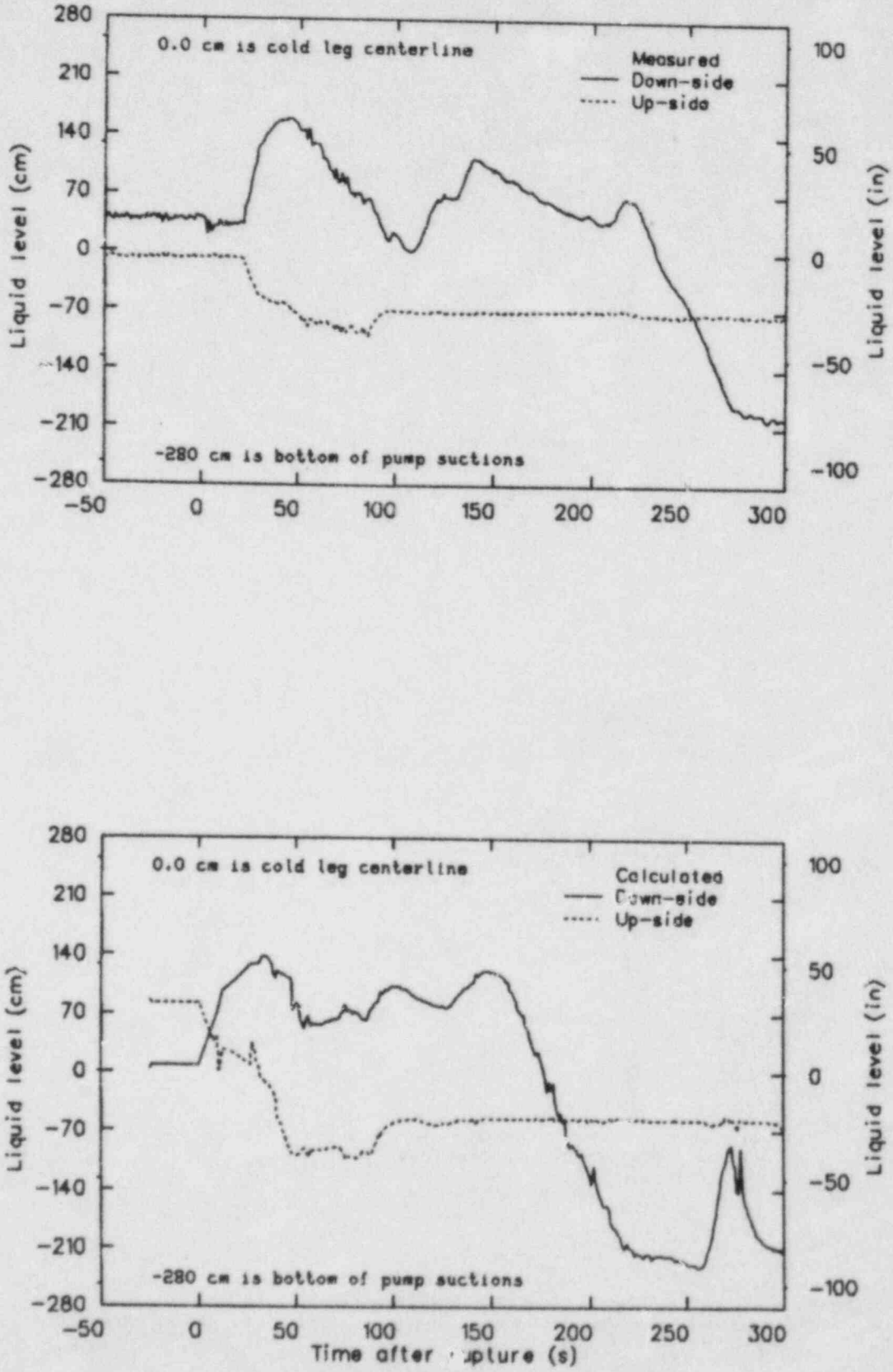

Figure B-13. Comparison of measured (S-LH-2) and calculated (RELAP5) broken loop pump suction collapsed liquid levels.

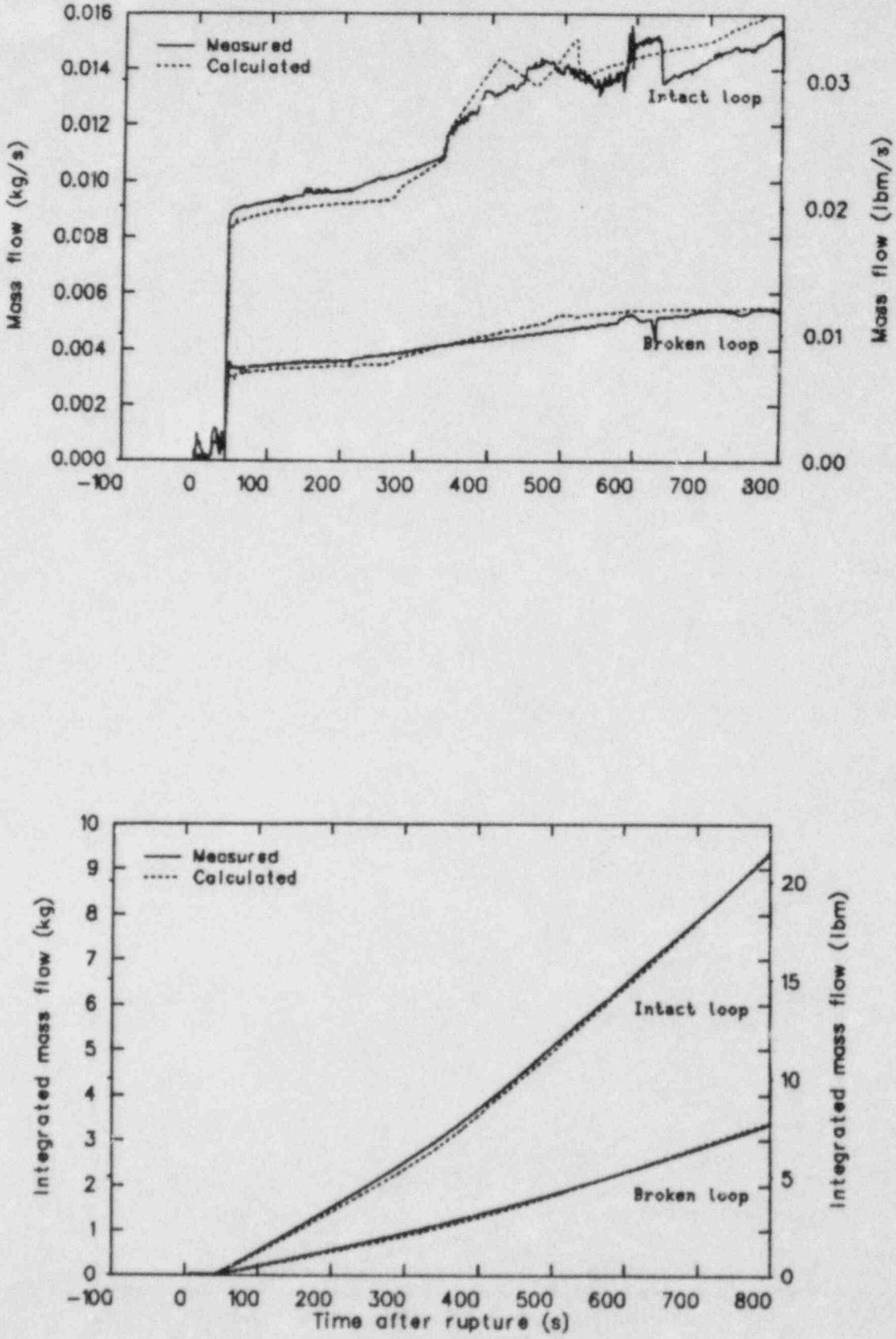

Figure B-14. Comparison of measured (S-LH-2) and calculated (RELAP5) HPIS mass flow rates.

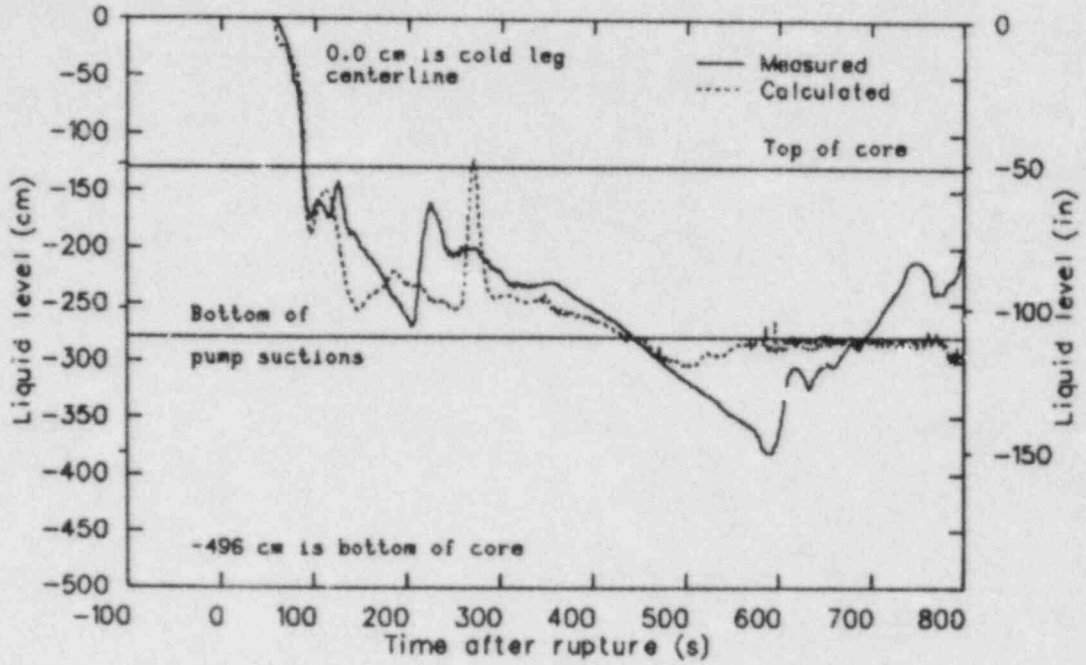

Figure B-15. Comparison of measured (S-LH-2) and calculated (RELAP5) vessel collapsed liquid levels during core boil-off.

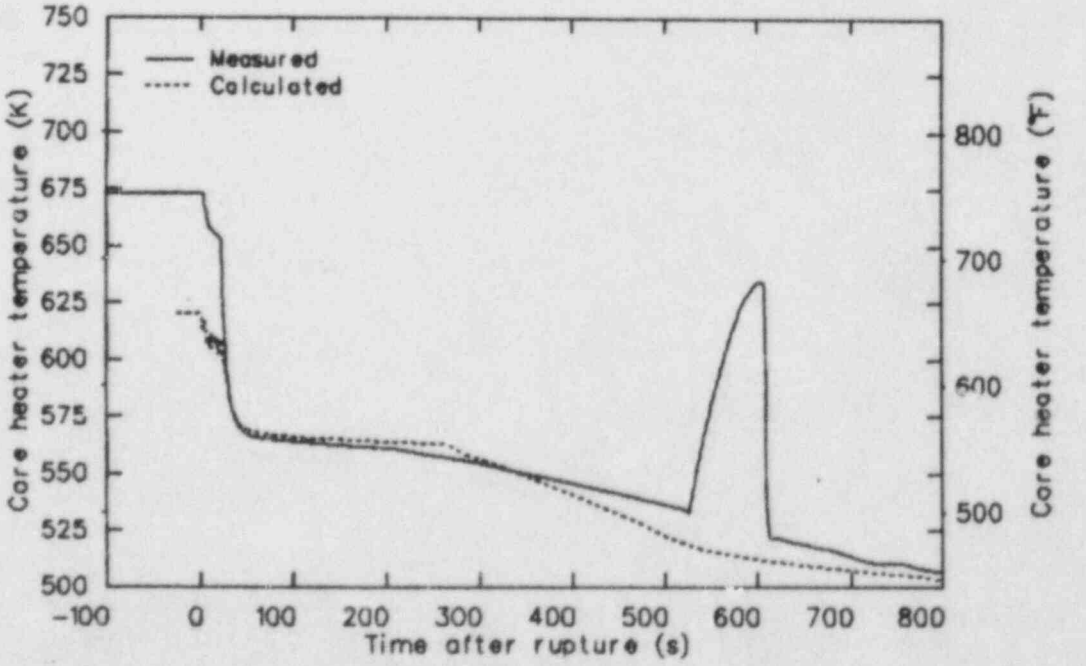

Figure B-16. Comparison of measured (S-LH-2) and calculated (RELAP5) maximum core heater rod temperatures during core boil-off.

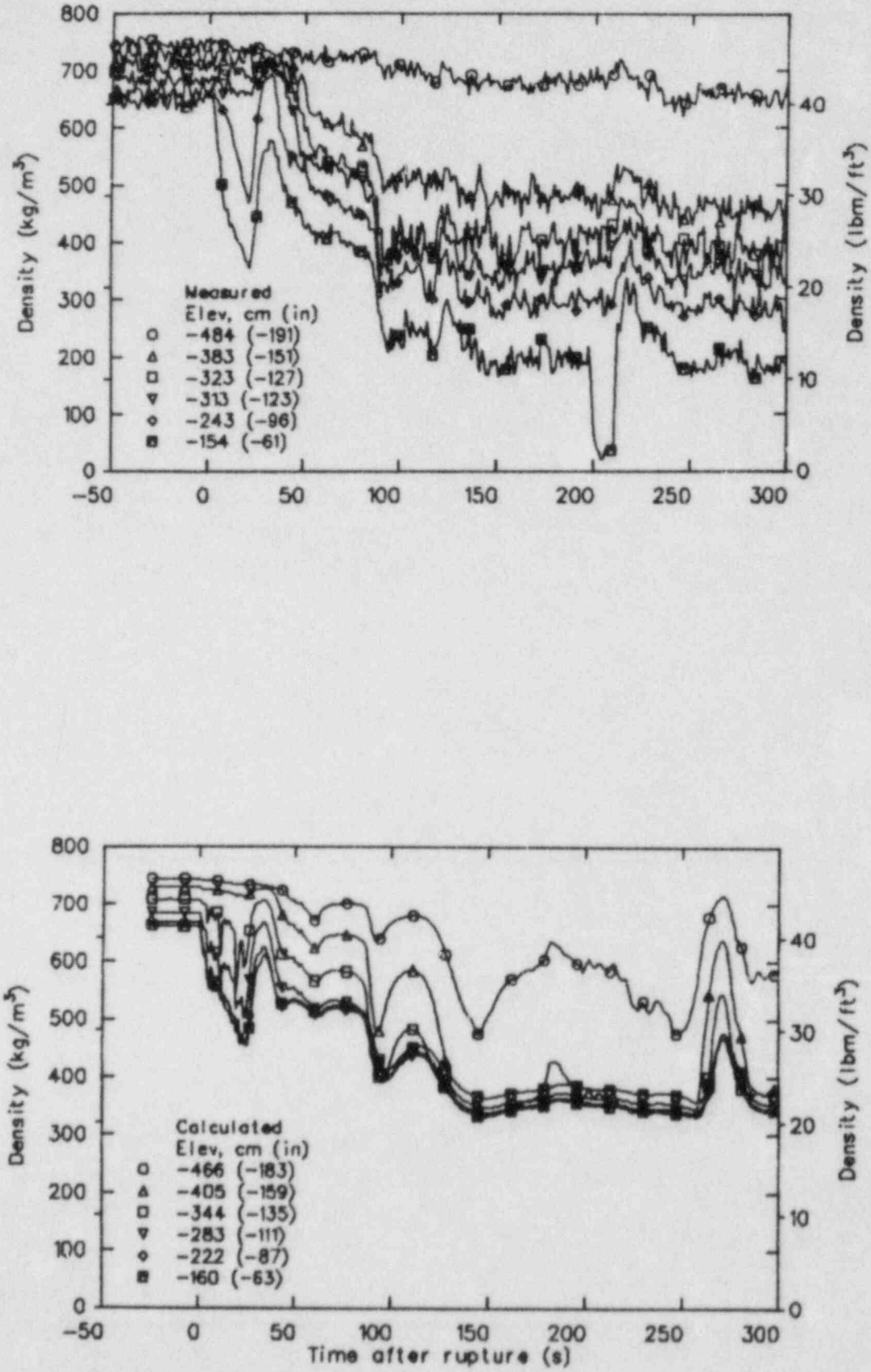

Figure B-17. Comparison of measured (S-LH-2) and calculated (RELAP5) core densities.

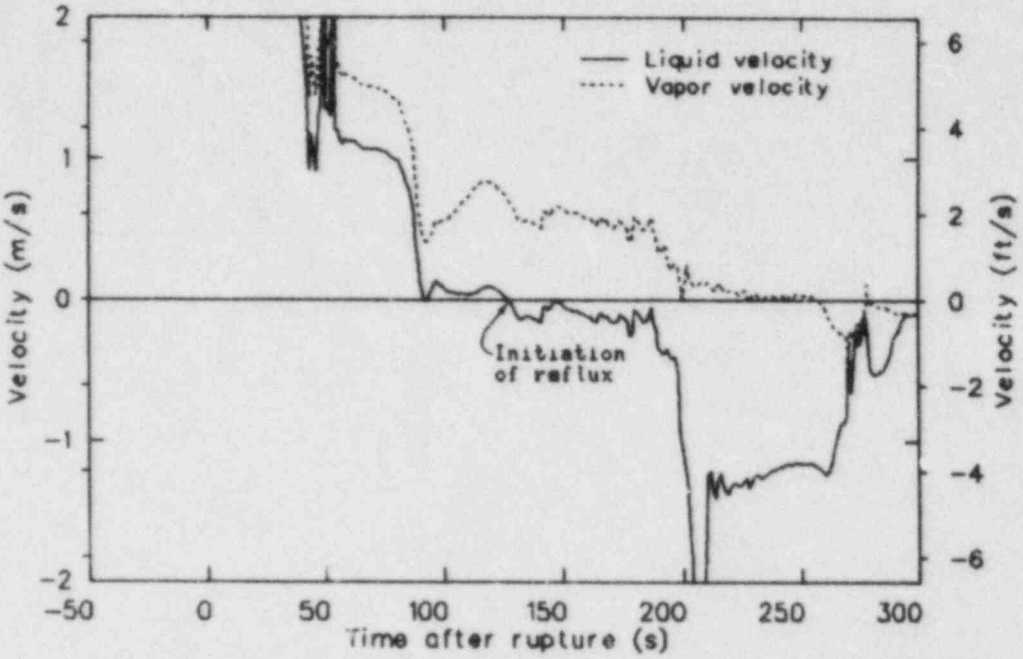

Figure B-18. Calculated (RELAP5) liquid and vapor velocities at the broken loop steam generator inlet for S-LH-2.

NRC FORM 335 (2-84) NRCM 1102, 3201, 3202

U.S. NUCLEAR REGULATORY COMMISSION

BIBLIOGRAPHIC DATA SHEET

SEE INSTRUCTIONS ON THE REVERSE

1. REPORT NUMBER (Assigned by TIDC, add Vol. No., if any)
NUREG/CR-4438
EGG-2424

2. TITLE AND SUBTITLE
Results of Semiscale Mod-2C
Small-Break Loss-of-Coolant Accident
Experiments S-LH-1 and S-LH-2

3. LEAVE BLANK

4. DATE REPORT COMPLETED
MONTH: 11 YEAR: 85

5. AUTHOR(S)
Guy G. Loomis
John E. Streit

6. DATE REPORT ISSUED
MONTH: 11 YEAR: 85

7. PERFORMING ORGANIZATION NAME AND MAILING ADDRESS (Include Zip Code)
EG&G Idaho, Inc.
Idaho Falls, Idaho 83415

8. PROJECT/TASK/WORK UNIT NUMBER

9. FIN OR GRANT NUMBER
A6038

10. SPONSORING ORGANIZATION NAME AND MAILING ADDRESS (Include Zip Code)
EG&G Idaho, Inc.
Idaho Falls, Idaho 83415

11a. TYPE OF REPORT
Research

b. PERIOD COVERED (Inclusive dates)

12. SUPPLEMENTARY NOTES

13. ABSTRACT (200 words or less)

Two experiments simulating small break (5%) loss-of-coolant accidents (5% SBLOCAs) were performed in the Semiscale Mod-2C facility. These experiments were identical except for downcomer-to-upper-head bypass flow (0.9% in Experiment S-LH-1 and 3.0% in Experiment S-LH-2) and were performed at high pressure and temperature [15.6 MPa (2262 psia) system pressure; 37 K (67°F) core differential temperature; 595 K (610°F) hot leg fluid temperature]. From the experimental results, the signature response and transient mass distribution are determined for a 5% SBLOCA. The core thermal-hydraulic response is characterized, including core void distribution maps, and the effect of core bypass flow on transient severity is assessed. Comparisons are made between postexperiment RELAP5 calculations and the experimental results, and the capability of RELAP5 to calculate the phenomena is assessed.

14. DOCUMENT ANALYSIS - a. KEYWORDS/DESCRIPTORS
Semiscale, small-break LOCA, RELAP5

15. AVAILABILITY STATEMENT

16. SECURITY CLASSIFICATION
(This page) Uncl.
(This report) Uncl.

17. NUMBER OF PAGES
117

18. PRICE

b. IDENTIFIERS/OPEN-ENDED TERMS

EG&G Idaho
P.O. Box 1625
Idaho Falls, Idaho
83415